PROGRESS REPORT

January 1, 1975 - June 30, 1975

NASA Grant NGR 47-003-078

A STUDY OF HEAVY-HEAVY NUCLEAR REACTIONS

Principal Investigator: Govind S. Khandelwal
Associate Professor
Department of Physics and Geophysical Sciences
School of Sciences
Old Dominion University

Submitted by: Old Dominion University Research Foundation
Norfolk, Virginia 23508

(NASA-CR-145401) A STUDY OF HEAVY-HEAVY NUCLEAR REACTIONS Progress Report, 1 Jan. - 30 Jun. 1975 (Calhoun Community Coll., Decatur, Ala.) 109 p HC $5.25 CSCL 03B

N76-10974

Unclas
G3/93 39362

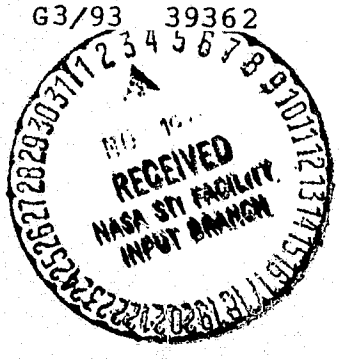

October 22, 1975

Mr. John W. Wilson, Technical Monitor
Astrophysics Section
Space Physics Branch
Environmental and Space Sciences Division
Langley Research Center

A STUDY OF HEAVY-HEAVY NUCLEAR REACTIONS

This report includes the progress of research in the study of determination of the reaction products in high energy collisions and of the atmospheric transport of particles such as protons, neutrons and other nucleons.

Dr. Joshi, research assistant professor, has submitted two articles on Magnetic Moments of Charmed Baryons for possible publication in Physical Review (see Attachments 1 and 2).

Mr. Chris Costner, graduate research assistant, and Mr. John W. Wilson, technical monitor of this project, have been successful in obtaining total cross sections which are required for cosmic heavy ion transport and shielding studies (see attachment 3).

Mr. John W. Wilson, technical monitor, and Dr. G. S. Khandelwal, principal investigator, have obtained close parameter values for Rad and Rem dose deposition functions in tissue for high energy protons (up to 10 GeV). Their results are given in the table on the following page.

Work is now in progress on various extensions, modifications, and refinements of the above mentioned results in collaboration with Mr. Wilson.

TABLE

Parameter Values for Rad and Rem Dose Deposition Functions

E, MeV	Rad			Rem		
	a_1	a_2	a_3	a_1	a_2	a_3
50*	1.069	---	1.60 (-1)	1.480	---	2.00 (-3)
100	1.119	---	9.96 (-2)	1.500	---	1.00 (-2)
200	1.190	---	4.38 (-2)	1.554	---	7.29 (-2)
300	1.220	---	3.14 (-2)	1.680	---	4.08 (-2)
400	1.240	---	2.28 (-2)	1.770	---	3.05 (-2)
730	1.400	5.0 -5	1.50 (-2)	3.210	1.7 -4	1.77 (-2)
1,000*	1.45	4.0 -4	1.28 -2	4.300	9.4 -4	1.50 -2
1,500	1.595	1.9 -3	1.13 -2	5.200	2.9 -3	1.20 -2
3,000	1.708	2.0 -3	6.14 -3	5.350	3.0 -3	6.44 -3
10,000	1.800	2.1 -3	2.30 -3	5.600	3.1 -3	2.39 -3

* Values obtained by extrapolation or interpolation

$$F(E,t) = (a_1 + a_4 t + a_2 t^2) \exp(-a_3 t)$$

$$a_4 = \frac{1}{r} \exp(a_3 r) - \frac{a_1}{r} - a_2 r$$

ATTACHMENT 1

MAGNETIC MOMENTS OF CHARMED BARYONS I

A. L. CHOUDHURY

Department of Mathematics
Elizabeth City State University
Elizabeth City, N.C. 27909

and

V. JOSHI §

Department of Physics
Old Dominion University
Norfolk, Va

§ Work partially supported by NASA, Langley, Va.

Abstract

The magnetic moments of all baryons belonging to the totally symmetric $\underline{20}$ - representation, the mixed symmetry $\underline{20}'$- representation and the totally antisymmetric $\underline{4}$ - representation have been compared under the U(4) and the SU(4) symmetry separately. For the $\underline{20}'$- representation the usual results of the SU(3) symmetry remains unchanged except the relation $\mu(\Lambda^0) = -\mu(\Sigma^0)$. This result is no more valid in U(4). In SU(4) , an interesting new relation results, which is $\mu(p) = -\mu(n)$. The magnetic moments of all charmed particles have been expressed in terms of the moments of proton , neutron and lambda-particles in the U(4) symmetry, whereas in SU(4) all moments can be expressed in terms of just the proton and the lambda particle magnetic moments.

I. Introduction

The recent discovery of the ψ-particles [1] has lead to the renewed interest of introducing a new quark c with charmed quantum number 1, in addition to the three quarks, a pair u and d, the isotopic soin doublet and s, an isotopic soin singlet with charm assignment zero. The ψ- particle is assumed to be the quark-antiquark, $c\bar{c}$ combination and a vector meson with associated quantum numbers, $J^{PG} = 1^{--}$. The introduction of c as an additional quark, with isotopic spin $I = 0$, and hypercharge $Y = -2/3$, has lead to the renewed interest in extending the SU(3) symmetry classification to SU(4), a theory in which four quarks have to play the fundamental role in the reproduction of the other particles that appear in nature.

The SU(4) - group [2] for the classification of the fundamental particles has been suggested earlier by Glashow, Iliopoulos and Maiani [3], to eliminate the strangness nonconserving neutral currents. In this model, a large number of new charmed particles show up, in addition to the usual noncharmed particles. In strong interaction, the charm quantum number is supposed to be stricly conserved. As soon as the discovery of the ψ- particle has been announced, a large number of explanations on the nature of the particle have been proposed [4]. Based on the SU(4) model Borchardt, Mathur and Okubo [5] proposed that ψ-particle is $c\bar{c}$ - state and suggested an extension of the Gell-Mann - Nishijima formula as follows :

$$Q = I_z + \frac{Y}{2} + C \qquad \ldots (1)$$

The quantum number C in (1) stands for the charm of the particles which is assumed to be zero for all particles known until now. In the quark model, for the u-, d- and s-quarks we assume $C = 0$ and the C value of the fourth quark to be one. The assignment of the other quantum numbers are to be done according to the fractional scheme of Glashow, Iliopoulos and Maiani [3]. We also assume here that all the baryons are obtained by the combination of qqq, where q is a quark.

A large number of experimental and theoretical works since then have been carried out. Assuming that the SU(4) classification would show up a promising future, we have decided to calculate the magnetic moments of the baryons in light

of the U(4) and SU(4) symmetry.

The calculation of the magnetic moments for the SU(3) baryon octets has been done by Glashow and Coleman [7]. Okubo [8] has also shown that the same results could be reproduced from a very general consideration of the transformation property property of the charge operator. Afterwards Okubo [9] has indicated how the higher order correction to the moments, assuming more complex magnetic moment operator, could be obtained. A more general formulation can also be found in the paper of Rosen [10], who gave a close form of the magnetic moment operator in terms of the U-spin and the charge of the particles.

All these calculations have been very much improved by extending the symmetry group to SU(6), with the inclusion of intrinsic spin of the particles. Beg, Lee and Pais [11] assumed that the baryon octets and the decouplets belong to the $\underline{56}$ - dimensional representation of SU(6) and the magnetic moment operator transforms like a $(\underline{8}, \underline{3})$ - member of the $\underline{35}$ - representation. Their results gave us the ratio $\mu(p) / \mu(n) = -3/2$. Thirring [12] also obtained the same results straightforwardly from the quark model by vectorially adding the magnetic moments of the quarks which constitute the particle concerned.

We in a sequence of two papers would like at first to extend the calculations of SU(3) to that of U(4) and SU(4). Then enlarging the group to U(8) or SU(8), we would like to find out the magnetic moments of the charmed particles. In this paper, we would restrict ourselves to the smaller groups U(4) and SU(4). In section II, we would discuss the U(4) classification and introduce the conventional nomenclatures. We also would write down the corresponding baryon states with the help of a tensor $B_{\mu\nu\rho}$ [13]. In section III, we would construct very general currents [14], which appears in a magnetic moment tensor. In section IV, we would obtain the magnetic moments, assuming the U(4) symmetry. In section V, we would indicate what modifications results when we go over to the SU(4) symmetry from the U(4). In section VI, we would discuss the general aspects of the results obtained.

II. U(4) Classification of Baryons

The baryons are to be obtained by the combination of three quarks qqq . In terms of the irreducible representation of U(4) , we know,

$$\underline{4} \otimes \underline{4} \otimes \underline{4} = \underline{20} + 2 \times \underline{20'} + \underline{4} \quad , \qquad \ldots (2)$$

where $\underline{20}$ is the dimension of the completely symmetric representation associated with the Young's tableaux $\square\square\square$, $\underline{20'}$ is the dimension of the representation of mixed symmetry $\begin{smallmatrix}\square\square\\\square\end{smallmatrix}$ and $\underline{4}$ is the dimension of the totally antisymmetric reoresentation associated with $\begin{smallmatrix}\square\\\square\\\square\end{smallmatrix}$.

On the other hand if we express $\underline{20}$ multiplet in terms of SU(3) $\otimes$ U_c indices , we find,

$$\underline{20} = (10, 0) + (6, 1) + (3, 2) + (1, 3) , \qquad \ldots (3)$$

where (m, n) indicates m-dimensional SU(3) multiplet with a charm quantum number n. Similarly for $\underline{20'}$, we get,

$$\underline{20'} = (8, 0) + (6, 1) + (\bar{3}, 1) + (3, 2) . \qquad \ldots (4)$$

In the equation (4) , $(\bar{3}, 1)$ represents the contragradient triplet states with charm quantum number 1 . The multiplet $\underline{4}$ is given by

$$\underline{4} = (\bar{3}, 1) + (1, 0) . \qquad \ldots (5)$$

The baryon wavefunction for the $\underline{20}$ - representation can be exoressed in terms of the U(4) indices by a totally symmetric tensor $B^{20}_{\mu\nu\rho}$ which is normalized to the

number of particles in the multiplet. The tensor $B^{20}_{\mu\nu\rho}$ can be expressed in terms of the SU(3) multiplets as follows:

$$B^{20}_{\mu\nu\rho} = \delta^i_\mu \delta^j_\nu \delta^k_\rho d_{ijk} + \frac{1}{\sqrt{3}} (\delta^i_\mu \delta^j_\nu \delta^4_\rho + \delta^4_\mu \delta^i_\nu \delta^j_\rho + \delta^i_\mu \delta^4_\nu \delta^j_\rho) S^*_{ij}$$

$$+ \frac{1}{\sqrt{3}} (\delta^i_\mu \delta^4_\nu \delta^4_\rho + \delta^4_\mu \delta^i_\nu \delta^4_\rho + \delta^4_\mu \delta^4_\nu \delta^i_\rho) T^{*(2)}_i$$

$$+ \delta^4_\mu \delta^4_\nu \delta^4_\rho S^{*(3)}_o \quad . \qquad ..(6)$$

In the above expression d_{ijk} represents the decouplets of SU(3) and the indices i, j and k only run from 1 through 3 , whereas μ , ν and ρ run from 1 through 4. $S^{*(1)}_{ij}$ represents the sextuplet charm one baryons and is totally symmetric in i and j. The states $T^{*(2)}_i$ are the SU(3) triplets, with charm quantum number 2. The state $S^{*(3)}_o$ is the (1,3) state of the equation (3) [15] .

Similarly we find for 20',

$$B^{20'}_{\mu\nu\rho} = \delta^i_\mu \delta^j_\nu \delta^k_\rho N_{\{ik\}j} + \frac{1}{\sqrt{2}} (\delta^i_\mu \delta^j_\nu \delta^4_\rho - \delta^i_\rho \delta^j_\nu \delta^4_\mu) S^{(1)}_{ij}$$

$$+ \frac{1}{\sqrt{6}} (2 \delta^i_\mu \delta^4_\nu \delta^j_\rho + \delta^4_\mu \delta^i_\nu \delta^j_\rho - \delta^j_\mu \delta^i_\nu \delta^4_\rho) T^{(1)}_{\{ij\}}$$

$$+ \frac{1}{\sqrt{2}} (\delta^i_\mu \delta^4_\nu \delta^4_\rho - \delta^i_\rho \delta^4_\mu \delta^4_\nu) T^{(2)}_i . \qquad ..(7)$$

In the above expression, whenever we have put two indices within the curly brackets

the terms are antisymmetric with respect to those indices. Here again the Greek indices run from 1 through 4 , whereas the Latin indices run from 1 through 3. The symbols $N_{\{ik\}j}$, $S^{(1)}_{ij}$, $T^{(1)}_{\{ij\}}$ and $T^{(2)}_{i}$ stand for a baryon octet , a sextuplet with charm 1, a contragradient triplet with charm 1 and a triplet with charm 2 respectively. The baryon octet can be expressed in terms of the wellknown symbol N^{i}_{j} by the formula

$$N_{\{ik\}j} = \frac{1}{\sqrt{2}} \epsilon_{ikl} N^{l}_{j} \qquad ..(7a)$$

Here ϵ_{ijk} is the Levi-Civita totally antisymmetric tensor in three dimension.

Finally for the baryon $\underline{4}$ - multiplet , we can write ,

$$B^{4}_{\{\mu\nu\rho\}} = \frac{1}{\sqrt{3}} (\delta^{i}_{\mu} \delta^{j}_{\nu} S^{4}_{\rho} + \delta^{4}_{\mu} \delta^{i}_{\nu} \delta^{j}_{\rho} - \delta^{i}_{\mu} \delta^{4}_{\nu} \delta^{j}_{\rho}) T^{(1)'}_{\{ij\}}$$

$$+ \frac{1}{\sqrt{6}} \delta^{i}_{\mu} \delta^{j}_{\nu} \delta^{k}_{\rho} \epsilon_{ijk} S^{o'} \qquad ..(8)$$

where $T^{(1)'}_{\{ij\}}$ stands for the charm one contragradient triplet and $S^{o'}$ is the singlet with charm zero.

Here we would exclusively follow the identification of the particles as introduced by Gaillard , Lee and Rosner [2] . Thus for the sextuplet belonging to the $\underline{20}$ - representation, we define

$$S^{*(1)}_{11} = C^{*++}_{1} \quad , \quad S^{*(1)}_{12} = \frac{C^{*+}_{1}}{\sqrt{2}} \quad , \quad S^{*(1)}_{22} = C^{*o}_{1} \quad ,$$

$$S^{*(1)}_{13} = \frac{S^{*+}}{\sqrt{2}} \quad , \quad S^{*(1)}_{23} = \frac{S^{*o}}{\sqrt{2}} \quad , \qquad ..(9a)$$

and $$S^{*(1)}_{33} = T^{*o}$$

For the triplet members, (3, 2) , of the 20 - representation, we identify the particles as

$$T_1^{*(2)} = X_u^{*++} \quad , \quad T_2^{*(2)} = X_d^{*+} \quad , \text{ and } \quad T_3^{*(2)} = X_s^{*+} \qquad ..(9b)$$

The new baryons belonging to 20'- representation, the members of the sextuplet $S_{ij}^{(1)}$ ((6,1)) are given by the equations (9a) just by dropping the asterisks. Similarly the multiplets (3,2) of the 20'- representation is given by the equations (9b), where we have also to drop the asterisks. For the multiplet $(\bar{3}, 1)$, we write

$$T_{\{12\}}^{(1)} = \frac{1}{\sqrt{2}} C_o^+ \quad , \quad T_{\{23\}}^{(1)} = \frac{1}{\sqrt{2}} A^o \quad , \quad T_{\{31\}}^{(1)} = \frac{1}{\sqrt{2}} A^+ \qquad ..(9c)$$

For $(\bar{3}, 1)$ belonging to 4 , we go over to the particles by adding a prime (') to the relations in the equation (9c).

III Most General Currents

In calculating magnetic moment coming from the first order electromagnetic interaction , we need to constuct the most general current tensors $J^{\mu}_{\ \kappa}$ [14] with the help of the multiplet wavefunctions B given by the equations (6) , (7) and (8). For 20 - representation , the most general current that we can form is

$$J(D) = \mu_o \bar{B}^{\mu\nu\rho}_{20} B^{20}_{\kappa\nu\rho} + g_o \delta^{\mu}_{\kappa} \langle \bar{B} B \rangle_{20} \qquad ..(10)$$

where μ_o and g_o are two arbitrary constants and $\langle \bar{B} B \rangle_{20}$ stands for the trace of the tensor defined as follows:

$$\langle \bar{B} B \rangle_{20} = \bar{B}^{\mu\nu\rho}_{20} B^{20}_{\mu\nu\rho} \qquad ..(10a)$$

So far we have only considered the representation to be in U(4) . If we want to restrict the particle wavefunctions to be in SU(4) , the trace of $J(D)^{\mu}_{\ \kappa}$ must vanish, yielding the condition,

$$\mu_o + 4 g_o = 0 \qquad ..(11)$$

The most general current $J(N)^{\mu}_{\kappa}$ that can be constructed with the tensors $\bar{B}$ and B belonging 20'- representation is given by

$$J(N)^{\mu}_{\ \kappa} = D^{\mu}_{\ \kappa} + \delta^{\mu}_{\kappa} G^{\alpha}_{\ \alpha} \qquad ..(12)$$

where

$$D^{\mu}{}_{\kappa} = a_1 \bar{B}^{\{\mu\rho\}\nu}_{20'} B^{20'}_{\{\kappa\rho\}\nu} + a_2 \bar{B}^{\{\rho\nu\}\mu}_{20'} B^{20'}_{\{\kappa\rho\}\nu} + a_3 \bar{B}^{\{\nu\mu\}\rho}_{20'} B^{20'}_{\{\kappa\rho\}\nu}$$

$$+ b_1 \bar{B}^{\{\mu\rho\}\nu}_{20'} B^{20'}_{\{\rho\nu\}\kappa} + b_2 \bar{B}^{\{\rho\nu\}\mu}_{20'} B^{20'}_{\{\rho\nu\}\kappa} + b_3 \bar{B}^{\{\nu\mu\}\rho}_{20'} B^{20'}_{\{\kappa\rho\}\nu} \quad ..(13)$$

$$+ c_1 \bar{B}^{\{\mu\rho\}\nu}_{20'} B^{20'}_{\{\nu\kappa\}\rho} + c_2 \bar{B}^{\{\rho\nu\}\mu}_{20'} B^{20'}_{\{\nu\kappa\}\rho} + c_3 \bar{B}^{\{\nu\mu\}\rho}_{20'} B^{20'}_{\{\nu\kappa\}\rho}$$

and G^{α}_{α} is an expression obtained from $D^{\mu}{}_{\kappa}$ by setting $\mu = \kappa = \alpha$ and replacing the constants a_i , b_i and c_i-s by new constants a'_i , b'_i and c'_i-s.

By using the following symmetry relations :

$$B^{20'}_{\{\mu\nu\}\rho} + B^{20'}_{\{\nu\rho\}\mu} + B^{20'}_{\{\rho\mu\}\nu} = 0 \quad ..(14)$$

$$B^{20'}_{\{\mu\nu\}\rho} = - B^{20'}_{\{\nu\mu\}\rho} \quad ..(15)$$

$$\bar{B}^{\{\rho\nu\}\mu}_{20'} B^{20'}_{\{\rho\nu\}\kappa} = - 2 \bar{B}^{\{\rho\nu\}\mu}_{20'} B^{20'}_{\{\kappa\rho\}\nu} \quad ..(16)$$

$$\bar{B}^{\{\mu\rho\}\nu}_{20'} B^{20'}_{\{\rho\nu\}\kappa} = \bar{B}^{\{\rho\nu\}\mu}_{20'} B^{20'}_{\{\kappa\rho\}\nu} \quad ..(17)$$

we can simplify the equation (12) into a very convenient form. We should notice that equation (15) and (16) are the outcome of the equations (13) and (14) . We finally get

$$J(N)^{\mu}{}_{\kappa} = \mu_x \bar{B}^{\{\mu\rho\}\nu}_{20'} B^{20'}_{\{\kappa\rho\}\nu} + \mu_y \bar{B}^{\{\rho\nu\}\mu}_{20'} B^{20'}_{\{\kappa\rho\}\nu} + g_x \delta^{\mu}_{\kappa} \bar{B}^{\{\alpha\rho\}\nu}_{20'} B^{20'}_{\{\alpha\rho\}\nu}$$

$$+ g_y \delta^{\mu}_{\kappa} \bar{B}^{\{\rho\nu\}\alpha}_{20'} B^{20'}_{\{\alpha\rho\}\nu} \quad ..(18)$$

If we require that instead of U(4) , the symmetry should be SU(4) , then the current $J(N)^{\mu}_{\kappa}$ should be traceless. Hence the tracelessness condition subjects the constants to the restriction

$$\mu_x - \frac{1}{2}\mu_y = -4 g_o \qquad \ldots(19)$$

where

$$g_o = g_x - \frac{1}{2} g_y \qquad \ldots(20)$$

Similarly for the representation $\underline{4}$, which is totally antisymmetric, the current tensor

$$J(A)^{\mu}_{\kappa} = \mu_1 \bar{B}_4^{\{\mu\nu\rho\}} B^4_{\{\kappa\nu\rho\}} + g_1 \delta^{\mu}_{\kappa} \langle \bar{B} B \rangle_4 \qquad \ldots(21)$$

where again μ_1 and g_1 are two arbitrary constants and

$$\langle \bar{B} B \rangle_4 = \bar{B}_4^{\{\mu\nu\rho\}} B^4_{\{\mu\nu\rho\}} \qquad \ldots(22)$$

The SU(4) limit leads us to a constraint in the constants μ_1 and g_1 as expressed by the following equation

$$\mu_1 + 4 g_1 = 0 \qquad \ldots(23)$$

In the next section we would use the currents in the equation (10), (18) and (21) to obtain the magnetic moments.

IV Magnetic Moments in U(4)

As shown by Glashow and Coleman [3] that the magnetic moment for baryons can be obtained by forming the trace of $\bar{B}BQ$ in all possible contraction, where Q is the charge operator, a 4 x 4 matrix and can be written as

$$Q^{\kappa}_{\mu} = q_{\mu}\,\delta^{\kappa}_{\mu} \qquad \ldots(21)$$

where $q_1 = q_4 = 2/3$ and $q_2 = q_3 = -1/3$, are the charges of the quarks. We follow Okubo et al's [5] prescription of the charge operator as given by the equation (1).

We assume that for a low momentum case the expectation value of the magnetic moment operator is proportional to

$$J(X)^{\mu}_{\kappa}\, Q^{\kappa}_{\mu} \qquad \ldots(22)$$

where X stands for either D, N or A. We have altogether suppressed the spin part of the magnetic moment as a first approximation.

A. 20- representation.

For (10,0) members of the 20-representation, we find using equations (6), (10) and (25) that

$$\mu(N^{*++}) = \frac{2}{3}\mu_o + \frac{2}{3}g_o \quad , \quad \mu(N^{*+}) = \frac{1}{3}\mu_o + \frac{2}{3}g_o$$

$$\mu(N^{*o}) = \frac{2}{3}g_o \quad , \quad \mu(N^{*-}) = -\frac{1}{3}\mu_o + \frac{2}{3}g_o \qquad \ldots (26)$$

and

$$\mu(Y^{*+}) = \mu(N^{*+})$$

$$\mu(Y^{*0}) = \mu(\Xi^{*0}) = \mu(N^{*0}) \qquad ..(27)$$

$$\mu(Y^{*-}) = \mu(\Xi^{*-}) = \mu(\Omega^{-}) = \mu(N^{*-})$$

For sextuplet (6,1)

$$\mu(C_1^{*++}) = \mu(N^{*++}) \quad , \quad \mu(C_1^{*+}) = \mu(S^{*+}) = \mu(N^{*+})$$

$$\mu(C_1^{*0}) = \mu(S^{*0}) = \mu(T^{*0}) = \mu(N^{*0}) \qquad ..(28)$$

Similarly for the triplet (3, 2)

$$\mu(X_u^{*++}) = \mu(N^{*++}), \quad \mu(X_d^{*+}) = \mu(X_s^{*+}) = \mu(N^{*+}) \qquad ..(29)$$

For the singlet (1,3) (identifying $S^{*}(3) = R^{*++}$) , we find

$$\mu(R^{*++}) = \mu(N^{*++}) \qquad ..(30)$$

B. 20'- representation

If we now go to 20'- representation and use the equations (7), (18) and (25), the magnetic moments of the baryon octet (8, 0) come out to be

$$\mu(p) = \mu(\Sigma^{+}) = \frac{1}{6}\mu_x - \frac{1}{3}\mu_y + \frac{2}{3}g_o \qquad ..(31a)$$

$$\mu(n) = \mu(\Xi^0) = \frac{1}{6}\mu_x + \frac{1}{6}\mu_y + \frac{2}{3}g_0 \qquad \ldots(31b)$$

$$\mu(\Xi^-) = \mu(\Sigma^-) = -\frac{1}{3}\mu_x + \frac{1}{6}\mu_y + \frac{2}{3}g_0 \qquad \ldots(31c)$$

$$\mu(\Sigma^0) = -\frac{1}{12}\mu_x - \frac{1}{12}\mu_y + \frac{2}{3}g_0 \qquad \ldots(31d)$$

$$\mu(\Lambda^0) = \frac{1}{12}\mu_x + \frac{1}{12}\mu_y + \frac{2}{3}g_0 \qquad \ldots(31d')$$

The transition moments are given by

$$\langle \Sigma^0 | \mu | \Lambda^0 \rangle = \langle \Lambda^0 | \mu | \Sigma^0 \rangle = -\frac{1}{4\sqrt{3}}\mu_x - \frac{1}{4\sqrt{3}}\mu_y \qquad \ldots(31e)$$

If we compare these results with U(3) results as quoted by Okubo [8], we find the unchanged relations are

$$\mu(p) = \mu(\Sigma^+) \quad , \quad \mu(\Xi^0) = \mu(n) \quad , \quad \mu(\Xi^-) = \mu(\Sigma^-) \qquad \ldots(31$$

$$\mu(p) + \mu(\Sigma^-) + 4\mu(n) = 6\mu(\Lambda^0) \qquad \ldots(31$$

and

$$\mu(\Sigma^+) + \mu(\Sigma^-) = 2\mu(\Sigma^0) \qquad \ldots(31$$

However we should notice that

$$\mu(\Sigma^0) \neq -\mu(\Lambda^0) \qquad \ldots(31$$

in U(4) in contrast to the result $\mu(\Sigma^0) = \mu(\Lambda^0)$ in U(3).

For the charmed sextuplet (6, 1)

$$\mu(C_1^{++}) = \frac{2}{3}\mu_x - \frac{1}{3}\mu_y + \frac{2}{3}g_o \qquad \ldots(32a)$$

$$\mu(C_1^{+}) = \mu(S^{+}) = \frac{5}{12}\mu_x - \frac{1}{12}\mu_y + \frac{2}{3}g_o \qquad \ldots(32b)$$

and

$$\mu(C_1^{o}) = \mu(S^{o}) = \mu(T^{o}) = \mu(n) \qquad \ldots(32c)$$

In terms of $\mu(p)$, $\mu(n)$ and $\mu(\Lambda^{o})$, we can write

$$\mu(C_1^{++}) = 2\mu(p) + 5\mu(n) - 6\mu(\Lambda^{o}) \qquad \ldots(32d)$$

and

$$\mu(C_1^{+}) = \mu(p) + 3\mu(n) - 3\mu(\Lambda^{o}) \qquad \ldots(32e)$$

For the charmed baryon triplet (3, 2) , we find

$$\mu(X_u^{++}) = \mu(C_1^{++}) \qquad \ldots(33a)$$

$$\mu(X_d^{+}) = \mu(X_1^{+}) = \mu(p) \qquad \ldots(33b)$$

If we now go over to the contragradient baryon triplet ($\bar{3}$, 1), we find

$$\mu(C_o^{+}) = \mu(A^{+}) = \frac{1}{4}\mu_x - \frac{1}{4}\mu_y + \frac{2}{3}g_o \qquad \ldots(34a)$$

$$\mu(A^{o}) = -\frac{1}{6}\mu_x - \frac{1}{6}\mu_y + \frac{2}{3}g_o \qquad \ldots(34b)$$

Expressing (34a) and (34b) in terms of proton, neutron and lambda particle magnetic moments, we find

$$\mu(C_o^+) = \mu(p) + \mu(n) - \mu(\Delta^o) \qquad \ldots(34c)$$

and

$$\mu(A^o) = -3\mu(n) + 4\mu(\Delta^o) \qquad \ldots(34d)$$

Due to the degeneracy of quantum numbers of some baryon sextuplet particles with the contragradient triplets, we find that transition magnetic moments appear between sextuplet and triplet particles. The results come out to be the followings:

$$-\langle C_1^+ | \mu | C_o^+ \rangle = -\langle C_o^+ | \mu | C_1^+ \rangle = \langle S^+ | \mu | A^+ \rangle$$
$$= \langle A^+ | \mu | S^+ \rangle = \langle \Sigma^o | \mu | \Delta^o \rangle \qquad \ldots(35)$$

C. $\underline{4}$ - representation

For the particles belonging to the totally antisymmetric representation $\underline{4}$, the magnetic moments for the contragradient triplets can be found out using equations (8), (21), and (25). We get for the contragradient charmed triplets

$$\mu(A'^o) = \frac{2}{3} g_1 \qquad \ldots(36a)$$

and

$$\mu(A'^+) = \mu(C_o'^+) = \frac{1}{3}\mu_1 + \frac{2}{3} g_1 \qquad \ldots(36b)$$

For the singlet (1,0) we get

$$\mu(S'^o) = \mu(A'^o) \qquad \ldots(37)$$

V SU(4) Magnetic Moments

The SU(4) constraints (11), (19) and (23) introduce some modifications in the results of U(4) magnetic moments quoted in the section IV.

A. 20 - representation

Here we find for (10, 0) member

$$\mu(N^{*++}) = 3\,\mu(N^{*+}) = -3\,\mu(N^{*0}) = -\mu(N^{*-}) = \frac{1}{2}\,\mu_0 \qquad ..(38a)$$

$$3\,\mu(Y^{*+}) = -3\,\mu(Y^{*0}) = -\mu(Y^{*-}) = \frac{1}{2}\,\mu_0 \qquad ..(38b)$$

$$-3\,\mu(\Xi^{*0}) = -\mu(\Xi^{*-}) = \frac{1}{2}\,\mu_0 \qquad ..(38c)$$

and

$$-\mu(\Omega^{-}) = \frac{1}{2}\,\mu_0 \qquad ..(38d)$$

Strictly speaking, the new relations which are absolutely due to the tracelessness are quoted in the equations (38a) through (38d). The other equalities like $\mu(N^{*+}) = \mu(Y^{*+})$, $\mu(N^{*0}) = \mu(Y^{*0}) = \mu(\Xi^{*0})$ and $\mu(N^{*-}) = \mu(Y^{*-}) = \mu(\Xi^{*-}) = \mu(\Omega^{-})$, follow also from U(4) consideration.

For the sextuplet (6,1), the relations given in the equation (28) remain unchanged. However due to the equation (38a), we get a new relationship

$$\mu(C_1^{*++}) = 3\,\mu(C_1^{*+}) = -3\,\mu(C_1^{*0}) = \frac{1}{2}\,\mu_0 \qquad ..(39)$$

For the triplet (3,2) , the equations (29) remains also unchanged, however due to (38a) , we get

$$\mu(X_u^{*++}) = 3\,\mu(X_d^{*+}) = \frac{1}{2}\,\mu_o \qquad ..(40)$$

For the singlet (1,3) , naturally the equation (30) stays unchanged.

B. 20' - representation

The restriction , relation (19) , now does not change the equations (31f) through (31h). We get however an altogether new relationship between the magnetic moments of the proton and the neutron as follows:

$$\mu(p) = -\mu(n) = -\frac{1}{4}\,\mu_y \qquad ..(41)$$

This result is quite an improvemnt over the SU(3) result, where they are completely unrelated.

For the sextuplet, we get

$$\mu(C_1^{++}) = \frac{1}{2}\mu_x - \frac{1}{4}\mu_y \qquad ..(42a)$$

$$\mu(C_1^{+}) = \frac{1}{4}\,\mu_x \qquad ..(42b)$$

whereas (32c) stays completely unaltered. The equations(32d) and (32e) due to the equation (41) reduces to

$$\mu(C_1^{++}) = 3\,\mu(n) - 6\,\mu(\Lambda^o) \qquad ..(43a)$$

and

$$\mu(C_1^+) = 2\mu(n) - 3\mu(\Delta^0) \qquad ..(43b)$$

The triplet (3,2) magnetic moments given by the equations (33a) and (33b) do not change at all.

The contragradient triplet $(\bar{3},1)$ magnetic moment relation (34c) changes into

$$\mu(C_o^+) = \mu(A^+) = -\mu(\Delta^0) = \frac{1}{12}\mu_x - \frac{1}{6}\mu_y \qquad ..(44)$$

whereas the relation (34d) remains unchanged.

Finally, the transition moment relation (35) between the sextuplet- and the contragradient triplet- particles stays unchanged.

C. 4 - representation

Due to the relation (23), the equations (36a), (36b) and (35) modify into

$$-\mu(A'^0) = \mu(A'^+) = \mu(C_o'^+) = -\mu(S'^0) = \frac{1}{6}\mu_1 \qquad ..(45)$$

VI Concluding Remarks

We have calculated the magnetic moments in the low frequency limit in U(3) and SU(4), assuming that the magnetic moment operator is proportional to the charge operator. The expectation value of the magnetic moment could thus be written as in the equation (25). This equation finally has produced the results quoted in the sections IV and V. Almost all results of U(3) have been reproduced in U(4). The only different result U(4) yields is

$$\mu(\Sigma^0) \neq -\mu(\Lambda^0)$$

If we now go over to SU(4) magnetic moments, we obtain a very interesting result, namely, $\mu(p) = -\mu(n)$. We have also derived the magnetic moments of all new charmed baryons in terms of the magnetic moments of the proton, the neutron and Λ^0- particle in the $\underline{20}'$- representation and in terms of the magnetic moments of the N^*-s in the $\underline{20}$ - representation, for both U(4) and SU(4) symmetries.

In a separate paper we would show, how the results of SU(4) can be extended for the case U(8) or SU(8).

Acknowledgement

The authors like to express their sincerest thanks to Professor L. C. Biedenharn Jr. of Duke University , Durham , N.C. for encouragement and some fruitful suggestions. The first author (A.L.C.) also expresses his gratitude to the Department of Physics , University of North Carolina at Chapel Hill for allowing him to use the facilities of the department during the summer months. He is particularly grateful to Professors J.W. Straley, E. Merzbacher and H. van Dam for helpful cooperation.

Reference:

1. J.J.Aubert et al : Phys. Rev. Lett.,33 , 1404 (1974).

J.E.Augustine et al : ibid , 33, 1406 (1974)

C. Bacci et al : ibid , 33 , 1408 (1974).

2. For SU(4) review see M.K. Gaillard , B.W. Lee and J.L.Rosner: Rev.Mod.Phys. ,47 , 227(1975).

3. S. L. Glashow , J. Iliopoulos and L. Maiani : Phys.Rev. , D2 , 1285 (1970).

4. S. Borchardt, V.S. Mathur, and S. Okubo : Phys. Rev. Lett., 34 ,38(1975).

A. S. Goldhaber and M. Goldhaber : ibid, 34, 36 (1975).

J. Schwinger : ibid, 34, 37 (1975).

R. Michael Barnett : ibid, 34, 41 (1975).

T. Applequist and H.D. Politzer : ibid, 34, 43 (1975).

A. De Rújula and S.L. Glashow : ibid , 34 , 46 (1975).

H.T.Nieh, T.T.Wu and C.N.Yang : ibid, 34 , 49(1975).

C. G. Callan et al : ibid , 34 , 52 (1975).

J.J. Sakurai : ibid , 34, 56 (1975).

5. S. Okubo, V. S. Mathur and S. Borchardt : Phys. Rev. Lett. , 34 , 236 (1975).

6. Other possible choices of quantum number assignments can be found in ref. 6. For other possible combination of the quarks to construct a baryon see : D. Amati, H. Bacry , J. Nuyts, and J. Prentki : Phys.Lett., 11 , 190 (1964) ; Nouvo Cimento, 34 , 1732 (1964). See also J.W. Moffat : SU(4) and SU(8) Mass Splitting etc., Univ. of Toronto Preprint (1975) and V.Rabl,G.Cambell and K.C.Wali: Syracuse Univ. Preprint SU 4206 -50 (1975)

7. S. Coleman and S. L. Glashow : Phys. Rev. Lett . , 6 , 423 (1961).

8. S. Okubo : Prog. Theoret. Phys.,27 , 949 (1962).

9. S. Okubo : Phys. Lett., 4 , 14 (1963).

10. S. P. Rosen : Phys. Rev. Lett., 11 , 100 (1963).

11. M. A. B. Bég , B.W. Lee and A. Pais : Phys. Rev. Lett., 13 , 514 (1964).

12. W. Thirring : Acta Physica Austriaca , Suppl. II, 205 (1965).

13. See also S. Okubo : SU(4) and SU(8) Mass Formula etc. Technical Report UR-524, Univ. of Rochester (1975).

14. B. Sakita : Phys. Rev. , 136 , B1756 (1964).

A. Salam, R. Delbourgo and J. Strathdee : Proc. Roy. Soc. , A284, 146 (1965).

15. Actually we should indicate here that there is a certain amount of arbitrariness in choosing the constants in front of each states. If we write (with real α, β , γ , δ)

$$B^{20}_{\mu\nu\rho} = \alpha B^{10}_{\mu\nu\rho} + \beta B^{6}_{\mu\nu\rho} + \gamma B^{3}_{\mu\nu\rho} + \delta B^{1}_{\mu\nu\rho}$$

and normalize B^{10} to 10 , B^{6} to 6 etc., then we get

$$20 = \alpha^2 10 + \beta^2 6 + \gamma^2 3 + \delta^2$$

We have made the choice $\alpha = \beta = \gamma = \delta = 1$.

ATTACHMENT 2

MAGNETIC MOMENTS OF CHARMED BARYONS II

A. L. CHOUDHURY

Department of Mathematics
Elizabeth City State University
Elizabeth City, N.C.27909

and

V. JOSHI §

Department of Physics
Old Dominion University
Norfolk, Va.

§ Work partially supported by NASA, Langley, Va.

Abstract

Assuming that the magnetic moment operator is a tensor transforming as the $(\underline{15}, 3)$ - member of the U(8) or the SU(8) representation, we have compared the magnetic moments of all the baryons belonging to the $\underline{120}$ - representation. The moments of the conventional particles like the SU(3) decouplets or octets stay unchanged. The charmed baryon moments are expressed in terms of the magnetic moment of the proton.

I Introduction

In a recent paper [1] the authors calculated the magnetic moments of the charmed baryons assuming that the magnetic moment operator transforms as the charge operator in the U(4) and the SU(4) symmetry. We have suppressed there the intrinsic spin of the particles as a first step. However, more realistic approach would be to incorporate the intrinsic spin of the particles.

It is wellknown that similar extensions have been achieved earlier, when Gürsey and Radicati and independently Sakita [2] first proposed to extend SU(3), the internal symmetry group, into SU(6) to give every particle in this classification a definite spin. It has been found out by Pais [4] that SU(6) gives the correct D/F ratio for the baryon current. Taking this group as the basis of the baryon classification Bég, Lee and Pais [3] calculated the magnetic moments of the basic baryons belonging to the 56 - representation. They conjectured there that the magnetic moment operator transforms as (8,3) member of the 35- representation and obtained in the effective low frequency limit the electromagnetic moments of all the particles in terms of the magnetic moment of the proton.

With the discovery of ψ - particles [5], many physicists are hoping that more charmed particles are about to emerge. The enlarged group SU(4) [6], with a fourth quark c , it is hoped , should enable us to explain many previously unanswered questions, and all the recent particles showering in as the new discoveries.

There are already suggestions [7] put forward to extend the SU(4) symmetry to SU(8), to incorporate the intrinsic spin of the particles. This group has been used to deduce the spin dependent mass equations to predict the masses of the charmed baryons.

In our work , we have assumed that the classification is given by U(8)-representation. As an extension of the work of Bég , Lee and Pais [3], we have assumed that the magnetic moment operator transforms as the (15, 3) member of the 63 - representation (Young's tableaux specification (2111111)) . The magnetic moments are finally expressed in terms of the magnetic moment of the proton.

In section II, we have constructed a tensor B_{ABC} which should represent the group of particles given by 20 - representation of U(4) with spin 3/2 and the 20'- representation with spin 1/2. In section II , we have constructed the most general currents . We have evaluated the magnetic moments in section IV. In section V we have discussed our results.

II. U(8) or SU(8) Classifications of the Baryons

The enlargement from U(4) to U(8) group permits us to place both $\underline{20}$ and $\underline{20'}$ representations of U(4) into the same irreducible representation $\underline{120}$ of U(8). The representation $\underline{120}$ is totally symmetric in terms of the tensor indices and can be designated by the Young's tableaux $\square\square\square$. If we now express $\underline{120}$ in terms of the U(4) $\otimes$ SU(2) indices , where SU(2) should be the group of the intrinsic spin of the particles , we find

$$\underline{120} = (\underline{20}, 4) + (\underline{20'}, 2) \qquad \ldots(1)$$

The symbol $(\underline{m}, n)$ now stands for a $\underline{m}$ - dimensional multiplet under U(4) or SU(4) classification and simultaneously the multiplet is also n-dimensional SU(2) representation. Thus the $\underline{120}$ - multiplet stands for $\underline{20}$ - U(4) totally symmetric spin 3/2 and $\underline{20'}$ spin 1/2 with U(4) mixed symmetry particles.

We are aware of the fact that the totally symmetric representation as that of equation (1) has the intrinsic problem of statistics . To improve the situation we have to introduce different colored quarks as suggested by Gell-Mann [8]. However we would not bother ourselves with such questions. This may be considered in future extension of the calculation where one includes also the colored quarks.

The totally symmetric tensor which represents the $\underline{120}$ - multiplet is given by B_{ABC} , where A, B and C stand for the pairs (μ, a) , (ν, b) and (ρ, c) respectively. The Greek indices stand for the U(4) labeling , all of which run from 1 through 4 , whereas a, b , c etc are used to express the SU(2)

labeling which run from 1 to 2. We would use for U(3) or SU(3) the labeling i , j, k etc. , which run from 1 through 3. The baryon multiplets are now given by

$$B_{ABC} = B_{\mu\nu\rho\,;\,abc}$$

$$= B^{20}_{\mu\nu\rho}\,\chi_{abc} + \frac{1}{3}\left(\epsilon_{ab}\chi_c\, B^{20'}_{\{\mu\nu\}\rho} + \epsilon_{bc}\chi_d\, B^{20'}_{\{\nu\rho\}\mu}\right.$$

$$\left. + \epsilon_{ca}\chi_b\, B^{20'}_{\{\rho\mu\}\nu}\right). \qquad ..(2)$$

In the equation (2) we have put for 20 - representation,

$$B^{20}_{\mu\nu\rho} = \delta^i_\mu\,\delta^j_\nu\,\delta^k_\rho\, d_{ijk} + \frac{1}{\sqrt{3}}\left(\delta^i_\mu\,\delta^j_\nu\,\delta^4_\rho + \delta^4_\mu\delta^i_\nu\,\delta^j_\rho + \delta^i_\mu\,\delta^4_\nu\,\delta^j_\rho\right) S^*_{ij}$$

$$+ \frac{1}{\sqrt{3}}\left(\delta^i_\mu\,\delta^4_\nu\,\delta^4_\rho + \delta^4_\mu\,\delta^i_\nu\,\delta^4_\rho + \delta^4_\mu\,\delta^4_\nu\,\delta^i_\rho\right) T^{*(2)}_i$$

$$+ \delta^4_\mu\,\delta^4_\nu\,\delta^4_\rho\, S^{*(3)}_o \,. \qquad ..(3)$$

The detailed explanation of the symbols in equation (3) can be found in part one of the present work [1]. The quantity $B^{20'}_{\mu\nu\rho}$ is the baryon mixed tensor and is given by

$$B^{20'}_{\{\mu\rho\}\nu} = \delta^i_\mu\,\delta^j_\nu\,\delta^k_\rho\, N_{\{ik\}j} + \frac{1}{\sqrt{2}}\left(\delta^i_\mu\,\delta^j_\nu\,\delta^4_\rho - \delta^i_\rho\,\delta^j_\nu\,\delta^4_\mu\right) S^{(1)}_{ij}$$

$$+ \frac{1}{\sqrt{6}}\left(2\,\delta^i_\mu\,\delta^4_\nu\,\delta^j_\rho + \delta^4_\mu\,\delta^i_\nu\,\delta^j_\rho - \delta^j_\mu\,\delta^i_\nu\,\delta^4_\rho\right) T^{(1)}_{\{ij\}}$$

$$+\frac{1}{\sqrt{2}}\left(\delta^{i}_{\mu}\,\delta^{4}_{\nu}\,\delta^{4}_{\rho} - \delta^{i}_{\rho}\,\delta^{4}_{\mu}\,\delta^{4}_{\nu}\right) T^{(2)}_{i} \qquad ..(4)$$

Again for the detailed explanation of the symbols see the earlier paper CJ I [1]. In the equation (2) the states χ_{abc} stands for totally symmetric SU(2) tensor representing 3/2 - spin states normalized to 4 , the dimension of the representation (see also Beg et al [3]) . We can write

$$\chi_{111} = u_{3/2} \quad , \quad \chi_{112} = \frac{1}{\sqrt{3}} u_{1/2} \quad , \quad \chi_{122} = \frac{1}{\sqrt{3}} u_{-1/2}$$

$$\text{and} \qquad \chi_{222} = u_{-3/2} \qquad ..(5)$$

where u_i-s are the i-th spin states. The symbol χ_i stands for spin half states and is also normalized to the value 2 , the total number of the states . We set

$$\chi_1 = v_{1/2} \qquad \text{and} \qquad \chi_2 = v_{-1/2} \qquad ..(6)$$

Again v_i-s are the i-th spin states. In equation (4) ϵ_{ab} is the Levi-Civita symbol in two dimension.

The SU(8) classification is exactly similar and keeps everything discussed uptil now unchanged. We have just to remember that in contrast to U(8), the mixed tensors T^{ν}_{μ} has to be traceless in SU(8).

III Current Tensor

We can now construct the most general mixed tensor, which we would call the current tensor by contracting just a pair of B and $\bar{B}$. We find due to the symmetry of the indices of B , it is given by

$$J^{A'}_{A} = \mu_o \, \bar{B}^{A'BC} B_{ABC} + g_o \, \delta^{A'}_{A} \bar{B}^{DBC} B_{DBC} \qquad \ldots(7)$$

where $$\delta^{A'}_{A} = \delta^{\mu}_{\kappa} \, \delta^{a}_{d} \, . \qquad \ldots(7a)$$

Substituting the expression of the tensor B from equation (2) into the equation (7), we obtain

$$J^{A'}_{A} = J^{A'}_{A}(\bar{20}, 20) + J^{A'}_{A}(\bar{20}, 20') + J^{A'}_{A}(\bar{20}', 20) + J^{A'}_{A}(\bar{20}', 20') \quad \ldots(\varepsilon$$

where $J^{A'}_{A}(\bar{m}, n)$ means terms in which $\bar{B}^{m} B_{n}$ appears with m and n being the dimensionality of the of the U(4) - representation. The first term comes straightforwardly as

$$J^{A'}_{A}(\bar{20}, 20) = \frac{1}{2} \, \delta^{a}_{d} \langle \bar{\chi} \chi \rangle_{3/2} \left[\mu_o \, \bar{B}^{\mu\nu\rho}_{20} \, B^{20}_{\kappa\nu\rho} + 2 \, g_o \, \delta^{\mu}_{\kappa} \langle \bar{B} \, B \rangle_{20} \right]$$

$$+ \frac{1}{2} \, \vec{\sigma}^{\,a}_{\,d} \cdot \langle \bar{\chi} \vec{\sigma} \chi \rangle_{3/2} \; \mu_o \, \bar{B}^{\mu\nu\rho}_{20} \; B^{20}_{\kappa\nu\rho} \qquad \ldots(9)$$

To obtain the final form of the equation (9) , we have used the abbreviations

$$\left\langle \bar{\chi}\chi \right\rangle_{3/2} = \bar{\chi}^{abc}\,\chi_{abc} \qquad \ldots(10)$$

$$\left\langle \bar{B}\,B \right\rangle_{20} = \bar{B}^{\alpha\nu\rho}_{20}\; B^{20}_{\alpha\nu\rho} \qquad \ldots(11)$$

and

$$\left\langle \bar{\chi}\vec{\sigma}\chi \right\rangle_{3/2} = \bar{\chi}^{abc}\,\vec{\sigma}^{\,d}_{\ a}\,\chi_{dbc} \qquad \ldots(12)$$

They have been introduced by using the following identity:

$$\vec{\sigma}^{\,a}_{\ b}\cdot\vec{\sigma}^{\,c}_{\ d} = 2\,\delta^{a}_{\ d}\,\delta^{c}_{\ b} - \delta^{a}_{\ b}\,\delta^{c}_{\ d} \qquad \ldots(13)$$

In actuality we have expressed $J^{A'}_{\ A}(\bar{20},\ 20)$ in terms of two terms, the first part being $(\underline{15}+1,\ 1)$ member of the $\underline{63}$ - representation and the second being $(15,3)$-member of the same.

Using the symmetry relation mentioned in the paper CJ-I(the equations (14) through (17) there), we find,

$$J^{A'}_{\ A}(\bar{20}',\ 20') = \tfrac{1}{3}\,\delta^{\,a}_{\ d}\left\langle \bar{\chi}\chi \right\rangle_{1/2}\Big[\mu_o\left\{\bar{B}^{\{\mu\rho\}\nu}_{20'}\;B^{20'}_{\{\kappa\rho\}\nu} - \bar{B}^{\{\rho\nu\}\mu}_{20'}\;B^{20'}_{\{\kappa\rho\}\nu}\right\}$$

$$+\,2\,g_o\delta^{\mu}_{\kappa}\left\{\bar{B}^{\{\alpha\rho\}\nu}_{20'}\;B^{20'}_{\{\alpha\rho\}\nu} - \bar{B}^{\{\rho\nu\}\alpha}_{20'}\;B^{20'}_{\{\alpha\rho\}\nu}\right\}\Big] \qquad \ldots(14)$$

$$-\frac{\mu_o}{9}\,\vec{\sigma}^{\,a}_{\ b}\cdot\left\langle \bar{\chi}\vec{\sigma}\chi \right\rangle_{1/2}\Big[\bar{B}^{\{\mu\rho\}\nu}_{20'}\;B^{20'}_{\{\kappa\rho\}\nu} + 5\,\bar{B}^{\{\rho\nu\}\mu}_{20'}\;B^{20'}_{\{\kappa\rho\}\nu}\Big]$$

We should notice that the second term in (14) does not have any g_o dependence . Such term vanishes due to the tracelessness of $\vec{\sigma}$.

For the cross currents we find,

$$J^{A'}_{A}(\overline{20}\ ,\ 20') = \frac{\mu_o}{3}\ \vec{\sigma}^{a}_{\ d} \cdot \langle \bar{\chi}_{3/2} \vec{\sigma}\ \chi_{1/2} \rangle\ \bar{B}^{\mu\nu\rho}_{20}\ B^{20'}_{\{k\nu\}\rho} \qquad \ldots(15)$$

and

$$J^{A'}_{A}(\overline{20}'\ ,\ 20) = \frac{\mu_o}{3}\ \vec{\sigma}^{a}_{\ d} \cdot \langle \bar{\chi}_{1/2} \vec{\sigma}\ \chi_{3/2} \rangle\ \bar{B}^{\{\mu\nu\}\rho}_{20'}\ B^{20}_{\kappa\nu\rho} \qquad \ldots(16)$$

In the equations (15) and (16), we have used the abbreviations

$$\langle \bar{\chi}_{3/2} \vec{\sigma}\ \chi_{1/2} \rangle = \bar{\chi}^{abc}\ \vec{\sigma}^{d}_{\ a}\ \epsilon_{db}\ \chi_{c} \qquad \ldots(17)$$

and

$$\langle \bar{\chi}_{1/2} \vec{\sigma}\ \chi_{3/2} \rangle = \epsilon^{ab}\ \bar{\chi}^{c}\ \vec{\sigma}^{d}_{\ a}\ \chi_{dbc} \ . \qquad \ldots(18)$$

It is worthwhile to notice that both $J^{A'}_{A}(\overline{20}\ ,\ 20')$ and $J^{A'}_{A}(\overline{20}',\ 20)$ are traceless. On the other hand only the second terms of the currents $J^{A'}_{A}(\overline{20},20)$ and $J^{A'}_{A}(\overline{20}',\ 20')$ are traceless. We should not be surprised by this outcome, because we are expressing U(8) multiplets in terms of the U(4) and the SU(2) contents and since the expressions like $\vec{\sigma}$ -s are traceless , we are automatically led to such results. More generally , however, out of the equation (7) we would get the condition of tracelessness as

$$\mu_o + 8\, g_o = 0 \qquad \ldots(19)$$

It is worth mentioning at this stage , that in $J^{A'}_{A}(\overline{20}',20')$ (equation (4)) the first term , which includes $(\underline{15},1)$ member of the $\underline{63}$ - representation, contains only F-type of current, whereas the second term, which is a $(\underline{15},3)$ member, contains both D and F types of currents for the baryon octets (in SU(3) sense) whose ratio is 3/2. This follows directly from the expansion of the terms within the square brackets.

IV Magnetic Moments

As Bég , Lee and Pais [3] have done , we would similarly make the assumption that the magnetic moment operator transforms like a $(\underline{15}, 3)$ member of a $\underline{63}$ - representation of U(8). Under this assumption , the effective low frequency limit of the electromagnetic vertex of the baryons may be written as

$$V = J^{A'}_{A} \left[e_o \, \phi \, \delta^{d}_{a} + m_o \, \vec{\sigma}^{d}_{a} \cdot \vec{n} \right] Q^{\kappa}{}_{\mu} \qquad \ldots(20)$$

where e_o and m_o are two arbitrary constants and $\vec{n} = \vec{q} \times \vec{\epsilon}$, $\vec{q}$ being the momentum of the baryon and $\vec{\epsilon}$ is a polarization vector perpendicular to $\vec{q}$. We have intentionally kept the constants e_o , m_o , μ_o and g_o (the last two appearing in $J^{A'}_{A}$) arbitrary. In equation (20), ϕ is the electrostatic potential.

If we write the component of the equation (20) which contributes to the magnetic moments as $M(\bar{m}, n)$ between the n and m dimensional representations belonging to U(4) , we find

$$M(\bar{20}, 20) = \mu_o \, m_o \, \vec{n} \cdot \langle \bar{\chi} \vec{\sigma} \chi \rangle_{3/2} \; \bar{B}^{\mu\nu\rho}_{20} \; B^{20}_{\kappa\nu\rho} \; Q^{\kappa}{}_{\mu} \qquad \ldots(21)$$

$$M(\bar{20}', 20') = -\frac{2}{9} \mu_o \, m_o \, \vec{n} \cdot \langle \bar{\chi} \vec{\sigma} \chi \rangle_{1/2} \left[\bar{B}^{\{\mu\rho\}\nu}_{20'} \; B^{20'}_{\{\kappa\rho\}\nu} + 5 \, \bar{B}^{\{\rho\nu\}\mu}_{20'} \; B^{20'}_{\{\kappa\rho\}\nu} \right] Q^{\kappa}{}_{\mu} \qquad \ldots(22)$$

$$M(\bar{20}, 20') = \frac{2}{3} \mu_o \, m_o \, \vec{n} \cdot \langle \bar{\chi}_{3/2} \vec{\sigma} \chi_{1/2} \rangle \; \bar{B}^{\mu\nu\rho}_{20} \; B^{20'}_{\{\kappa\nu\}\rho} \; Q^{\kappa}{}_{\mu} \qquad \ldots(23)$$

and $$M(\bar{20}', 20) = \frac{2}{3} \mu_o \, m_o \, \vec{n} \cdot \langle \bar{\chi}_{1/2} \vec{\sigma} \chi_{1/2} \rangle \; \bar{B}^{\{\mu\nu\}\rho}_{20'} \; B^{20}_{\kappa\nu\rho} \; Q^{\kappa}{}_{\mu} \qquad \ldots(24)$$

Let us now write, for the expectation values of the magnetic moment of a particle X between the maximum z-component of the spin, $\mu(X)$; that is,

$$\mu(X) = \left\langle X;\ J,\ J_z = J \,\middle|\, M \,\middle|\, X;\ J,\ J_z = J \right\rangle \qquad \ldots(25a)$$

For the transition magnetic moment between X and Y , assuming X belongs to $\underline{20}'$-representation and Y to $\underline{20}$ - representation , we would write

$$\left\langle Y \,\middle|\, \mu \,\middle|\, X \right\rangle = \left\langle Y;\ \tfrac{3}{2},\ \tfrac{1}{2} \,\middle|\, M \,\middle|\, X;\ \tfrac{1}{2},\ \tfrac{1}{2} \right\rangle \qquad \ldots(25b)$$

Then we can find out all the magnetic moments and the transition moments by using the equations (21) through (24).

A. $\underline{20}$ - representation

We find, for the (10,0) members,

$$\tfrac{1}{2}\,\mu(N^{*++}) = \mu(N^{*+}) = \mu(Y^{*+}) = -\mu(N^{*-}) = -\mu(Y^{*-})$$

$$= -\mu(\Xi^{*-}) = -\mu(\Omega^{-}) = \mu(p) \qquad \ldots(26a)$$

and

$$\mu(N^{*o}) = \mu(Y^{*o}) = \mu(\Xi^{*o}) = 0 \qquad \ldots(26b)$$

For the sextuplet (6,1) members , we get,

$$\tfrac{1}{2}\,\mu(C_1^{*++}) = \mu(C_1^{*+}) = \mu(S^{*+}) = \mu(p) \qquad \ldots(27a)$$

and

$$\mu(C_1^{*o}) = \mu(S^{*o}) = \mu(T^{*o}) = 0 \qquad \ldots(27b)$$

For the triplet (3,2) particles , we find,

$$\frac{1}{2}\,\mu\,(X_u^{*++}) \;=\; \mu\,(X_d^{*+}) \;=\; \mu\,(X_s^{*+}) \;=\; \mu(p) \qquad \ldots(28)$$

Finally for the singlet (1,3) , we have,

$$\frac{1}{2}\,\mu(R^{*++}) \;=\; \mu(p) \qquad \ldots(29)$$

We can easily notice that the magnetic moments satisfy the relation,

$$\mu_{\underline{20}}(X) \;=\; Q_X\,\mu(p) \qquad \ldots(30)$$

B. $\underline{20}'$- representation

For the baryon octets (8, 0) , we get,

$$-\frac{3}{2}\,\mu(n) \;=\; \mu(\Sigma^+) \;=\; -\frac{3}{2}\mu(\Xi^0) \;=\; -\,3\mu(\Sigma^-) \;=\; -\,3\mu(\Xi^-)$$

$$=\; -\,(\Delta^0) \;=\; 3\mu(\Sigma^0) \;=\; \mu(p) \qquad \ldots(31)$$

We find for the sextuplet (6,1) particles ,

$$\frac{2}{3}\,\mu(C_1^{++}) \;=\; -\frac{3}{2}\,\mu\,(C_1^0) \;=\; -\frac{3}{2}\,\mu(S^0) \;=\; -\frac{3}{2}\mu(T^0) = \mu(p) \qquad \ldots(32a)$$

and

$$\mu(C_1^+) \;=\; \mu\,(S^+) \;=\; 0 \qquad \ldots(32b)$$

For the contragradient triplet $(\bar{3},\,1)$, the moments are given by,

$$\mu\,(C_o^+) \;=\; \mu(A^+) \;=\; \mu(A^0) \;=\; \frac{2}{3}\,\mu\,(p) \qquad \ldots(33)$$

For the triplet (3,2) , we have,

$$\frac{3}{2}\,\mu\,(X_u^{++}) \;=\; \mu\,(X_d^{+}) \;=\; \mu\,(X_s^{+}) \;=\; \mu(p) \qquad \ldots(34)$$

Finally the nonvanishing transition moments within this multiplet, with spin states $J_z = \frac{1}{2}$, are

$$\langle \Sigma^{o} | \mu | \Delta^{o} \rangle \;=\; -\,\langle C_1^{+} \,|\, \mu \,|\, C_o^{+} \rangle \;=\; \langle S^{+} | \mu \,|\, A^{+} \rangle \;=\; \frac{1}{3}\,\mu(p) \qquad \ldots(35)$$

For the above transition moments the following relation is also satisfied :

$$\langle X \,|\, \mu \,|\, Y \rangle \;=\; \langle Y \,|\, \mu \,|\, X \rangle \qquad \ldots(35a)$$

C. Transition moments between $\underline{20'}$ and $\underline{20}$ - representations

The transition moments between the (8,0) and (10,0) members are given by[9],

$$\langle N^{*+} | \mu \,|\, p \rangle \;=\; -\,\langle Y^{*+} \,|\, \mu | \Sigma^{+} \rangle \;=\; \langle N^{*o} | \mu | n \rangle \;=\; 2\,\langle Y^{*o} | \mu \,|\, \Sigma^{o} \rangle$$

$$=\; -\,\frac{\sqrt{3}}{2}\,\langle Y^{*o} | \mu \,|\, \Lambda^{o} \rangle \;=\; -\,\langle \Xi^{*o} | \mu | \Xi^{o} \rangle \;=\; \frac{2\sqrt{2}}{3}\,\mu(p) \qquad \ldots(36)$$

It also comes out very easily as in (35a) that

$$\langle Y \,|\, \mu \,|\, X \rangle \;=\; \langle X \,|\, \mu \,|\, Y \rangle \qquad \ldots(37)$$

All other transition moments between the (8,0) and the (10,0) members are zero.

The only nonvanishing moments between the triplet, $(\bar{3}, 1)$ of $\underline{20'}$ representation and the sextuplet , (6,1) of $\underline{20}$ - representation are,

$$\left\langle C_1^{*+} \middle| \mu \middle| C_o^{+} \right\rangle = - \left\langle S^{*+} \middle| \mu \middle| A^{+} \right\rangle = \frac{2}{3} \mu(p) \qquad \ldots(38)$$

The equation (37) is also valid for such transitions.

V Concluding Remarks

We have started with a general group U(8) and classified the particles in terms of $U(4) \otimes SU(2)$ specifications, where U(4) gives us the internal symmetry and SU(2) incorporates the intrinsic spin of the particles. Then assuming that the magnetic moment operator transforms as $(\underline{15}, 3)$ - member of $\underline{63}$ - representation, we obtained the magnetic moments of all the baryons in terms of the magnetic moments of proton $\mu(p)$. The SU(3) - decouplet and octet magnetic moments come out in the present case same as that of SU(6) calculation of Bég , Lee and Pais [3] . We have also determined the magnetic moments of the charmed baryons. These moments would be useful if such particles appear to be reality.

It is worthwhile to mention that the transition from U(8) to SU(8) can be achieved by replacing g_o from the moment expressions by equation (19). A glance through the equations (21) through (24) reveals that the M-operators do not depend g_o at all . Hence the results obtained are also valid for SU(8).

It would be quite interesting to see whether introduction of colored quarks have any influence on the magnetic moments. This would be something worth studying, because in the real world , we need to introduce them to incorporate the correct statistics for the baryons. This point is now being pursued by the authors.

Acknowledgement

The authors would like to express their deepest gratitude to Professor L. C. Biedenharn Jr., of Duke University for encouragement and helping them to crystalize some of the ideas of the paper. The first author (A . L. C.) also expresses his gratitude to the Department of Physics , UNC-Chapel Hill, N.C., for allowing him to use the facilities of the department during the summer months. He is also particularly grateful to Professors J.W. Straley, E. Merzbacher and H. van Dam for many helpful cooperations.

Reference

1. A. L. Choudhury and V. Joshi : Magnetic Moments of Charmed Baryons I. ECSU Preprint (1975) . To be denoted as CJ I.

2. F. Gürsey and L. A. Radicati : Phys. Rev. Lett. 13 , 173(1964)
B. Sakita : Phys. Rev. 136 , B1756 (1964)

3. M. A. B. Bég , B. W. Lee and A. Pais : Phys. Rev. Lett. 13, 514 (1964)
See also W. Thirring : Acta Physica Austriaca Suppl. II, 205 (1965)

4. A. Pais : Phys. Rev. Lett. 13 , 175 (1964)

5. J. J. Aubert et al : Phys. Rev. Lett. 33 , 1404 (1974)
J. E. Augustine et al : ibid 33, 1406 (1964)
C. Bacci et al : ibid 33 , 1408 (1974)

6. S. L. Glashow , J. Iliopoulos and L. Maiani : Phys. Rev. D2, 1285 (1970)

7 S. Okubo : SU(4), SU(8) Mass Formula and Weak Interaction: Technical Report UR 524 , University of Rochester (1975)
J. W. Moffat : SU(4) and SU(8) Mass Splitting etc. Preprint , University of Toronto (1975)
D. B. Lichtenberg : Charmed Baryons etc. Indiana University Preprint (1975)

8. M. Gell-Mann: Acta Physica Austriaca Suppl. IX , 733(1972)

9. It should be pointed out here that in contrast to Beg et al's results [3] the equation (36) contains extra negative signs in front of the expressions
$\frac{3}{2}\langle \Sigma^{*0}|\mu|\Lambda^{0}\rangle$ and $\langle \Xi^{*0}|\mu|\Xi^{0}\rangle$.

ATTACHMENT III

PROSPECTIVE TN

ATTACHMENT 3

PROSPECTIVE TN

NUCLEON AND HEAVY ION TOTAL AND ABSORPTION CROSS SECTION WITH SELECTED NUCLEI

By John W. Wilson
Langley Research Center

and

Christopher M. Cosner
Old Dominion University

ABSTRACT

Approximations to the solution of the coupled channel equations of composite particle scattering are considered with view to the nuclear scattering problem. Application of the eikonal formalism within a small angle approximation to calculate the coherent elastic scattered amplitude is made from which total and absorption cross sections are derived. Detailed comparison with nucleon-nucleus experiments show agreement within 5% except at lower energies where the eikonal approximation is of questionable accuracy. Even then, global agreement is within 15%. Tables of cross sections required for cosmic heavy ion transport and shielding studies are presented.

SYMBOLS

a	parameter in Woods-Saxon function, fm
A	nuclear mass number, dimensionless
a_c	parameter for Woods-Saxon charge density, fm
a_p	proton root-mean-square charge radius, fm
a_{P_ℓ}	the ℓ^{th} transition moment of the projectile, $(fm)^\ell$
a_{T_ℓ}	the ℓ^{th} transition moment of the target, $(fm)^\ell$
$\vec{b}$	projectile impact parameter vector, fm
$B(e)$	average of slope parameters of nucleon-nucleon scattering amplitude, fm^2
B_{pp}, B_{np}	slope parameter for proton-proton and neutron-proton scattering, fm^2
e	two-nucleon kinetic energy in their center-of-mass frame, MeV
E	projectile laboratory energy per unit mass, GeV/amu
$\bar{f}(\vec{q})$	heavy ion scattering amplitude, fm
$\bar{f}^B(\vec{q})$	Born approximation to $\bar{f}(q)$, fm
$f(e,\vec{q})$	average two-nucleon scattering amplitude, fm
$f_e(\vec{q})$	heavy ion coherent scattering amplitude, fm
$f_i(e,q)$	two-nucleon scattering amplitude for $i = pp, np, fm$
$F(\vec{q})$	nuclear form factor, dimensionless
$g_{P_m}(\vec{\xi}_P)$	projectile internal wave function for state m, $fm^{-3/2}$
$g_{T_\mu}(\vec{\xi}_T)$	target internal wave function for state μ, $fm^{-3/2}$
G_c	coherent propagator or coherent Green's function, dimensionless
J_m, J_μ	total internal angular momentum quantum numbers for the projectile in state m and target in state μ, dimensionless

1	$\vec{k}$	projectile momentum vector relative to target in
2		the initial state, fm^{-1}
3	$\vec{k}_f$	projectile momentum vector relative to the target in
4		the final state, fm^{-1}
5	ℓ	orbital angular momentum quantum number, dimensionless
6	m	nucleon mass, 938 MeV/c^2
7	N	total number of nuclear constituents, dimensionless
8	N_p, N_T	neutron numbers of the projectile and target, dimensionless
9	$\vec{q}$	momentum transfer $(\vec{q} = \vec{k}_f - \vec{k})$, fm^{-1}
10	$\vec{r}$	position vector relative to the nuclear center of mass, fm
11	r_u	nuclear equivalent uniform radius, fm
12	$r_{0.5}, R$	nuclear half-density radius, fm
13	t	nuclear skin thickness, fm
14	t_C	nuclear charge skin thickness, fm
15	$t_{\alpha j}(\vec{x}_\alpha, \vec{x}_j)$	two-nucleon transition operator for nucleons α and j
16		at positions $\vec{x}_\alpha$ and $\vec{x}_j$, MeV
17	$\tilde{t}$	average two-nucleon transition amplitudes, MeV
18	t_{nn}, t_{pp}, t_{np}	two-nucleon transition amplitudes for neutron-neutron,
19		proton-proton, and neutron-proton scattering, MeV
20	$\bar{U}(x)$	optical potential matrix, MeV^2
21	$U_c(x)$	coherent optical potential, MeV^2
22	$V_{m\mu,m'\mu'}(\vec{x})$	matrix elements of the optical potential operator, MeV
23	$V_{opt}(\vec{\xi}_p, \vec{\xi}_T, \vec{x})$	optical potential operator, MeV
24	$\vec{x}$	relative position vector of the projectile $(\vec{x} = \vec{b} + \vec{z})$, fm
25	$\vec{y}$	two-nucleon relative position vector, fm

1	z	projection of $\vec{x}$ along the beam, fm
2	$\hat{z}$	unit vector along the beam, dimensionless
3	α_{pp}, α_{np}	ratio of real to imaginary parts of nucleon-nucleon
4		scattering amplitudes, dimensionless
5	$\bar{\delta}$	entrance channel unit vector, dimensionless
6	θ	scattering angle, radians
7	$\vec{\xi}_p, \vec{\xi}_T$	collections of constituent relative coordinates for
8		projectile and target, fm
9	$\rho_n(r), \rho_p(r)$	neutron and proton densities in the nucleus, fm^3
10	$\rho_{C_A}(\vec{r})$	nuclear charge density, fm^{-3}
	$\rho_{C_p}(\vec{r})$	proton charge density, fm^{-3}
11	$\rho_A(\vec{r})$	nuclear single particle density, fm^{-3}
12	σ_{pp}, σ_{np}	two-nucleon total cross sections, fm^2 (mb)
13	$\sigma_{Tot}, \sigma_s, \sigma_{abs}$	heavy ion total, scattering, and absorption cross
14		sections, fm^2 (mb)
15	$\bar{\phi}(\vec{x})$	the coupled channel phase operator, dimensionless
16	$\bar{\chi}(\vec{b})$	the eikonal phase shift, dimensionless
17	$\bar{\psi}(x)$	the coupled channel scattered wave, $fm^{-3/2}$
18	$\psi_{m\mu}(x)$	components of $\bar{\psi}(x)$
19	$\bar{\psi}_i(\vec{x})$	the i^{th} term of the multiple excitation series for $\bar{\psi}(x)$
20	$\bar{\psi}^{(i)}(\vec{x})$	the i^{th} iterate of the perturbation approximation to $\bar{\psi}(x)$
21	$\bar{\psi}_p(x)$	entering plane wave state, $fm^{-3/2}$
22	Ω	coupled channel wave operator, dimensionless
23	Ω_c	coherent wave operator, dimensionless
24		
25		

INTRODUCTION

The high-energy heavy ions of the cosmic radiation pose an ever present hazard to spacecraft and high-altitude aircraft. In particular, for manned space missions of long duration or for crew members of high-altitude aircraft flight in which career lifetimes may approach 25 years, the potential adverse affects on nonregenerative tissues is of extreme importance (refs. 1 and 2). In that the range of such energetic particles is large compared to space craft walls and the overhead airmass at very high altitudes, an attractive means of radiation protection appears to be through attenuation and breakup in nuclear reaction. To make effective use of nuclear attenuation, the corresponding cross sections must be accurately known since even modest cross section uncertainty can, because of the non-linear relation of cross section to transmitted flux, produce large errors in such calculations. For example, a 25% uncertainty in absorption cross section produces an order of magnitude uncertainty in flux after only three mean free paths. In addition, the uncertainty in production cross sections for the reaction products produces further uncertainty in the transmitted flux which may also be large as demonstrated by Curtis and Wilkinson (ref. 3).

In the present report, we will examine a recent high-energy heavy-ion reaction model for potential use in estimating the required nuclear parameters (refs. 4 and 5). The model consists of a coupled channel Schroedinger equation derived assuming high-energy and closure of the internal nuclear states. We will consider approximation procedures for solution of the coupled equations and examine in detail the lowest order approximation. Comparisons with available nuclear cross section measure-

ments will be made.

HEAVY ION DYNAMICAL EQUATIONS

In this section we will examine the coupled channel equations for composite particle scattering. Particular attention will be given to the relation between the coherent elastic scattered wave, the Born approximation, Chew's form of the impulse approximation, the distorted wave Born approximation (DWBA), and various approximation procedures to the coupled equations. Finally, we will show how the coupled equations can be solved assuming small angle scattering and a simplified expression for the elastic and all of the inelastic scattering amplitudes will be derived. We will further discuss the usual use of the optical theorem to estimate total cross sections from the coherent elastic scattered wave and, in particular, shed some light on the reasons why this estimate of total cross section is so successful.

Coupled channel equations. The starting point for the present discussion is the coupled channel (Schroedinger) equation relating the entrance channel to all excited states of the target and projectile which was derived assuming high energy and closure for the accessible internal eigenstates of the target and projectile (refs. 4 and 5). These coupled equations are given as

$$(\nabla_x^2 + \vec{k}^2)\,\psi_{m\mu}(\vec{x}) = \left(\frac{2mA_pA_T}{N}\right)\sum_{m'\mu'} V_{m\mu,m'\mu'}(\vec{x})\,\psi_{m'\mu'}(\vec{x}) \qquad (1)$$

where subscripts m and μ label the eigenstates of the projectile and target, A_p and A_T are projectile and target mass number, m is constituent mass, $\vec{k}$ is projectile momentum relative to the center of mass, $\vec{x}$ is the projectile position vector relative to the target, with

$$V_{m\mu,m'\mu'}(\vec{x}) = \langle g_{P_m}(\vec{\xi}_P)\, g_{T_\mu}(\vec{\xi}_T) \,|\, V_{opt}(\vec{\xi}_P, \vec{\xi}_T, \vec{x}) \,|\, g_{P_{m'}}(\vec{\xi}_P)\, g_{T_{\mu'}}(\vec{\xi}_T) \rangle \tag{2}$$

$g_{P_m}(\vec{\xi}_P)$ and $g_{T_\mu}(\vec{\xi}_T)$ are the projectile and target internal wave functions, $\vec{\xi}_P$ and $\vec{\xi}_T$ are collections of internal coordinates of the projectile and target constituents, $V_{opt}(\vec{\xi}_P, \vec{\xi}_T, \vec{x})$ is the effective potential operator derived in ref. 4 and given by

$$V_{opt}(\vec{\xi}_P, \vec{\xi}_T, \vec{x}) = \sum_{\alpha,j} t_{\alpha j}(\vec{x}_\alpha, \vec{x}_j) \tag{3}$$

where $t_{\alpha j}(\vec{x}_\alpha, \vec{x}_j)$ is the two-body transition operator for the j-constituent of the projectile at position $\vec{x}_j$ and the α-constituent of the target at $\vec{x}_\alpha$ and N is the total constituent number

$$N = A_P + A_T \tag{4}$$

We simplify the notation by introducing the wave vector

$$\vec{\psi}(\vec{x}) = \begin{bmatrix} \psi_{00}(\vec{x}) \\ \psi_{01}(\vec{x}) \\ \psi_{10}(\vec{x}) \\ \psi_{11}(\vec{x}) \\ \vdots \end{bmatrix} \tag{5}$$

and the potential matrix

$$\bar{U}(\vec{x}) = \left(\frac{2mA_T A_P}{N}\right) \begin{bmatrix} V_{00,00}(\vec{x}) & V_{00,01}(\vec{x}) & V_{00,10}(\vec{x}) & \cdots \\ V_{01,00}(\vec{x}) & V_{01,01}(\vec{x}) & V_{01,10}(\vec{x}) & \cdots \\ V_{10,00}(\vec{x}) & V_{10,01}(\vec{x}) & V_{10,10}(\vec{x}) & \cdots \\ V_{11,00}(\vec{x}) & V_{11,01}(\vec{x}) & V_{11,10}(\vec{x}) & \cdots \\ \vdots & \vdots & \vdots & \end{bmatrix} \tag{6}$$

The coupled equations are then written in matrix form as

$$(\nabla_x^2 + \vec{k}^2)\,\bar{\psi}(\vec{x}) = \bar{U}(\vec{x})\,\bar{\psi}(\vec{x}) \tag{7}$$

for which we now seek approximations.

Born approximation. The Born approximation of the coupled equations is written as

$$\bar{f}^B(\vec{q}) = -\frac{1}{4\pi} \int e^{-i\vec{q}\cdot\vec{x}}\, \bar{U}(\vec{x})\, d^3\vec{x} \tag{8}$$

which is a matrix of approximate scattering amplitudes relating all possible entrance channels to all possible final channel states. For example, diagonal elements relate to all possible elastic scatterings of the system where the elastic channel is defined by the entrance channel. Recalling the definition of the potential matrix in equation (2), we write

$$f^B_{m'\mu';m\mu}(\vec{q}) = -\frac{1}{4\pi}\left(\frac{2mA_T^2A_2^2}{N}\right) F_{P_{m'm}}(\vec{q})\, F_{T_{\mu'\mu}}(\vec{q})\, \tilde{t}(k,\vec{q}) \tag{9}$$

where $F_{P_{m'm}}(\vec{q})$ and $F_{T_{\mu'\mu}}(\vec{q})$ are the projectile and target form factors. Equation (9) corresponds to a generalized version of Chew's impulse approximation (ref. 6) or single scattering approximation (ref. 7). This is consistent with the idea that solution of the optical model implicitly sums the multiple scattering corrections. As noted in ref. 3 , the Born series is term by term equivalent to the multiple-scattering series.

It follows from the form of eq. (9) that

$$\bar{f}^{B}_{m'\mu';m\mu}(\vec{q}) \sim \left[\delta_{m'm} + a_{P_{\ell_P}} |\vec{q}|^{\ell_P}\right]\left[\delta_{\mu'\mu} + a_{T_{\ell_T}} |\vec{q}|^{\ell_T}\right] t(k,\vec{q}) \tag{10}$$

at small momentum transfer where

$$\ell_P = \text{Max}\{|J_{m'} - J_m|, 1\} \tag{11}$$

and

$$\ell_T = \text{Max}\{|J_{\mu'} - J_\mu|, 1\} \tag{12}$$

where $J_{\mu'}, J_\mu$ $(J_{m'}, J_m)$ are the internal angular momentum quantum numbers of the target (projectile) in the final and entering states respectively. The $a_{T_{\ell_T}}$ and $a_{P_{\ell_P}}$ are the lowest order nonvanishing transition moments of the target and projectile respectively. On the basis of the Born approximation, we see a very strong threshold effect on the various excitation processes which causes an ordering in the contribution of specific excitation channels in going from small to large momentum transfer. Clearly at zero momentum transfer, only the elastic channel is open. As the momentum transfer increases, the single dipole transitions for either the target or projectile but not both are displayed first. Note that this severly restricts the accessible angular momentum states in the excitation process. At slightly higher momentum transfer, coincident dipole transitions in projectile and target and single quadrapole transitions are in competition with and may eventually dominate the single dipole transitions at sufficiently high momentum transfer. Similarly at higher momentum transfer, transitions to higher angular momentum states are possible.

Perturbation Expansion and DWBA. According to the above discussion, we see that over a restricted range of momentum transfer the off diagonal elements of the "Born" matrix of scattering amplitudes are small compared to the elastic-scattering amplitudes for the various channels found along

the diagonal. Noting that these amplitudes are proportional to the potential, we may consider the decomposition

$$\bar{\mathcal{U}}(\vec{x}) = \bar{\mathcal{U}}_d(\vec{x}) + \bar{\mathcal{U}}_o(\vec{x}) \tag{13}$$

where $\bar{\mathcal{U}}_d(\vec{x})$ are the diagonal parts of $\bar{\mathcal{U}}(\vec{x})$ and $\bar{\mathcal{U}}_o(\vec{x})$ are the corresponding off diagonal parts. Clearly we may assume

$$\bar{\mathcal{U}}_d(\vec{x}) >> \bar{\mathcal{U}}_o(\vec{x}) \tag{14}$$

in accordance with the above discussion. We will treat the off diagonal contribution as a perturbation and consider the iterated solution.

We rewrite eq. (7) as

$$[\nabla_x^2 + \vec{k}^2 - \bar{\mathcal{U}}_d(\vec{x})]\,\bar{\psi}(\vec{x}) = \bar{\mathcal{U}}_o(\vec{x})\,\bar{\psi}(\vec{x}) \tag{15}$$

and take as a first approximation

$$[\nabla_x^2 + k^2 - \bar{\mathcal{U}}_d(\vec{x})]\,\bar{\psi}_o(\vec{x}) = 0 \tag{16}$$

The only nonzero component of $\bar{\psi}_o(\vec{x})$ is the elastic coherent scattered wave. If the initial prepared states are in their ground states then we solve for the coherent elastic wave from

$$(\nabla_x^2 + \vec{k}^2)\,\psi_c(\vec{x}) = \mathcal{U}_{oo,oo}(\vec{x})\,\psi_c(\vec{x}) \tag{17}$$

and the first approximation is

$$\bar{\psi}_o(\vec{x}) = \begin{bmatrix} \psi_c(\vec{x}) \\ 0 \\ 0 \\ 0 \\ \vdots \end{bmatrix} \tag{18}$$

Estimating the perturbation via use of eq. (18) we now correct the result as

$$[\nabla_x^2 + \vec{k}^2 - \bar{\mathcal{U}}_d(\vec{x})]\,\bar{\psi}^{(1)}(\vec{x}) = \bar{\mathcal{U}}_o(\vec{x})\,\bar{\psi}_o(\vec{x}) \tag{19}$$

The right hand side is a term describing the source of excitation caused by the interaction of the coherent amplitude and is of the form

$$\bar{\mathcal{U}}_o(\vec{x})\,\bar{\psi}_o(\vec{x}) = \begin{bmatrix} 0 \\ \mathcal{U}_{01,00} \\ \mathcal{U}_{10,00} \\ \mathcal{U}_{11,00} \\ \vdots \end{bmatrix} \psi_c(\vec{x}) \tag{20}$$

Noting that the first component of the source of excitation is zero, we see that the equation for the first component of eq. (19) is

$$\left[\nabla_x^2 + \vec{k}^2 - \mathcal{U}_{00,00}(\vec{x})\right] \psi_{00}^{(1)}(\vec{x}) = 0 \tag{21}$$

from which we see that the iteration of the elastic channel obtains again the coherent elastic amplitude

$$\psi_{00}^{(1)}(\vec{x}) = \psi_c(\vec{x}) \tag{22}$$

The remaining components of (19) are

$$\left[\nabla_x^2 + \vec{k}^2 - \mathcal{U}_{m\mu,m\mu}(\vec{x})\right] \psi_{m\mu}^{(1)}(\vec{x}) = \mathcal{U}_{m\mu,00}(\vec{x})\, \psi_c(\vec{x}) \tag{23}$$

This process of successive iteration is equivalent to the series approximation

$$\bar{\psi}(\vec{x}) = \bar{\psi}_0(\vec{x}) + \bar{\psi}_1(\vec{x}) + \bar{\psi}_2(\vec{x}) + \cdots \tag{24}$$

where

$$\left[\nabla_x^2 + \vec{k}^2 - \bar{\mathcal{U}}_d(\vec{x})\right] \bar{\psi}_0(\vec{x}) = 0 \tag{25}$$

and

$$\left[\nabla_x^2 + \vec{k}^2 - \bar{\mathcal{U}}_d(\vec{x})\right] \bar{\psi}_i(\vec{x}) = \bar{\mathcal{U}}_0(\vec{x})\, \bar{\psi}_{i-1}(\vec{x}) \tag{26}$$

The iterated solution and series solution are related as

$$\bar{\psi}_i(\vec{x}) = \bar{\psi}^{(i)}(\vec{x}) - \bar{\psi}^{(i-1)}(\vec{x}) \tag{27}$$

and the $i^{\underline{\text{th}}}$ iterate is the $i^{\underline{\text{th}}}$ partial sum of the series.

Further insight can be gained by considering the formal solution to the coupled equations (25) and (26). We introduce the diagonal coherent propagator

$$G_c = \left[\nabla_x^2 + \vec{k}^2 - \bar{\mathcal{U}}_d(\vec{x})\right]^{-1} \tag{28}$$

and the coherent wave operator

$$\Omega_c = 1 + (\nabla_x^2 + \vec{k}^2)^{-1} \bar{\mathcal{U}}_d(\vec{x}) \tag{29}$$

with which the solution to eq. (26) is written as

$$\bar{\psi}_i(\vec{x}) = G_c\, \bar{\mathcal{U}}_0(\vec{x})\, \bar{\psi}_{i-1}(\vec{x}) \tag{30}$$

and note that

$$\bar{\psi}_0 = \Omega_c\, \bar{\psi}_p \tag{31}$$

where $\bar{\psi}_p$ is the entering plane wave state. The series (24) may now be written as

$$\bar{\psi} = \Omega_c \bar{\psi}_p + G_c \bar{U}_o \Omega_c \bar{\psi}_p + G_c \bar{U}_o G_c \bar{U}_o \Omega_c \bar{\psi}_p + \cdots \equiv \Omega \bar{\psi}_p \tag{32}$$

The first term is the coherent elastic scattered wave as noted above and represents attentuation and propagation of the incident plane wave in matter. Since Ω_c is diagonal, this propagation is in undisturbed matter. The second term relates to the excitation caused by the presence of the coherent elastic wave followed by coherent propagation in disturbed matter. Note that the second term has no contribution in the elastic channel. The third term relates to further excitation caused by the presence of the scattered waves formed exclusively by coherent excitation and the first correction to the elastic channel due to incoherent processes. Hence, the coherent elastic wave is correct up to third-order terms in off-diagonal elements of the potential matrix which shows considerable damping or suppression at small momentum transfer as shown in connection with eq. (10). This may well be the reason why the coherent elastic amplitude has been so successful in nuclear applications (refs. 5 and 8).

It is obvious from the structure of the second term in the series (32), that it is the usual distorted-wave Born approximation (ref. 9) or single inelastic scattering approximation (ref. 10) and the entire series could be aptly referred to as the distorted-wave Born series. However, recalling that the terms of the series correspond to a successively larger number of changes in states of excitation (i.e., the first term contains no excitation, the second term transforms the coherent elastic wave to the excited states, the third term transforms the excited states of the second term to new excitation levels and so on); a more appropriate name for the series would be the "multiple excitation series."

Full coupled channel amplitudes. We consider now the solution to the coupled equations (7) within a small angle approximation. We will in effect sum the multiple excitation series to all orders and as a final result give expressions for the scattering amplitudes connecting all possible entrance channels to all possible final channels. Making now the forward scattering assumption, we take the boundary condition as

$$\lim_{z\to-\infty} \bar{\psi}(\vec{x}) = (\tfrac{1}{2\pi})^{3/2} \exp(i\vec{k}\cdot\vec{x})\,\bar{\delta} \tag{33}$$

where $-\hat{z}$ is the direction to the beam source and $\bar{\delta}$ is a constant vector with a unit entry at the entrance channel element and zero elsewhere. Equation (33) simply states that no particles are scattered backwards. Physically, this assumption is justified since the backward scattered component for most high-energy scattering is many orders of magnitude less than the forward scattered component. We will seek a solution to eq. (7) of the form

$$\bar{\psi}(\vec{x}) = (\tfrac{1}{2\pi})^{\frac{3}{2}} \exp[i\,\bar{\phi}(\vec{x})] \exp(i\vec{k}\cdot\vec{x})\,\bar{\delta} \tag{34}$$

where the boundary condition (33) implies

$$\lim_{z\to-\infty} \bar{\phi}(\vec{x}) = 0 \tag{35}$$

as a boundary condition on $\bar{\phi}(\vec{x})$. Using eq. (34) we may write an equation for $\bar{\phi}(\vec{x})$ as

$$i\nabla_x^2\,\bar{\phi}(\vec{x}) - [\nabla_x\,\bar{\phi}(\vec{x})]^2 - 2\vec{k}\cdot\nabla_x\,\bar{\phi}(\vec{x}) - \bar{u}(\vec{x}) = 0 \tag{36}$$

If $\bar{u}(\vec{x})$ is small compared to the kinetic energy

$$\bar{u}(\vec{x}) << k^2 \tag{37}$$

and if the change in $\bar{u}(\vec{x})$ is small over one oscillation of the incident wave as

$$\nabla_x\,\bar{u}(\vec{x}) << \vec{k}\,\bar{u}(\vec{x}) \tag{38}$$

where inequalities refer to magnitudes of elements on each side of (37) and (38); then we may approximate (36) by

$$2k\,\frac{\partial}{\partial z}\,\bar{\phi}(\vec{x}) = -\,\bar{u}(\vec{x}) \tag{39}$$

which has a solution as

$$\bar{\phi}(\vec{x}) = -\frac{1}{2k}\int_a^z \bar{u}(\vec{x}')\,d\vec{z}' \tag{40}$$

where the value a is fixed by the boundary condition (35) to be $-\infty$.

We may now write the scattered wave (34) as

$$\bar{\psi}(\vec{x}) = \left(\frac{1}{2\pi}\right)^{\frac{3}{2}} \exp\left[-\frac{i}{2k}\int_{-\infty}^{z} \bar{u}(\vec{x}')\,d\vec{z}'\right] \exp(i\vec{k}\cdot\vec{x})\,\bar{\delta} \tag{41}$$

We note that the wave operator is approximated by

$$\Omega \approx \exp\left[-\frac{i}{2k}\int_{-\infty}^{z} \bar{u}(\vec{x}')\,d\vec{z}'\right] \tag{42}$$

The scattering amplitudes are given by

$$\begin{aligned}\bar{f}(\vec{q})\,\bar{\delta} &= -\sqrt{\frac{\pi}{2}}\int \exp(-i\vec{k}_f\cdot\vec{x})\,\bar{u}(\vec{x})\,\bar{\psi}(\vec{x})\,d^3\vec{x} \\ &= -\frac{1}{4\pi}\int \exp(-i\vec{q}\cdot\vec{x})\,\bar{u}(\vec{x})\exp\left[-\frac{i}{2k}\int_{-\infty}^{z}\bar{u}(\vec{x}')\,d\vec{z}'\right]\bar{\delta}\,d^3\vec{x}\end{aligned} \tag{43}$$

where $\vec{k}_f$ is the final projectile momentum and $\vec{q}$ the momentum transfer is given by

$$\vec{q} = \vec{k}_f - \vec{k} \tag{44}$$

We define a cylindrical coordinate system with cylinder axis along the beam direction and write

$$\vec{x} = \vec{b} + \vec{z} \tag{45}$$

where $\vec{b}$ is the impact parameter vector and note that

$$\vec{q}\cdot\vec{x} = \vec{q}\cdot\vec{b} + O(\theta^2) \tag{46}$$

where θ is the scattering angle which we assume small. Using then the small angle approximation we obtain

$$\bar{f}(\vec{q}) = -\frac{1}{4\pi}\int \exp(-i\vec{q}\cdot\vec{b})\,\bar{u}(\vec{b}+\vec{z})\exp\left[-\frac{i}{2k}\int_{-\infty}^{z}\bar{u}(\vec{b}+\vec{z}')\,d\vec{z}'\right]d^2\vec{b}\,d\vec{z} \tag{47}$$

which we rewrite as

$$\bar{f}(\vec{q}) = -\frac{ik}{2\pi}\int \exp(-i\vec{q}\cdot\vec{b})\left\{\exp[i\bar{\chi}(\vec{b})] - 1\right\}d^2\vec{b} \tag{48}$$

where

$$\bar{\chi}(\vec{b}) = -\frac{1}{2k}\int_{-\infty}^{\infty}\bar{u}(\vec{b}+\vec{z})\,d\vec{z} \tag{49}$$

Equation (48) gives the matrix of scattering amplitudes of all possible entrance channels to all possible final channels of the system.

We may inquire as to the relation between the eikonal result for the full scattering amplitude (48) and the various approximate results discussed earlier in this section. First, we consider the expansion in powers of $\bar{\chi}$ of the integrand of equation (48)

$$\bar{f}(\vec{q}) = -\frac{ik}{2\pi}\int e^{-i\vec{q}\cdot\vec{b}}\left[i\bar{\chi} - \tfrac{1}{2}\bar{\chi}^2 - \tfrac{1}{3!}i\bar{\chi}^3 + \cdots\right] d^2\vec{b} \qquad (50)$$

The first term is the Born approximation at small angles. Higher order terms are multiple-scattering corrections to the Born result. Recall that the Born approximation for the optical potential is equivalent to Chew's impulse approximation. A more interesting result is obtained by separating the $\bar{\chi}$ matrix into its diagonal and off-diagonal parts as

$$\bar{\chi}(\vec{b}) = \bar{\chi}_d(\vec{b}) + \bar{\chi}_o(\vec{b}) \qquad (51)$$

which corresponds to the diagonal and off-diagonal parts of the matrix potential $\bar{U}(\vec{x})$. If we now make an expansion in powers of the off-diagonal part of $\bar{\chi}$ in equation (48) we obtain

$$\bar{f}(\vec{q}) = -\frac{ik}{2\pi}\int e^{-i\vec{q}\cdot\vec{b}}\left[e^{i\bar{\chi}_d(\vec{b})} - 1\right] d^2\vec{b}$$
$$-\frac{ik}{2\pi}\int e^{-i\vec{q}\cdot\vec{b}}\, e^{i\bar{\chi}_d(\vec{b})}\left[i\bar{\chi}_o - \tfrac{1}{2}\bar{\chi}_o^2 - \tfrac{1}{3!}i\bar{\chi}_o^3 + \cdots\right] d^2\vec{b} \qquad (52)$$

The first term is the elastic coherent amplitude, the second term is the distorted wave Born approximation, and the remaining terms are multiple excitation corrections.

THE ELASTIC CHANNEL

It was shown in the previous section that within a small angle approximation, the coupled channel equations could be solved. The principal difficulty in calculating the full coupled channel amplitude lies in our near complete lack of knowledge of the internal wave functions for the colliding nuclei for all orders of excitation. It was shown on very general principles for near forward scattering that transitions to the excited states are kinematically suppressed. This was the main motivation for expanding the solution in terms of off-diagnoal matrix elements of the potential. Near forward scattering, the scattering amplitude is then dominated by the on-diagonal elements. If elastic scattering is strongly forward then a reasonable approximation to the elastic amplitude is obtained by neglecting the off-diagonal contribution and, in addition, the eikonal small-angle approximation should be accurate. In this vien, we will now approximate the elastic channel amplitude by retaining only the first term in equation (52). We will justify this approximation by making detailed comparisons with experimental data.

It has been shown in ref. 5 that the elastic channel potential can be reduced to

$$\mathcal{U}_c(x) = \frac{2m A_T^2 A_P^2}{N} \int d^3\vec{z}\, \rho_T(\vec{z}) \int d^3\vec{y}\, \rho_P(\vec{x}+\vec{y}+\vec{z})\, \tilde{t}(k,\vec{y}) \tag{53}$$

where $\rho_T(\vec{z})$ and $\rho_P(\vec{z})$ are the target and projectile ground state single particle densities and $\tilde{t}(k,\vec{y})$ is the energy and space dependent two-body transition amplitudes averaged over the projectile and target constituent types as

$$\tilde{t} = \frac{1}{A_P A_T}\left[N_P N_T\, t_{nn} + Z_P Z_T\, t_{pp} + (N_P Z_T + Z_P N_T)\, t_{np}\right] \tag{54}$$

with N_p and N_T the projectile and target neutron numbers and Z_p and Z_T the corresponding proton numbers. The normalization of the t amplitudes are given by

$$\hat{t}(k,\vec{q}) = -\frac{1}{(2\pi)^3\mu}\int exp(i\vec{q}\cdot\vec{r})\, f(e,\vec{q})\, d^3\vec{q} \tag{55}$$

with the usual expression for the spin independent two-nucleon transition amplitudes as

$$f(e,\vec{q}) = \frac{\sqrt{me}\,\sigma(e)}{4\pi}[\alpha(e)+i]\,exp\left[-\tfrac{1}{2}B(e)\,\vec{q}^{\,2}\right] \tag{56}$$

where e is the constituent energy in the two-body center of mass frame, $\mu = m/2$ is the two-body reduced mass, $\sigma(e)$ is the energy dependent total two-body cross section, $\alpha(e)$ is the ratio of real to imaginary parts, and B(e) is the slope parameter. The elastic channel phase function may now be approximated by

$$\chi(\vec{b}) = \frac{-1}{2k}\int_{-\infty}^{\infty} U_c(\vec{b}+\vec{z})\, d\vec{z} \tag{57}$$

from which we may calculate the elastic channel amplitude by

$$f_c(\vec{q}) = -ik\int_0^\infty b\,db\, J_0(2kb\sin\tfrac{\theta}{2})\left\{exp[i\chi(\vec{b})]-1\right\} \tag{58}$$

where we have used the property that the phase function is cylindrically symmetric about the Z-direction. Applying now the optical theorem we find

$$\begin{aligned}\sigma_T &= \frac{4\pi}{k}\,Im[f_c(\vec{o})] \\ &= 4\pi\int_0^\infty b\,db\left\{1-exp[-\chi_i(\vec{b})]\cos[\chi_r(\vec{b})]\right\}\end{aligned} \tag{59}$$

where X_r and X_i are the real and imaginary parts of X. In that the scattering is strongly forward, we may calculate the total elastic cross section using the eikonal expression

$$\begin{aligned}\sigma_s &= \int|f(\vec{q})|^2 d\Omega_q \\ &\approx 4\pi\int_0^\infty b\,db\left\{1-exp[-\chi_i(\vec{b})]\cos[\chi_r(\vec{b})]\right\} \\ &\quad -2\pi\int_0^\infty b\,db\left\{1-exp[-2\chi_i(\vec{b})]\right\}\end{aligned} \tag{60}$$

from which we now find

$$\sigma_{abs} = \sigma_T - \sigma_S$$
$$\approx 2\pi \int_0^\infty b\,db \left\{1 - \exp\left[-2\chi_i(r)\right]\right\} \tag{61}$$

The use of approximations (59) through (61) have at least in part been justified by comparison with experiment (ref 5). In the following, we will attempt to quantify the accuracy of these approximations by further comparing with experiments.

THE PHYSICAL DATA

It was noted in the previous section that scattering in the elastic channel can be described in terms of the single particle density functions of the projectile and target and the nucleon-nucleon two-body transition amplitudes. For the present work, these functions will be determined from compilations of experimental results on electron scattering from nuclei (i.e., nuclear charge distributions) and nucleon-nucleon scattering experiments.

Single Particle Density.- The single particle densities are related to the nuclear wave functions by

$$\rho_A(\vec{r}) = \frac{1}{A}\sum_{i=1}^{A} \langle g_o(\vec{\xi}) \mid \delta(\vec{r} - \vec{r}_i) \mid g_o(\vec{\xi}) \rangle \tag{62}$$

which can be written as

$$\rho_A(\vec{r}) = \frac{1}{A}\left[N_A \rho_n(\vec{r}) + Z_A \rho_p(\vec{r}) \right] \tag{63}$$

where $\rho_n(\vec{r})$ and $\rho_p(\vec{r})$ are the corresponding neutron and proton densities. It can be assumed that in light nuclei that

$$\rho_n(\vec{r}) \approx \rho_p(\vec{r}) \tag{64}$$

since they differ only by the protons coulomb repulsion which is a small affect in light nuclei. The medium mass nuclei would probably have

$$\int \vec{r}^{\,2} \rho_p(\vec{r})\, d^3\vec{r} > \int \vec{r}^{\,2} \rho_n(\vec{r})\, d^3\vec{r} \tag{65}$$

strictly as a result of coulomb repulsion. The relation (65) may actually be reversed in very heavy nuclei due to the large neutron excesses and the fact that the proton's nuclear binding is greatly increased due to this excess. For example, the charge radius has been observed to be relatively reduced in isotopes with increasing neutron numbers (ref. 11). In the present work, we will assume

$$\rho_n(\vec{r}) = \rho_p(\vec{r}) \tag{66}$$

and take the proton densities from electron scattering experiments.

Measured in electron scattering experiments is the charge distribution of the nucleus. Had the proton been a point particle, then the charge and proton densities would be proportional. The structure of the proton requires us to extract the single particle (or proton) densities by removing the effects of the proton charge distribution.

The single particle density (63) is then related to the charge distribution as measured in electron scattering through the following

$$\rho_{c_A}(\vec{r}) = \int \rho_{c_p}(\vec{r}') \, \rho_A(\vec{r}+\vec{r}') \, d^3\vec{r}' \tag{67}$$

where $\rho_{c_p}(\vec{r})$ is the proton's charge distribution and $\rho_{c_A}(\vec{r})$ is the nuclear charge density. We must now solve the integral equation (67) for the nuclear single particle density $\rho_A(\vec{r})$.

The proton charge form factor is to a good approximation a guassian function (ref. 12) as

$$\rho_{c_p}(\vec{r}) = \left(\frac{3}{2\pi a_p^2}\right)^{\frac{3}{2}} \exp\left(-3\vec{r}^2/2a_p^2\right) \tag{68}$$

with $a_p \approx 0.8$ fm. Substituting (68) into (67) and simplifying yields

$$\rho_{c_A}(\vec{r}) = \left(\frac{2\pi a_p^2}{3}\right)^{-\frac{1}{2}} \left\{ \frac{a_p^2}{3r} \int_0^\infty e^{-s} \left[\rho_A\left(r-\sqrt{\tfrac{2a_p^2 s}{3}}\right) - \rho_A\left(r+\sqrt{\tfrac{2a_p^2 s}{3}}\right)\right] ds \right.$$
$$\left. + \sqrt{\frac{2a_p^2}{3}} \int_{-\infty}^{\infty} e^{-s^2} \rho_A\left(r+\sqrt{\tfrac{2a_p^2}{3}}\, s\right) ds \right\} \tag{69}$$

The first term in (69) contributes only when r is near the nuclear edge. We will estimate its importance there by assuming the worst case when $\rho_A(\vec{r})$ is a uniform model density and take r to be the equivalent uniform radius r_u. We estimate then, the two terms in (69) at $r = r_u$ as

$$\rho_{c_A}(\vec{r}) \approx \frac{1}{\sqrt{6\pi}} \frac{a_p}{r_u} \rho_o + \frac{1}{\sqrt{\pi}} \int_{-\sqrt{\frac{3}{2a_p^2}} r_u}^{0} e^{-s^2} \rho_o \, ds$$

$$\approx \frac{1}{\sqrt{6\pi}} \frac{a_p}{r_u} \rho_o + \frac{1}{2} \rho_o \tag{70}$$

Comparing the ratio of the first term to the second as

$$\left(\frac{2}{3\pi}\right)^{\frac{1}{2}} \frac{a_p}{r_u} \approx .36/r_u \leq .15 \tag{71}$$

with $r_u \geq 2.4$ fm we see that the first term is less than or on the order of 15%. We further tested the importance of the first term numerically for the typical Woods-Saxon density and found it less than 1%. We take, therefore,

$$\rho_{c_A}(\vec{r}) = \frac{1}{\sqrt{\pi}} \int_{-\infty}^{\infty} e^{-s^2} \rho_A\left(r + \sqrt{\frac{2a_p^2}{3}}\, s\right) ds \tag{72}$$

and use the gauss quadrature formula to obtain

$$\rho_{c_A}(\vec{r}) \approx \frac{1}{2}\left[\rho_A(r + a_p/\sqrt{3}) + \rho_A(r - a_p/\sqrt{3})\right] \tag{73}$$

which is equivalent to assuming that $\rho_A(r)$ is well approximated by a cubic over the range of $r \pm a_p$ (ref. 12). The formula (73) was shown to be 2% accurate as determined by numerical evaluation of (69).

In the present work, we assume the densities of nuclei heavier than helium to be approximately Woods-Saxon in shape as given by

$$\rho(r) = \left[1 + \exp\left(\frac{r-R}{a}\right)\right]^{-1} \tag{74}$$

except for an overall normalization factor. In equation (74), R is the radius ~~of~~ at half density

$$R = r_{0.5} \tag{75}$$

and a is related to the skin thickness t by

$$t = 4.4\, a \tag{76}$$

Values for the half density radius and skin thickness determined from electron scattering experiments have been compiled by Hofstadter and Collard (ref. 13) and are shown in figures 1 and 2.

It was found on the basis of equation (72) that the half-density radius of the charge distribution was equal to the half-density radius of the single particle densities. Hence, the half-density radius for $\rho_A(r)$ may be taken directly from the compilations of reference 13. The single particle skin thickness is yet to be determined from approximation (73). Except for the overall normalization, we use equation (73) evaluated at $r = R + a_p/\sqrt{3}$ to find

$$a = \frac{2}{\sqrt{3}} a_p \Big/ \ln\left[\frac{3z-1}{3-z}\right] \tag{77}$$

where

$$z = \exp\left(a_p/\sqrt{3}\, a_c\right) \tag{78}$$

with a_c as the charge density parameter and a as the single particle density parameter. Equations (77) and (78) were used to determine the single particle skin thickness

$$t = 4.4\, a \tag{79}$$

in terms of the charge skin thickness

$$t_c = 4.4\, a_c \tag{80}$$

and the proton root mean square charge radius a_p given by

$$a_p^2 = \int \vec{r}^{\,2}\, \rho_{c_p}(\vec{r})\, d^3\vec{r} \tag{81}$$

The charge skin thickness and proton rms radius are taken from reference 13. The nuclear single particle density skin thickness as determined from the nuclear charge skin thickness is shown in figure 3. The skin thickness calculated using euqations (77) to (81) were shown to satisfy equation (69) to within 1%.

For the purposes of the present calculations, we use the relation

$$r_{0.5} = 1.18 A^{\frac{1}{3}} - 0.48 \qquad (fm) \tag{82}$$

to obtain the half-density radius. Values for the single-particle skin thickness were obtained by spline interpolation between the values given in Table 1. The experimental deviations from equation (82) and interpolated values from Table 1 are given in Table 2 for several common elements used in scattering experiments.

Nucleon-Nucleon Scattering Amplitude.- The two-body amplitudes required for the present calculations are the proton-proton and proton-neutron scattering amplitudes. In the present work, we neglect the coulomb scattering contribution and use the following form

$$f_i(e,\vec{q}) = \frac{\sqrt{me}}{4\pi}\,\sigma_i(e)\,[\alpha_i(e)+i]\,\exp\left[-\tfrac{1}{2}\,\beta_i(e)\,\vec{q}^{\,2}\right] \tag{83}$$

for $i = np, pp$. The parameters σ_i , α_i and β_i were taken from the compilations of refs. 14 and 15. Graphs of these functions as estimated from refs. 14 and 15 are shown in figures 4 through 9 where the values are shown by dots at descrete energies and the range of experimental uncertainty are indicated by the two curves. The deviation of experimental values from the average values given by

$$\sigma(e) = \tfrac{1}{2}\left[\sigma_{pp}(e) + \sigma_{np}(e)\right] \tag{84}$$

$$\alpha(e) = \left[\sigma_{pp}(e)\,\alpha_{pp}(e) + \sigma_{np}(e)\,\alpha_{np}(e)\right] / \left[\sigma_{pp}(e) + \sigma_{np}(e)\right] \tag{85}$$

$$\beta(e) = \tfrac{1}{2}\left[\beta_{pp}(e) + \beta_{np}(e)\right] \tag{86}$$

are given in Table 3. The uncertainties in Table 3 will be used for the purpose of estimating uncertainty in the present calculations although in the calculations the average two-body amplitude is calculated essentially from equation (54) which deviates slightly from equations (84) and (85). Equation (86) will be used to estimate the average slope parameter for convenience and the error introduced will be negligible since this parameter contributes only a few percent to the nuclear cross sections for energies less than 30 GeV.

NUCLEON-NUCLEUS SCATTERING

The case of nucleon-nucleus scattering will be considered first since a large body of experimental data is available with which to make comparisons. Attention will be given to the targets of carbon, aluminum, copper, and lead since for these the data are most complete. The experimental cross sections are taken from the compilations of Barashenkov et al. (ref. 16) and the experiments of Schimmerling et al. (refs. 17, 18).

The neutron-nucleus scattering cross sections were calculated using the eikonal and coherent approximations discussed previously. The physical data required for the calculations is discussed in the previous section. Using equations (59) and (61), the total and absorption cross sections were calculated for the four aforementioned targets and the comparison of the calculations with the experimental results are shown in figures 10 through 17. The uncertainty in the theoretical results due to uncertainty in the input physical data is indicated by the two curves. These uncertainties in cross sections were estimated by determining the effect of uncertainty in each input parameter separately and using the rms value of each effect to obtain the total uncertainty. This process was done at each of the five energies shown in Table 3 with the results for each of the four targets in Table 4. The curves were obtained by linear interpolation in Table 4. The points between the curves are the cross section values calculated at the indicated energies.

Generally the agreement between the present calculations and experiment are quite good with the largest errors being about 15% which occurs below 300 MeV. This error is suspected to be in part due to the eikonal approximation. For example, the eikonal approximation requires a large number of partial waves to contribute. Note however the even in lead that the angular momentum

$$\ell \simeq k R_{Pb} = 12 \qquad (37)$$

which leads us to anticipate large corrections to the eikonal result. Above 300 MeV, the worst error is for carbon total cross section with differences on the order of 5%. There is a real disagreement for aluminum total cross sections above 300 MeV of a few percent while copper and lead agree within theoretical and experimental uncertainty. These errors may result from the effective potential approximation which tends to overestimate shadow effects.

The results for absorption cross sections show much better agreement with the experimental results. This, of course, is in part due to the greater scatter in the experimental values. Even so it appears that the absorption cross section is more accurately predicted than the elastic cross section. This is especially true below 300 MeV.

The results of comparison with experiments are that the coherent approximation to the elastic channel appears reasonable and that the eikonal approximation to the coherent amplitude is good above 300 MeV for nucleon-nucleus scattering. Below 300 MeV, it is expected that due to the small number of contributing partial waves, that the eikonal approximation contributes an error which is never more than about 15%.

The nucleon-nucleus cross sections are given as a function of energy in Tables 5 through 8.

Nucleus-Nucleus Scattering

On the basis of the approximations discussed in previous sections, we have calculated total and absorption cross sections for selected heavy ions with various target nuclei, the results of which are given in Tables 9-16. An attempt has been made to include projectiles which are likely to be available at heavy ion accelerators and common target materials. At the same time, most of the data of interest to cosmic ray shielding is either contained in the tables or can be obtained by interpolation in nuclear mass number. Although it is difficult to affix an error to the tables at the present time, they may surely be regarded as no worse than about 10% since the largest errors anticipated are due to the eikonal approximation which is most accurate for heavy ion collisions. An accurate assessment must yet await new experimental results.

CONCLUDING REMARKS

The solution of the coupled channel equation for heavy ion reaction has been examined and approximation of the elastic amplitude by neglecting terms related to internal excitation and terms higher than second order in scattering angle was indicated to be accurate. On this basis, the total and absorption cross sections were calculated for scattering nucleons from nuclei and comparison with experiments indicate errors are within 5% above 300 MeV and within 15% above 100 MeV. The 15% errors at low energy are believed due to the eikonal approximation. Tables of heavy ion cross sections were calculated for use in cosmic ray transport studies. The eikonal approximation for heavy ion scattering is believed to be adequate due to the larger number of contributing partial waves even at 100 MeV.

REFERENCES

1. Schaefer, H. J.: Public Health Aspects of Galactic Radiation Exposure at Supersonic Transport Altitudes. Aerosp. Med., vol. 39, no. 12, Dec. 1968, pp. 1298-1303.

2. Space Science Board: Radioboilogical Factors in Manned Space Flight. National Academy of Sciences, Washington, DC 1967. Publication 1487.

3. Curtis, S. B.; and Wilkinson, M. C.: The Heavy Particle Hazard--What Physical Data are needed?. Proceedings of the National Symposium on Natural and Manmade Radiation in Space. Las Vegas, Nevada, March 1-5, 1971. NASA TM X-2440, Jan. 1972.

4. Wilson, J. W.: Multiple Scattering of Heavy Ions, Glauber Theory, and Optical Model. Phys. Lett., vol. 52B, Sept. 1974, pp. 149-152.

5. Wilson, J. W.: Composite Particle Reaction Theory. Ph. D. Thesis, College of William and Mary, 1975. (To be published in Nucl. Phys. B.)

6. Chew, G. F.: High Energy Elastic Proton-Deuteron Scattering. Phys. Rev., second series, vol. 84, no. 5, Dec. 1, 1951, pp. 1057-1058.

7. Watson, K. M.: Multiple Scattering and the Many-Body Problem-Application to Photomeson Production in Complex Nuclei. Phys. Rev., vol. 89, no. 3, Feb. 1953, pp. 575-587.

8. Best, M. E.: Particle-Nucleus Scattering at Intermediate Energies. Con. J. Phys., vol. 50, 1974, pp. 1609-1613.

9. Austern, N.: Direct Reaction Theories, in "Fast Neutron Physics Part II," Ed. by J. B. Marion and J. L. Fowler, Interscience Publishers, New York, 1963, p. 1113.

10. Goldberger, M. L.; and Watson, K. M.: Collision Theory, John Wiley and Sons, New York, 1964, p. 818.

11. Bohr, A.; and Mottelson, B. R.: Nuclear Structure, W. A. Benjamin, Inc., New York, 1969, p. 162.

12. Krylov, V. I.: Approximate Calculation of Integrals. The Macmillan Co., New York, 1962, pp. 129-132.

13. Hofstadter, R.; and Collard, H. R.: Nuclear Radii Determined by Electron Scattering, in Nuclear Radii, Landolt-Bornstein Series, vol. 2, Springer-Verlag, New York, 1967.

14. Hellwege, K. -H. (ed.): Scattering of Elementary Particles, Landolt-Bornstein Series, vol. 7, Springer-Verlag, New York, 1973.

15. Particle Data Group: NN and ND Interactions (above 0.5 GeV/c)-A Compilation. University of California (Berkeley), UCRL-20000 NN, August 1970.

16. Barashenkov, V. S.; Gudima, K. K.; and Toneev, V. D.: Cross Sections for Fast Particles and Atomic Nuclei, Fort. Phys., vol. 17, 1969, pp. 683-725.

17. Schimmerling, W.; Devlin, T. J; Johnson, W. W.; Vosburgh, K. G.; and Mischke, R. E.: Neutron-Nucleus Total Cross Sections from 900 to 2600 MeV/c. Phys. Lett., vol. 37B, no. 2, Nov. 1971, pp. 177-180.

18. Schimmerling, W.; Devlin, T. J.; Johnson, W. W.; Vosburgh, K. G.; and Mischke, R. E.: Neutron-Nucleus Total and Inelastic Cross Sections: 900 to 2600 MeV/c. Phys. Rev., vol. 7C, no. 1, Jan. 1973, pp. 248-262.

TABLE 1.- Nuclear Skin Thickness

$A^{1/3}$	t, fm	$A^{1/3}$	t, fm
1.75	1.81	3.46	2.16
2.02	1.75	3.71	1.90
2.19	1.51	3.90	1.69
2.38	1.19	4.13	1.53
2.46	1.01	4.43	1.67
2.66	0.90	4.73	1.77
2.83	1.08	5.11	1.83
2.94	1.44	5.50	1.80
3.03	1.78	5.86	1.77
3.22	2.06	6.00	1.75

TABLE 2.- Percentage Uncertainty in Nucleon Density Parameters

Target Nucleus	Half-radius (r.5)	Skin Thickness (t)
C	2.7%	2.6%
Al	3.3%	4.6%
Cu	3.2%	7.8%
Pb	3.1%	10.9%

TABLE 3.- Percentage Uncertainty in Nucleon-Nucleon Collision Parameters

Incident Energy GeV/amu	Re fel/Im fel (α)	Nucleon-Nucleon Cross Section (σ)	Slope Parameter (B)
.1	47%	3.4%	7.8%
.5	53%	3.1%	7.1%
1.0	67%	.9%	6.3%
5.0	35%	2.7%	5.1%
10.0	33%	2.1%	6.1%

TABLE 4.- Percentage Uncertainty in Neutron-Nucleus Cross Sections

Incident Energy GeV/amu	C	Al	Cu	Pb
.1	1.8%	2.9%	4.2%	5.0%
.5	1.3%	2.0%	3.0%	4.0%
1.0	1.4%	2.3%	3.3%	4.3%
5.0	1.3%	2.1%	3.2%	4.2%
10.0	1.4%	2.1%	3.1%	4.1%

TABLE 5. - NEUTRON-NUCLEUS. TOTAL CROSS SECTION, MB

ENERGY MEV/AMU	HE	C	O	AL	A	FE	BR	AG	BA	PB
100	178	428	496	805	1128	1349	1670	2094	2457	3215
125	163	401	474	767	1076	1308	1633	2051	2413	3170
150	155	384	459	744	1046	1283	1610	2027	2388	3147
175	142	355	429	697	984	1221	1549	1959	2319	3079
200	128	321	391	636	903	1132	1453	1849	2203	2957
225	120	303	369	602	857	1080	1395	1780	2128	2875
250	115	289	353	576	821	1038	1346	1722	2065	2803
275	111	278	339	555	792	1003	1304	1671	2008	2735
300	108	271	332	542	775	981	1278	1639	1972	2692
350	107	267	326	533	763	964	1257	1612	1941	2653
400	108	268	326	534	764	962	1253	1606	1934	2641
500	118	289	348	570	817	1016	1315	1679	2018	2736
600	128	309	369	605	867	1068	1374	1749	2097	2827
700	133	321	381	624	894	1095	1404	1784	2136	2870
800	138	330	390	639	914	1116	1427	1811	2165	2903
900	141	337	398	651	930	1133	1446	1833	2188	2929
1000	144	342	404	659	941	1145	1459	1849	2206	2948
1250	148	350	413	673	958	1166	1482	1875	2233	2979
1500	150	355	419	680	966	1176	1493	1889	2248	2996
1750	152	358	423	685	972	1183	1502	1899	2259	3009
2000	154	360	426	689	977	1190	1510	1908	2269	3021
2500	154	361	428	691	978	1193	1514	1913	2274	3027
3000	154	360	427	688	974	1189	1511	1909	2269	3023
3500	153	358	425	685	969	1185	1507	1904	2264	3018
4000	152	356	423	681	965	1181	1502	1898	2258	3011
5000	151	353	420	678	960	1175	1496	1892	2251	3004
6000	150	351	417	673	954	1169	1489	1884	2243	2995
7000	148	348	414	668	947	1161	1481	1873	2231	2982
8000	147	346	412	664	941	1155	1473	1865	2222	2971
9000	147	344	410	661	937	1150	1469	1859	2215	2964
10000	147	343	409	659	934	1147	1465	1855	2211	2959
12500	147	342	408	656	930	1142	1460	1848	2204	2952
15000	146	340	406	653	924	1137	1454	1841	2196	2943
17500	146	338	404	649	919	1131	1447	1833	2187	2933
20000	145	337	403	645	913	1125	1441	1825	2179	2923
22500	145	336	402	643	910	1122	1437	1820	2173	2916

TABLE 6. - NEUTRON-NUCLEUS ABSORPTION CROSS SECTION, MB

ENERGY MEV/AMU	HE	C	O	AL	A	FE	BR	AG	BA	PB
100	111	246	271	447	629	726	884	1107	1295	1680
125	102	230	257	422	593	694	851	1067	1252	1633
150	97	222	249	409	577	678	835	1049	1233	1612
175	93	214	242	398	561	663	820	1031	1213	1592
200	90	208	237	388	548	650	807	1015	1197	1574
225	87	203	232	380	537	639	796	1002	1183	1559
250	85	199	228	374	529	632	788	993	1173	1548
275	84	197	226	370	524	627	783	987	1167	1542
300	84	196	225	369	522	625	781	985	1165	1540
350	84	196	225	369	523	626	783	987	1168	1543
400	85	198	228	373	529	631	789	995	1177	1553
500	92	211	241	395	560	661	822	1033	1221	1603
600	99	223	252	413	587	686	849	1065	1257	1643
700	102	230	258	423	601	699	863	1082	1275	1664
800	105	234	262	430	611	709	873	1093	1288	1678
900	107	238	265	436	618	715	880	1102	1297	1688
1000	108	240	268	439	622	720	885	1107	1303	1694
1250	110	243	271	443	626	724	890	1112	1308	1700
1500	111	244	273	444	628	726	892	1114	1310	1703
1750	112	246	274	446	629	728	894	1117	1313	1705
2000	113	246	275	447	630	729	895	1118	1314	1707
2500	113	247	276	447	629	729	895	1117	1313	1706
3000	113	246	275	445	626	727	893	1115	1310	1703
3500	112	245	274	443	624	725	891	1112	1307	1700
4000	112	244	274	442	622	723	890	1111	1306	1699
5000	111	243	273	441	621	722	889	1110	1305	1698
6000	111	242	272	440	619	720	887	1108	1303	1696
7000	110	241	271	438	617	718	885	1105	1300	1692
8000	110	241	271	437	615	717	883	1103	1298	1690
9000	110	240	271	437	614	717	883	1103	1298	1690
10000	110	241	271	437	615	717	884	1103	1298	1691
12500	111	241	272	438	615	718	885	1105	1300	1693
15000	111	241	273	438	614	718	886	1105	1300	1694
17500	111	241	273	437	613	717	885	1104	1299	1693
20000	111	241	273	437	612	716	885	1104	1298	1692
22500	111	241	273	437	612	716	885	1104	1299	1693

TABLE 7. - PROTON-NUCLEUS TOTAL CROSS SECTION, MB

ENERGY MEV/AMU	HE	C	O	AL	A	FE	BR	AG	BA	PB
100	178	428	496	817	1171	1377	1716	2148	2540	3319
125	163	401	474	780	1122	1337	1681	2106	2494	3267
150	155	384	459	756	1088	1310	1656	2078	2464	3234
175	142	355	429	707	1020	1246	1592	2008	2390	3160
200	128	321	391	644	931	1151	1488	1889	2263	3028
225	120	303	369	609	880	1097	1425	1816	2182	2940
250	115	289	353	581	841	1052	1373	1753	2111	2859
275	111	278	339	559	808	1014	1325	1696	2045	2779
300	108	271	332	546	789	991	1295	1659	2002	2727
350	107	267	326	536	773	971	1269	1626	1963	2677
400	108	268	326	536	772	967	1262	1616	1949	2658
500	118	289	348	569	816	1014	1311	1673	2008	2721
600	128	309	369	603	861	1062	1363	1734	2074	2795
700	133	321	381	622	886	1089	1393	1770	2114	2840
800	138	330	390	637	907	1111	1417	1799	2146	2878
900	141	337	398	649	923	1128	1437	1822	2173	2909
1000	144	342	404	658	936	1142	1453	1841	2194	2934
1250	148	350	413	673	957	1165	1482	1875	2234	2981
1500	150	355	419	680	967	1177	1496	1893	2254	3006
1750	152	358	423	685	973	1185	1506	1904	2267	3020
2000	154	360	426	690	979	1192	1515	1914	2278	3034
2500	154	361	428	691	981	1196	1520	1920	2285	3043
3000	154	360	427	689	978	1193	1518	1918	2283	3041
3500	153	358	425	686	974	1189	1514	1913	2278	3036
4000	152	356	423	682	969	1184	1508	1906	2270	3027
5000	151	353	420	678	962	1177	1499	1896	2258	3014
6000	150	351	417	674	956	1170	1492	1887	2249	3002
7000	148	348	414	668	949	1163	1484	1877	2238	2990
8000	147	346	412	664	943	1156	1476	1869	2228	2979
9000	147	344	410	661	939	1152	1471	1862	2221	2970
10000	147	343	409	659	935	1148	1466	1857	2214	2963
12500	147	342	408	656	929	1142	1459	1847	2202	2949
15000	146	340	406	652	923	1136	1452	1839	2193	2938
17500	146	338	404	648	917	1130	1445	1830	2183	2928
20000	145	337	403	645	912	1124	1439	1823	2175	2918
22500	145	336	402	643	909	1121	1435	1818	2170	2912

TABLE 8. - PROTON-NUCLEUS ABSORPTION CROSS SECTION, MB

ENERGY MEV/AMU	HE	C	O	AL	A	FE	BR	AG	BA	PB
100	111	246	271	452	647	738	905	1133	1336	1731
125	102	230	257	426	611	705	872	1093	1292	1684
150	97	222	249	414	593	688	854	1072	1268	1658
175	93	214	242	401	575	672	837	1052	1246	1633
200	90	208	237	391	561	659	823	1035	1227	1612
225	87	203	232	383	549	648	811	1022	1212	1596
250	85	199	228	377	540	640	803	1011	1201	1583
275	84	197	226	373	535	634	797	1004	1193	1574
300	84	196	225	371	531	631	793	1000	1188	1569
350	84	196	225	371	531	631	793	999	1187	1567
400	85	198	228	375	536	636	798	1005	1192	1573
500	92	211	241	395	562	662	824	1035	1224	1607
600	99	223	252	413	585	685	847	1062	1252	1637
700	102	230	258	423	598	697	859	1077	1268	1654
800	105	234	262	429	607	706	868	1087	1279	1667
900	107	238	265	434	614	713	875	1095	1288	1676
1000	108	240	268	438	618	717	880	1101	1294	1683
1250	110	243	271	442	624	723	887	1108	1302	1693
1500	111	244	273	444	626	725	890	1112	1307	1698
1750	112	246	274	446	628	727	893	1115	1310	1702
2000	113	246	275	447	629	729	894	1117	1312	1704
2500	113	247	276	447	628	729	895	1117	1313	1706
3000	113	246	275	445	626	727	893	1115	1311	1704
3500	112	245	274	444	624	725	891	1113	1308	1701
4000	112	244	274	442	622	723	890	1111	1306	1698
5000	111	243	273	441	620	722	887	1108	1303	1695
6000	111	242	272	440	618	720	885	1106	1300	1692
7000	110	241	271	438	616	718	883	1103	1297	1689
8000	110	241	271	437	614	716	882	1102	1295	1687
9000	110	240	271	437	614	716	882	1101	1295	1686
10000	110	241	271	437	614	716	882	1101	1295	1686
12500	111	241	272	437	614	716	882	1102	1295	1687
15000	111	241	273	437	613	716	883	1102	1296	1688
17500	111	241	273	437	612	716	883	1102	1295	1687
20000	111	241	273	436	611	715	882	1101	1294	1687
22500	111	241	273	436	611	715	882	1101	1294	1687

TABLE 9.- HELIUM-NUCLEUS TOTAL CROSS SECTION, MB

ENERGY MEV/AMU	HE	C	O	AL	A	FE	BR	AG	BA	PB
100	466	880	953	1432	1938	2154	2544	3092	3557	4462
125	442	848	924	1389	1881	2101	2491	3030	3491	4390
150	428	830	907	1365	1849	2072	2461	2995	3453	4349
175	403	797	876	1321	1791	2016	2404	2930	3382	4272
200	372	753	834	1262	1714	1943	2327	2842	3287	4168
225	353	727	809	1226	1669	1899	2282	2790	3231	4106
250	339	705	788	1197	1631	1863	2244	2747	3184	4055
275	327	686	770	1171	1598	1831	2210	2708	3142	4009
300	320	674	759	1155	1577	1810	2189	2684	3116	3980
350	315	665	749	1141	1559	1793	2171	2663	3093	3955
400	315	663	747	1139	1556	1790	2167	2659	3089	3950
500	336	693	775	1178	1607	1838	2217	2716	3151	4018
600	357	723	804	1218	1658	1888	2269	2776	3215	4088
700	368	739	820	1240	1687	1916	2298	2809	3251	4127
800	377	752	833	1258	1710	1938	2321	2835	3279	4159
900	384	763	843	1272	1728	1955	2339	2856	3302	4184
1000	390	771	851	1283	1741	1969	2354	2872	3319	4203
1250	399	785	865	1301	1764	1992	2378	2900	3349	4236
1500	404	792	873	1311	1776	2004	2392	2915	3365	4254
1750	407	798	879	1318	1784	2013	2402	2926	3377	4268
2000	410	802	884	1325	1791	2021	2410	2935	3387	4279
2500	412	805	888	1328	1795	2026	2416	2941	3394	4287
3000	411	804	887	1327	1792	2024	2414	2939	3391	4285
3500	409	802	885	1324	1789	2021	2411	2935	3387	4280
4000	408	800	883	1321	1784	2016	2407	2930	3382	4274
5000	405	796	880	1316	1778	2011	2401	2924	3375	4266
6000	403	793	876	1311	1772	2005	2395	2917	3367	4258
7000	400	788	872	1306	1765	1998	2388	2908	3358	4248
8000	398	785	869	1301	1759	1992	2382	2902	3351	4241
9000	396	783	868	1299	1755	1989	2379	2898	3347	4236
10000	396	782	867	1297	1753	1987	2377	2896	3345	4234
12500	395	781	866	1295	1749	1985	2375	2893	3342	4231
15000	394	780	866	1293	1746	1982	2373	2891	3339	4228
17500	392	777	864	1290	1741	1979	2370	2886	3334	4224
20000	391	775	863	1287	1737	1975	2366	2883	3330	4219
22500	390	774	862	1286		1973	2365	2881	3328	4217

TABLE 10. - HELIUM-NUCLEUS ABSORPTION CROSS SECTION, MB

ENERGY MEV/AMU	HE	C	O	AL	A	FE	BR	AG	BA	PB
100	269	487	519	778	1054	1153	1348	1635	1875	2335
125	252	464	498	747	1013	1115	1310	1590	1827	2283
150	244	453	487	733	993	1097	1291	1569	1804	2257
175	236	443	478	719	975	1080	1274	1549	1781	2234
200	230	434	470	707	959	1066	1259	1532	1763	2214
225	225	427	464	698	947	1054	1248	1519	1749	2198
250	221	422	459	691	938	1046	1239	1509	1738	2186
275	219	419	456	687	932	1041	1234	1502	1731	2179
300	218	418	455	685	930	1038	1231	1499	1728	2176
350	218	418	455	686	930	1039	1232	1500	1729	2177
400	221	422	458	690	936	1045	1238	1507	1736	2185
500	234	440	476	714	968	1075	1269	1543	1775	2226
600	246	456	491	736	996	1101	1296	1574	1808	2263
700	252	465	499	748	1011	1116	1311	1591	1827	2284
800	257	471	505	756	1022	1126	1322	1603	1840	2298
900	260	476	510	762	1030	1134	1329	1612	1850	2309
1000	263	479	513	766	1036	1139	1335	1619	1857	2316
1250	266	483	517	772	1042	1145	1342	1626	1865	2325
1500	267	485	520	774	1045	1149	1346	1630	1869	2330
1750	269	487	522	777	1047	1151	1349	1633	1873	2334
2000	270	488	523	778	1048	1153	1351	1636	1875	2337
2500	270	489	524	778	1048	1153	1351	1636	1876	2338
3000	269	488	523	777	1046	1152	1350	1634	1873	2335
3500	268	487	522	775	1043	1150	1348	1632	1871	2333
4000	267	486	521	774	1042	1148	1346	1630	1869	2331
5000	267	485	521	773	1040	1146	1345	1628	1867	2328
6000	266	483	519	771	1038	1144	1343	1625	1864	2325
7000	265	482	518	769	1035	1142	1340	1623	1861	2322
8000	264	481	517	768	1033	1141	1339	1621	1859	2320
9000	264	481	517	768	1033	1141	1339	1621	1859	2320
10000	264	481	518	768	1033	1141	1339	1621	1860	2321
12500	265	483	519	769	1034	1142	1341	1623	1862	2323
15000	266	483	520	770	1034	1143	1343	1624	1863	2325
17500	266	483	521	770	1034	1143	1343	1624	1863	2325
20000	265	483	521	770	1033	1143	1343	1624	1863	2325
22500	266	484	522	770	1033	1143	1343	1625	1863	2326

TABLE 11. - CARBON-NUCLEUS TOTAL CROSS SECTION, MB

ENERGY MEV/AMU	HE	C	O	AL	A	FE	BR	AG	BA	PB
100	880	1441	1523	2150	2802	3029	3480	4130	4671	5697
125	848	1402	1487	2099	2736	2969	3420	4062	4598	5619
150	830	1379	1466	2071	2699	2935	3386	4023	4556	5574
175	797	1338	1428	2019	2633	2873	3323	3951	4479	5491
200	753	1283	1376	1950	2546	2791	3239	3856	4378	5381
225	726	1251	1346	1909	2494	2742	3189	3800	4317	5316
250	705	1224	1321	1876	2452	2702	3148	3754	4268	5263
275	686	1201	1299	1846	2416	2667	3112	3713	4224	5215
300	674	1187	1285	1828	2393	2645	3089	3688	4197	5186
350	664	1175	1274	1813	2374	2628	3071	3667	4175	5162
400	663	1173	1272	1811	2372	2625	3068	3664	4171	5158
500	692	1209	1306	1857	2430	2680	3124	3727	4239	5231
600	722	1247	1341	1904	2489	2736	3181	3792	4309	5306
700	739	1267	1361	1930	2522	2767	3213	3828	4347	5348
800	752	1284	1377	1951	2547	2792	3239	3857	4378	5382
900	762	1297	1390	1967	2568	2812	3260	3880	4403	5408
1000	770	1307	1400	1980	2584	2827	3276	3898	4422	5429
1250	784	1325	1418	2002	2610	2853	3303	3928	4454	5465
1500	792	1335	1428	2014	2624	2868	3319	3945	4473	5485
1750	797	1342	1435	2023	2634	2878	3330	3958	4486	5500
2000	802	1348	1442	2030	2642	2887	3340	3969	4498	5513
2500	805	1352	1447	2036	2648	2894	3347	3976	4505	5522
3000	804	1351	1446	2034	2645	2892	3346	3974	4503	5520
3500	802	1349	1444	2031	2641	2888	3343	3970	4499	5516
4000	799	1346	1441	2027	2635	2884	3338	3965	4493	5509
5000	796	1341	1437	2022	2629	2877	3331	3958	4486	5501
6000	792	1337	1433	2016	2622	2871	3325	3950	4478	5493
7000	788	1332	1429	2010	2614	2863	3317	3941	4468	5483
8000	785	1328	1425	2005	2608	2857	3311	3935	4461	5475
9000	783	1326	1423	2002	2604	2854	3308	3931	4457	5471
10000	782	1325	1423	2001	2602	2853	3307	3929	4455	5469
12500	780	1324	1422	1999	2599	2851	3306	3928	4454	5467
15000	779	1323	1422	1998	2596	2849	3305	3926	4452	5466
17500	777	1321	1421	1995	2592	2846	3302	3923	4448	5462
20000	775	1319	1419	1993	2588	2843	3299	3919	4444	5458
22500	774	[illegible]	[illegible]	1991	[illegible]	[illegible]	[illegible]	[illegible]	[illegible]	[illegible]

TABLE 12. - CARBON-NUCLEUS ABSORPTION CROSS SECTION, MB

ENERGY MEV/AMU	HE	C	O	AL	A	FE	BR	AG	BA	PB
100	486	778	814	1148	1500	1603	1828	2166	2444	2964
125	464	750	788	1113	1453	1560	1784	2116	2391	2907
150	453	737	775	1095	1430	1539	1764	2093	2366	2880
175	442	724	763	1079	1409	1520	1744	2071	2341	2854
200	434	713	754	1066	1391	1504	1728	2052	2322	2833
225	427	705	746	1055	1377	1491	1715	2037	2306	2816
250	422	698	740	1047	1367	1481	1706	2027	2294	2804
275	419	695	737	1042	1361	1476	1700	2020	2287	2796
300	417	693	735	1040	1358	1473	1697	2017	2284	2792
350	418	693	736	1040	1358	1474	1698	2018	2285	2793
400	421	698	740	1046	1365	1480	1704	2025	2293	2802
500	439	720	761	1074	1401	1514	1739	2064	2335	2847
600	455	740	780	1099	1434	1544	1769	2099	2372	2887
700	464	751	790	1113	1452	1561	1786	2118	2392	2909
800	471	759	798	1123	1464	1573	1799	2132	2407	2925
900	475	765	803	1131	1474	1581	1808	2142	2418	2937
1000	479	769	807	1136	1480	1588	1814	2149	2426	2945
1250	483	775	813	1142	1487	1595	1822	2158	2435	2955
1500	485	777	816	1146	1491	1599	1826	2163	2440	2961
1750	487	780	819	1148	1494	1603	1830	2166	2444	2965
2000	488	781	820	1150	1495	1605	1833	2169	2447	2969
2500	488	782	821	1151	1495	1605	1834	2170	2448	2970
3000	487	781	821	1149	1493	1604	1832	2168	2445	2968
3500	486	779	819	1148	1490	1601	1830	2165	2443	2965
4000	485	778	818	1146	1488	1599	1828	2163	2440	2963
5000	484	777	817	1144	1486	1598	1826	2161	2438	2960
6000	483	775	816	1143	1484	1595	1824	2159	2435	2957
7000	482	774	814	1140	1481	1593	1821	2156	2432	2954
8000	481	773	813	1139	1479	1591	1820	2154	2430	2952
9000	481	773	814	1139	1479	1591	1820	2154	2430	2952
10000	481	773	814	1140	1479	1592	1821	2154	2431	2953
12500	482	775	816	1141	1480	1594	1823	2157	2433	2955
15000	483	776	818	1142	1481	1595	1825	2159	2435	2958
17500	483	776	818	1143	1481	1595	1825	2159	2435	2958
20000	483	776	818	1143	1480	1595	1826	2159	2435	2958
22500	483	777	819	1143	1481	1595	1826	2159	2435	2958

TABLE 13. - OXYGEN-NUCLEUS TOTAL CROSS SECTION, MB

ENERGY MEV/AMU	HE	C	O	AL	A	FE	BR	AG	BA	PB
100	954	1526	1594	2252	2946	3153	3591	4268	4819	5849
125	924	1490	1562	2205	2883	3096	3537	4204	4750	5776
150	907	1469	1544	2179	2847	3065	3505	4167	4710	5734
175	876	1430	1509	2130	2783	3006	3447	4100	4638	5657
200	834	1379	1461	2065	2699	2928	3369	4010	4542	5554
225	809	1348	1433	2026	2649	2882	3322	3957	4485	5493
250	789	1323	1409	1994	2609	2844	3284	3914	4439	5443
275	771	1301	1389	1967	2574	2811	3250	3876	4398	5399
300	759	1287	1376	1949	2552	2791	3229	3852	4373	5372
350	750	1276	1365	1935	2534	2774	3212	3833	4352	5349
400	748	1274	1364	1933	2531	2771	3209	3830	4349	5346
500	776	1309	1396	1977	2588	2824	3262	3890	4413	5415
600	804	1344	1428	2021	2645	2877	3316	3951	4479	5486
700	821	1364	1447	2046	2677	2907	3346	3986	4516	5526
800	833	1380	1462	2066	2703	2931	3371	4014	4546	5558
900	844	1393	1474	2082	2723	2950	3390	4036	4570	5584
1000	852	1403	1484	2095	2738	2965	3406	4053	4588	5604
1250	866	1420	1501	2116	2764	2991	3433	4083	4620	5639
1500	874	1430	1512	2129	2779	3006	3449	4100	4639	5659
1750	880	1438	1520	2138	2789	3017	3461	4114	4652	5675
2000	885	1444	1527	2146	2798	3026	3471	4125	4664	5688
2500	888	1449	1532	2152	2803	3033	3479	4133	4673	5697
3000	888	1449	1533	2151	2801	3032	3478	4131	4671	5696
3500	886	1447	1531	2148	2797	3029	3475	4128	4668	5693
4000	884	1444	1529	2145	2793	3024	3471	4123	4662	5687
5000	880	1440	1525	2140	2786	3019	3465	4116	4655	5679
6000	877	1436	1521	2135	2780	3012	3459	4109	4648	5671
7000	873	1431	1517	2129	2772	3005	3452	4101	4639	5662
8000	870	1427	1514	2124	2766	3000	3447	4095	4632	5655
9000	868	1426	1512	2122	2762	2997	3444	4092	4629	5652
10000	868	1425	1512	2121	2760	2996	3443	4091	4628	5650
12500	867	1425	1513	2120	2758	2995	3443	4090	4627	5650
15000	866	1424	1514	2120	2756	2995	3444	4090	4627	5650
17500	865	1423	1513	2118	2753	2993	3442	4088	4624	5648
20000	863	1421	1512	2116	2749	2990	3440	4085	4621	5645
22500	863	1421	1512	2115	2748	2989	3440	4084	4620	5644

TABLE 14. - OXYGEN-NUCLEUS ABSORPTION CROSS SECTION, MB

ENERGY MEV/AMU	HE	C	O	AL	A	FE	BR	AG	BA	PB
100	519	816	842	1194	1569	1659	1875	2229	2511	3032
125	498	790	819	1160	1523	1619	1835	2182	2461	2979
150	488	777	808	1144	1501	1599	1816	2160	2438	2954
175	478	765	797	1129	1481	1581	1799	2139	2415	2930
200	470	755	789	1117	1464	1566	1784	2122	2396	2910
225	464	748	782	1107	1451	1554	1772	2108	2382	2895
250	459	742	777	1099	1441	1545	1763	2098	2371	2883
275	456	738	774	1095	1435	1540	1758	2092	2364	2876
300	455	737	772	1093	1432	1537	1756	2089	2361	2873
350	456	737	773	1093	1433	1538	1756	2090	2362	2874
400	459	741	777	1099	1439	1544	1763	2097	2370	2882
500	476	763	796	1126	1475	1577	1795	2134	2410	2925
600	491	782	813	1149	1506	1605	1823	2167	2445	2962
700	500	792	823	1163	1523	1621	1839	2185	2464	2983
800	506	800	830	1172	1536	1633	1851	2198	2479	2999
900	510	805	835	1179	1545	1641	1859	2208	2489	3010
1000	514	809	839	1184	1551	1647	1866	2215	2496	3018
1250	518	815	845	1191	1559	1655	1874	2224	2506	3028
1500	520	818	848	1194	1562	1659	1878	2229	2511	3034
1750	522	821	851	1197	1566	1663	1882	2233	2516	3039
2000	524	822	853	1199	1568	1665	1885	2236	2519	3043
2500	524	823	855	1201	1568	1666	1887	2238	2520	3044
3000	524	823	854	1199	1566	1665	1886	2236	2518	3043
3500	523	821	853	1198	1563	1663	1884	2234	2516	3040
4000	522	820	852	1196	1561	1661	1882	2232	2514	3038
5000	521	819	851	1195	1559	1659	1881	2230	2512	3036
6000	520	818	850	1193	1557	1657	1879	2227	2509	3033
7000	519	816	849	1191	1554	1655	1876	2225	2506	3030
8000	518	815	848	1190	1553	1654	1875	2223	2504	3028
9000	518	815	849	1190	1552	1654	1875	2223	2504	3028
10000	518	816	849	1191	1553	1654	1876	2224	2506	3029
12500	520	818	852	1193	1554	1657	1879	2227	2508	3033
15000	521	819	854	1194	1555	1659	1881	2229	2511	3035
17500	521	820	854	1195	1555	1659	1882	2230	2511	3036
20000	521	820	855	1195	1555	1659	1883	2230	2512	3037
22500	522	821	854	1195						

TABLE 15. - NITROGEN-NUCLEUS TOTAL CROSS SECTION, MB

ENERGY MEV/AMU	HE	C	O	AL	A	FE	BR	AG	BA	PB
100	914	1480	1554	2195	2870	3084	3526	4190	4736	5762
125	884	1442	1520	2147	2805	3027	3470	4125	4665	5687
150	867	1421	1501	2120	2769	2994	3437	4087	4625	5644
175	835	1381	1464	2069	2704	2934	3377	4018	4551	5565
200	793	1328	1415	2003	2620	2855	3297	3927	4453	5460
225	767	1297	1386	1964	2569	2808	3249	3873	4395	5397
250	746	1271	1362	1932	2528	2769	3210	3829	4348	5346
275	728	1249	1341	1903	2493	2736	3175	3789	4306	5300
300	716	1235	1328	1886	2470	2715	3154	3765	4280	5272
350	707	1223	1317	1871	2452	2697	3136	3745	4258	5249
400	705	1222	1315	1869	2450	2695	3133	3742	4255	5246
500	734	1257	1348	1914	2507	2748	3187	3804	4321	5317
600	763	1293	1382	1959	2564	2802	3242	3866	4388	5389
700	779	1313	1401	1984	2597	2833	3273	3901	4425	5430
800	792	1329	1416	2004	2622	2857	3298	3929	4455	5462
900	802	1342	1429	2021	2643	2876	3318	3952	4480	5488
1000	810	1352	1438	2033	2658	2891	3334	3969	4498	5508
1250	824	1370	1456	2055	2684	2917	3361	3999	4530	5544
1500	831	1380	1466	2067	2698	2932	3376	4016	4549	5564
1750	837	1387	1474	2076	2708	2943	3388	4029	4562	5579
2000	842	1394	1481	2084	2717	2952	3398	4040	4574	5592
2500	845	1398	1486	2089	2722	2958	3406	4048	4582	5601
3000	845	1397	1486	2088	2720	2957	3405	4046	4580	5600
3500	843	1395	1484	2086	2716	2954	3402	4043	4577	5596
4000	840	1392	1481	2082	2711	2949	3397	4038	4571	5590
5000	837	1388	1478	2077	2705	2943	3391	4031	4564	5582
6000	834	1384	1474	2071	2698	2937	3385	4024	4556	5574
7000	830	1379	1469	2065	2690	2930	3378	4015	4547	5564
8000	827	1375	1466	2061	2684	2924	3372	4009	4540	5557
9000	825	1374	1464	2058	2680	2921	3370	4006	4537	5553
10000	824	1373	1464	2057	2678	2920	3368	4004	4535	5552
12500	823	1372	1464	2056	2676	2919	3368	4003	4534	5551
15000	822	1371	1465	2055	2674	2918	3368	4003	4533	5551
17500	820	1370	1464	2053	2670	2915	3366	4000	4530	5548
20000	819	1368	1463	2051	2666	2913	3363	3997	4527	5545
22500	818	1367	1462	2050	2664	2911	3362	3996	4526	5543

TABLE 16. - NITROGEN-NUCLEUS ABSORPTION CROSS SECTION, MB

ENERGY MEV/AMU	HE	C	O	AL	A	FE	BR	AG	BA	PB
100	501	795	824	1167	1531	1627	1845	2192	2472	2992
125	479	768	800	1133	1485	1586	1804	2145	2421	2937
150	469	755	789	1116	1463	1566	1785	2122	2397	2911
175	459	742	778	1101	1443	1547	1766	2100	2374	2887
200	451	732	769	1088	1425	1531	1751	2083	2355	2866
225	444	724	761	1078	1412	1519	1739	2069	2340	2850
250	440	718	756	1070	1402	1510	1730	2058	2329	2838
275	437	715	753	1066	1396	1505	1724	2052	2321	2831
300	435	713	751	1063	1393	1502	1722	2049	2318	2828
350	436	714	752	1064	1393	1503	1723	2050	2319	2829
400	439	718	756	1069	1400	1509	1729	2057	2327	2837
500	457	739	776	1097	1436	1542	1762	2095	2368	2881
600	472	759	794	1121	1467	1571	1791	2128	2404	2919
700	481	769	804	1135	1485	1588	1808	2147	2424	2941
800	487	777	811	1144	1497	1599	1819	2160	2438	2956
900	491	783	816	1151	1506	1608	1828	2170	2449	2967
1000	495	787	820	1157	1513	1614	1834	2177	2456	2975
1250	499	792	826	1163	1520	1621	1842	2186	2465	2986
1500	501	795	829	1166	1524	1625	1847	2191	2470	2992
1750	503	798	832	1169	1527	1629	1851	2195	2475	2996
2000	504	799	834	1171	1529	1631	1854	2198	2478	3000
2500	505	800	835	1172	1529	1632	1855	2199	2479	3001
3000	504	799	834	1171	1527	1631	1854	2197	2477	2999
3500	503	798	833	1169	1524	1629	1852	2195	2474	2997
4000	502	797	832	1168	1522	1627	1850	2193	2472	2995
5000	501	796	831	1166	1520	1625	1848	2191	2470	2992
6000	500	794	830	1164	1518	1623	1846	2188	2467	2989
7000	499	793	829	1163	1515	1620	1844	2186	2464	2986
8000	498	792	828	1161	1513	1619	1842	2184	2463	2984
9000	498	792	828	1161	1513	1619	1843	2184	2463	2984
10000	498	792	829	1162	1514	1620	1844	2185	2464	2985
12500	500	794	831	1164	1515	1622	1846	2188	2466	2989
15000	501	795	833	1165	1516	1623	1848	2189	2468	2991
17500	501	796	834	1166	1516	1624	1849	2190	2469	2992
20000	501	796	834	1166	1515	1624	1849	2190	2469	2992
22500	501	797	835	1166	1516	1625	1850	2191	2470	2993

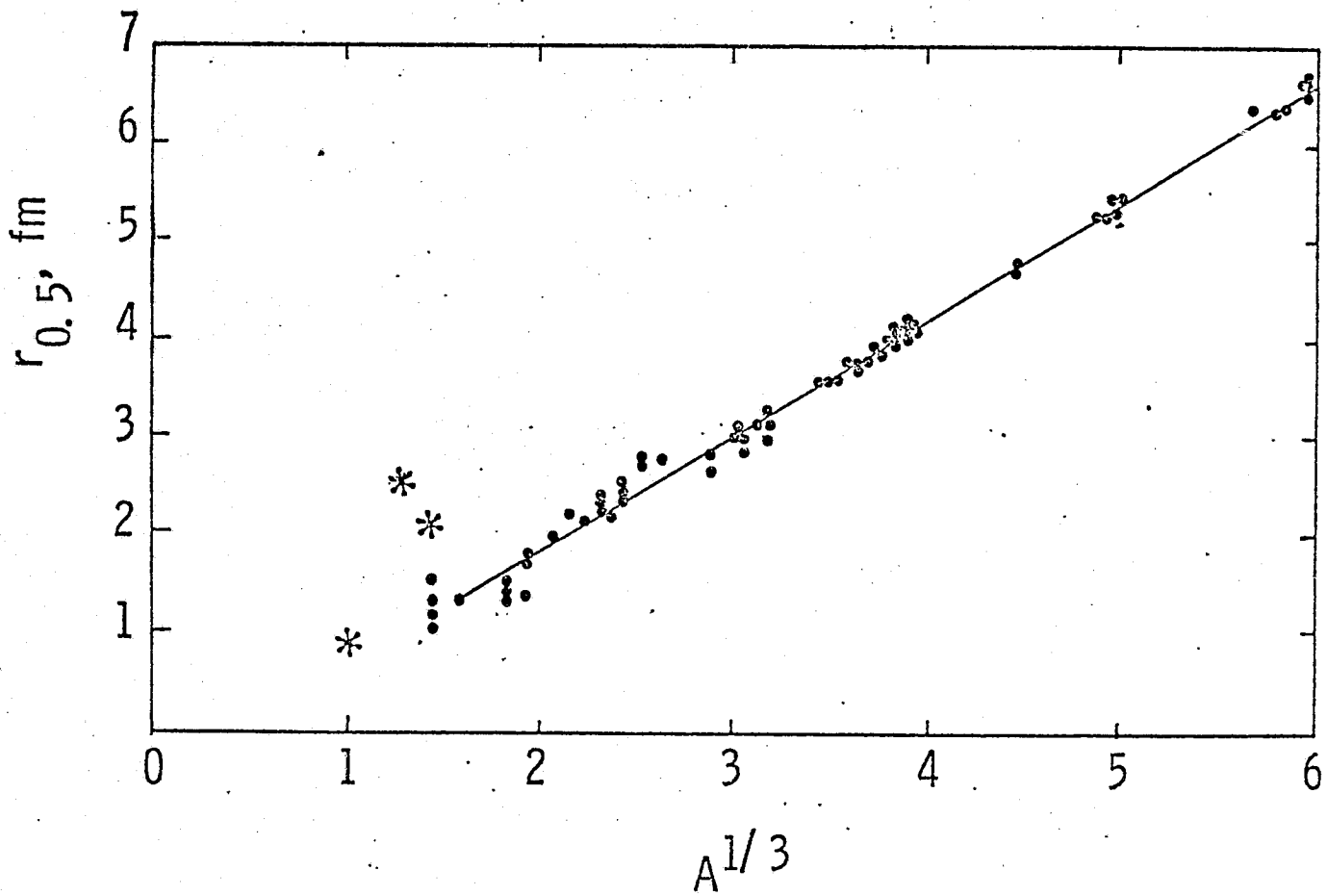

Fig. 1 Nuclear half-density radius as a function of mass number. Solid curve is used above He^4. Stars are values below He^4 obtained from assumed Gaussian density. Dots are data tabulated by Hofstadter and Collard.

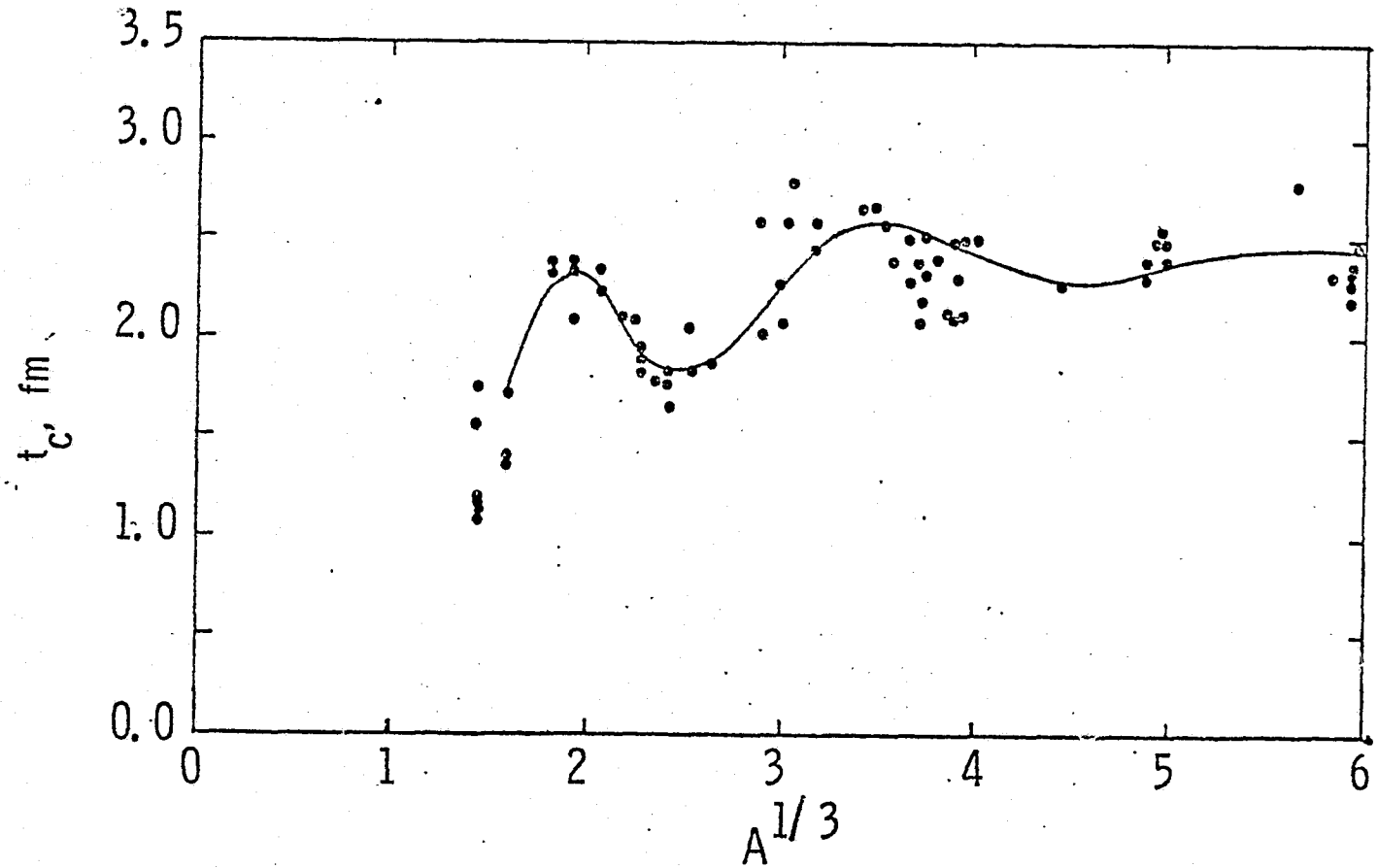

Fig. 2. Charge skin thickness as a function of mass number. Solid curve is used above He^4. Dots are data tabulated by Hofstadter and Collard.

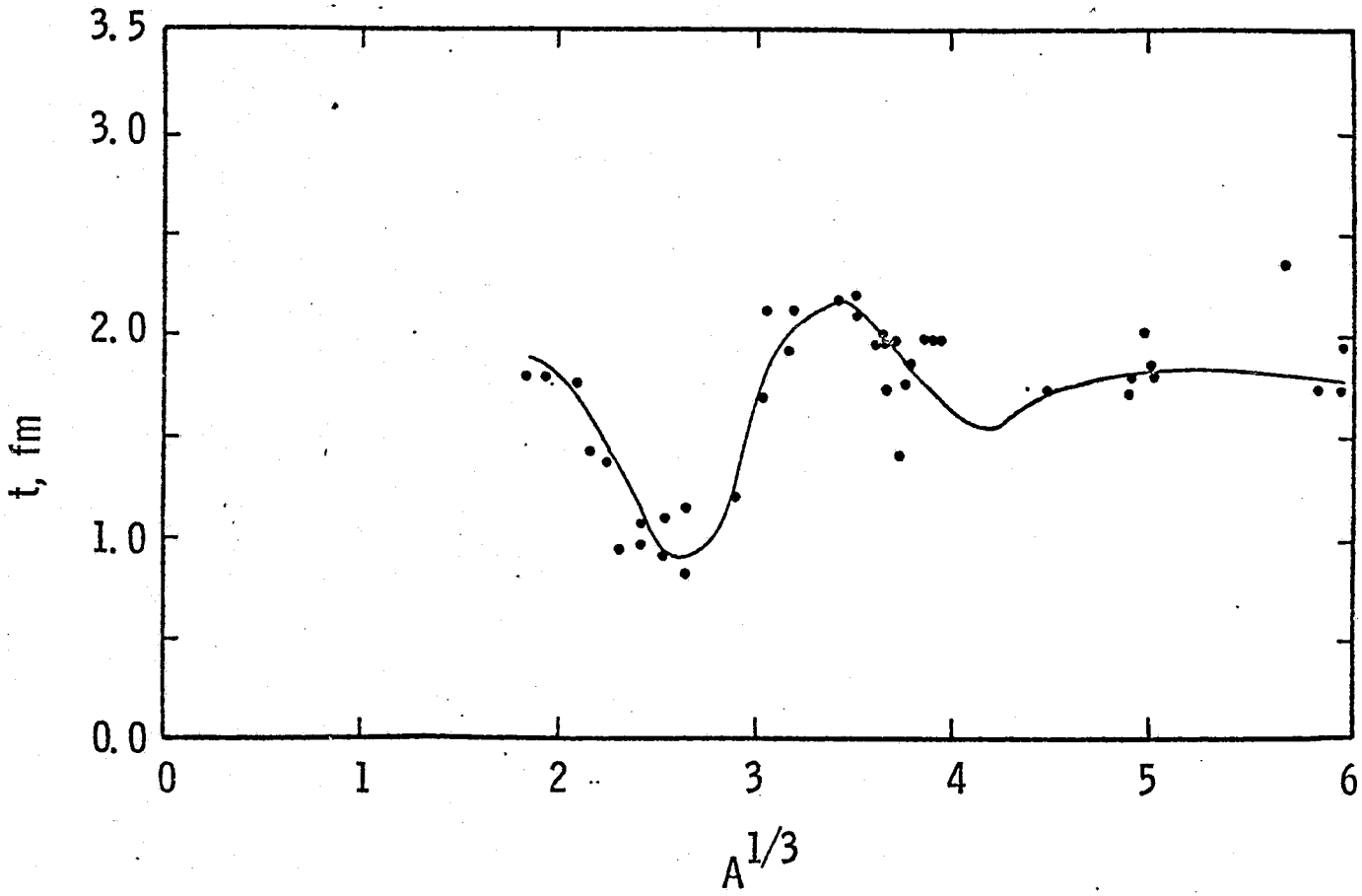

Fig. 3 Nuclear skin thickness as a function of mass number. Solid curve is used in the calculations. Dots are values determined from the tabulated values of Hofstadter and Collard.

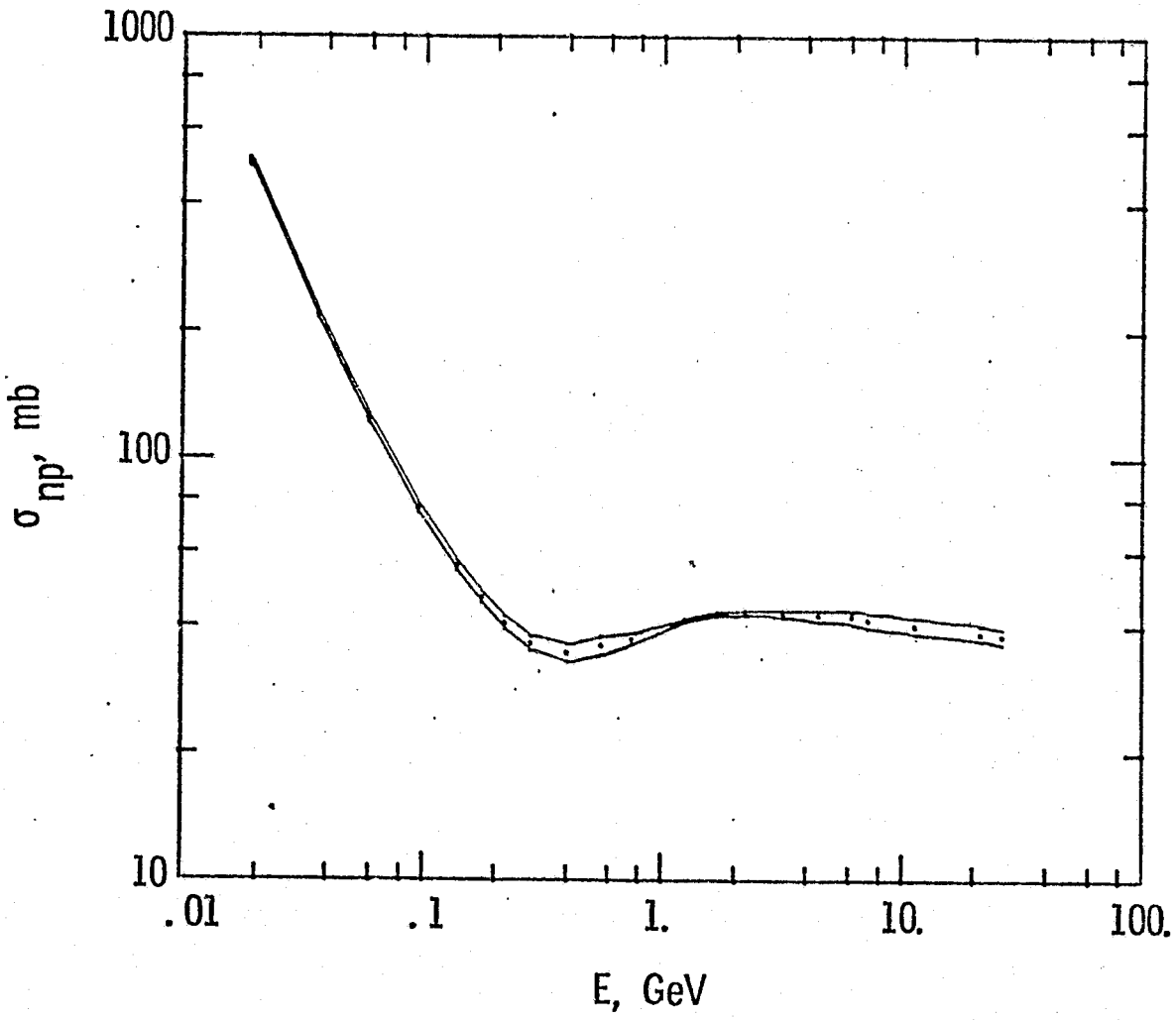

Fig. 4. Neutron-proton total cross section as a function of laboratory energy.

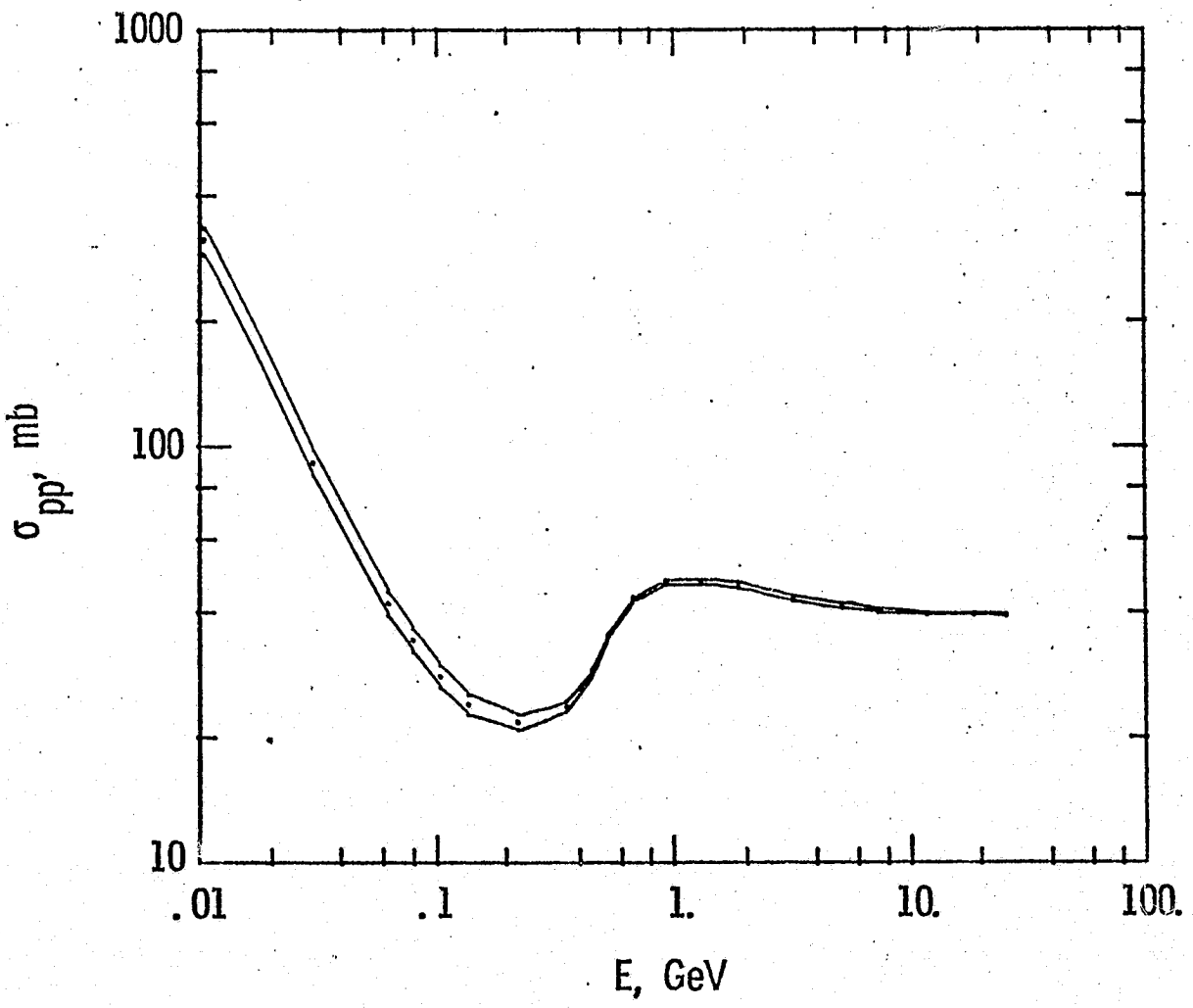

Fig. 5. Proton-proton total cross section as a function of laboratory energy.

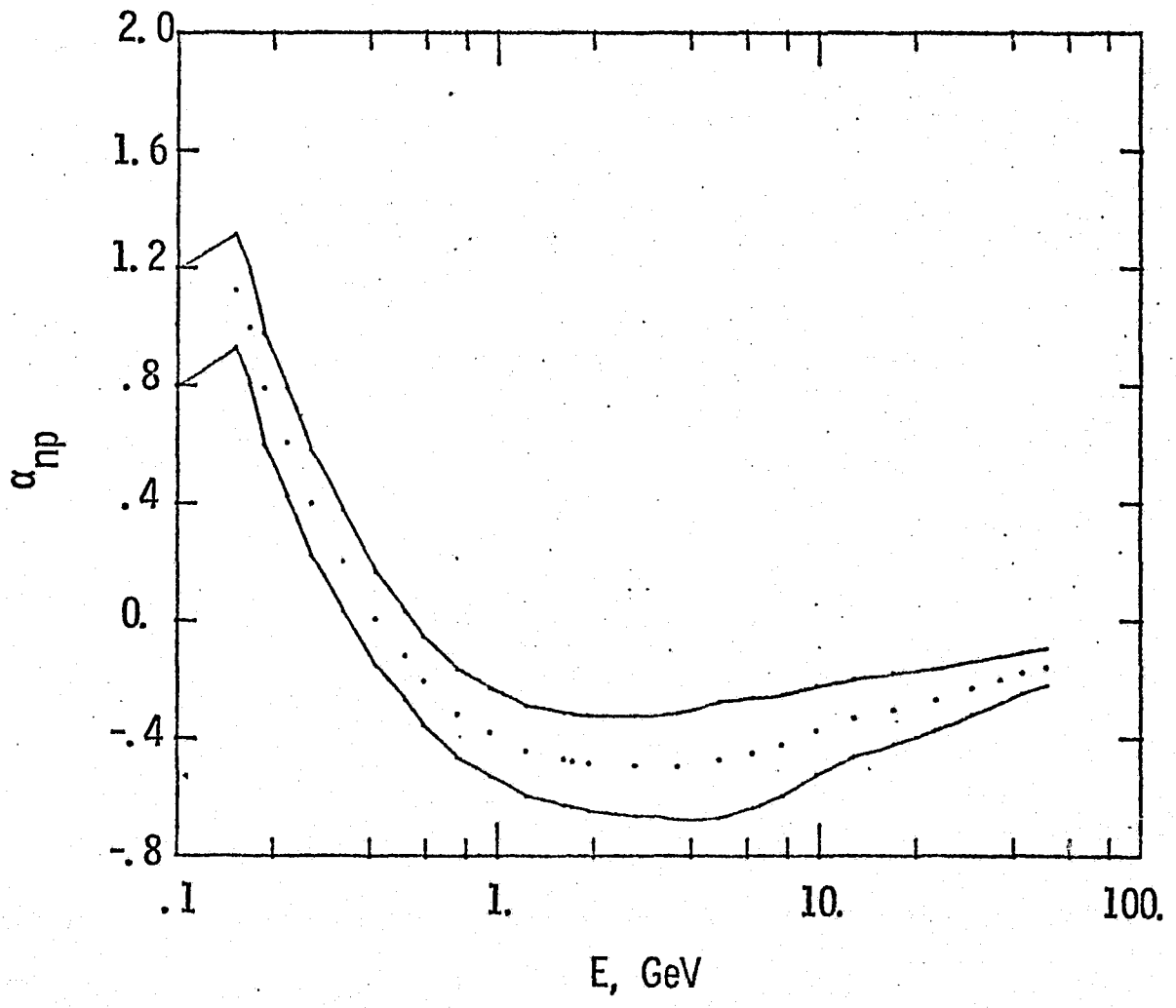

Fig. 6. Ratio of real-to-imaginary part of the forward neutron-proton scattering amplitude as a function of laboratory energy.

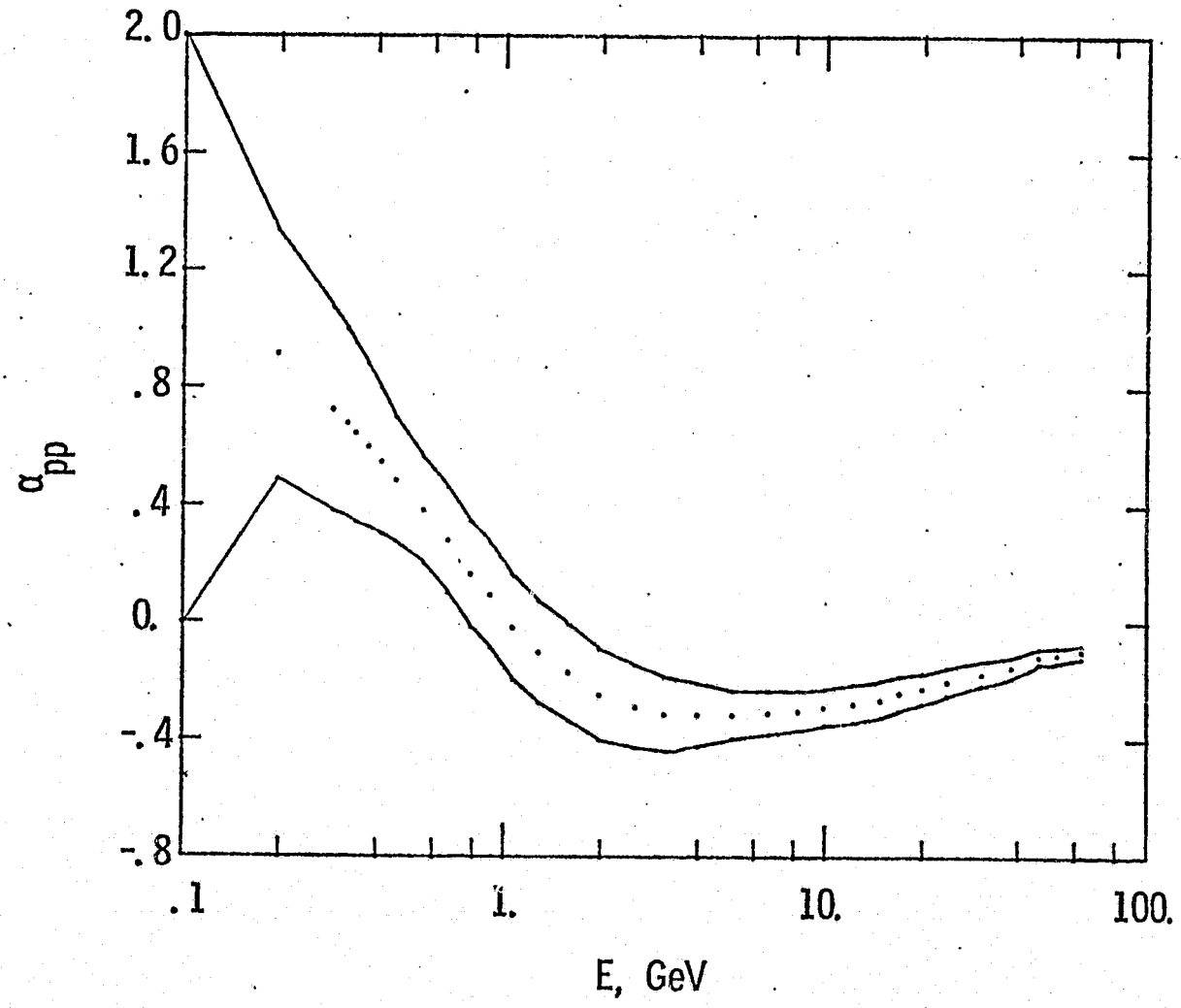

Fig. 7. Ratio of real-to-imaginary part of the forward proton-proton scattering amplitude as a function of laboratory energy.

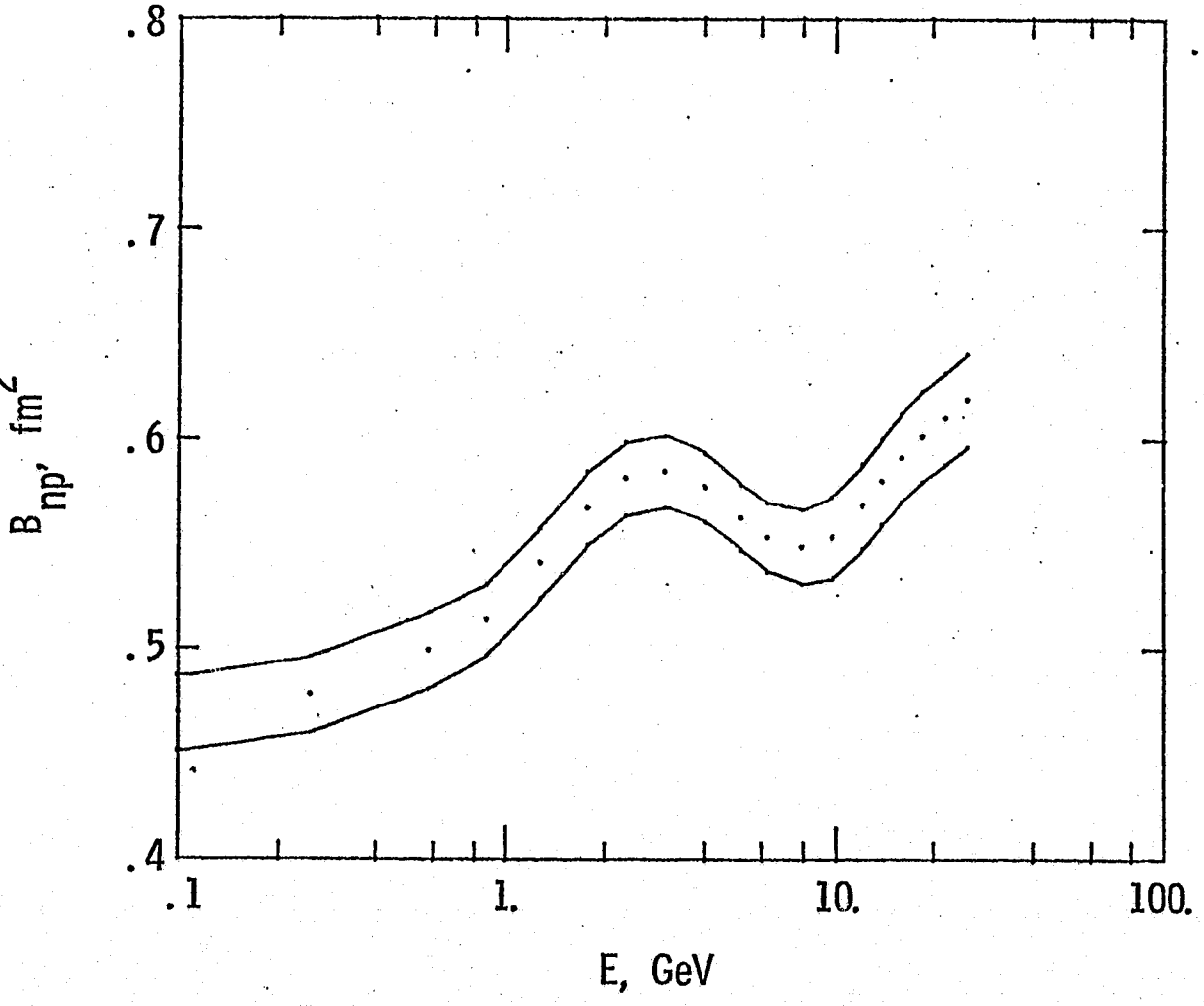

Fig. 8. Neutron-proton scattering slope parameter as a function of laboratory energy.

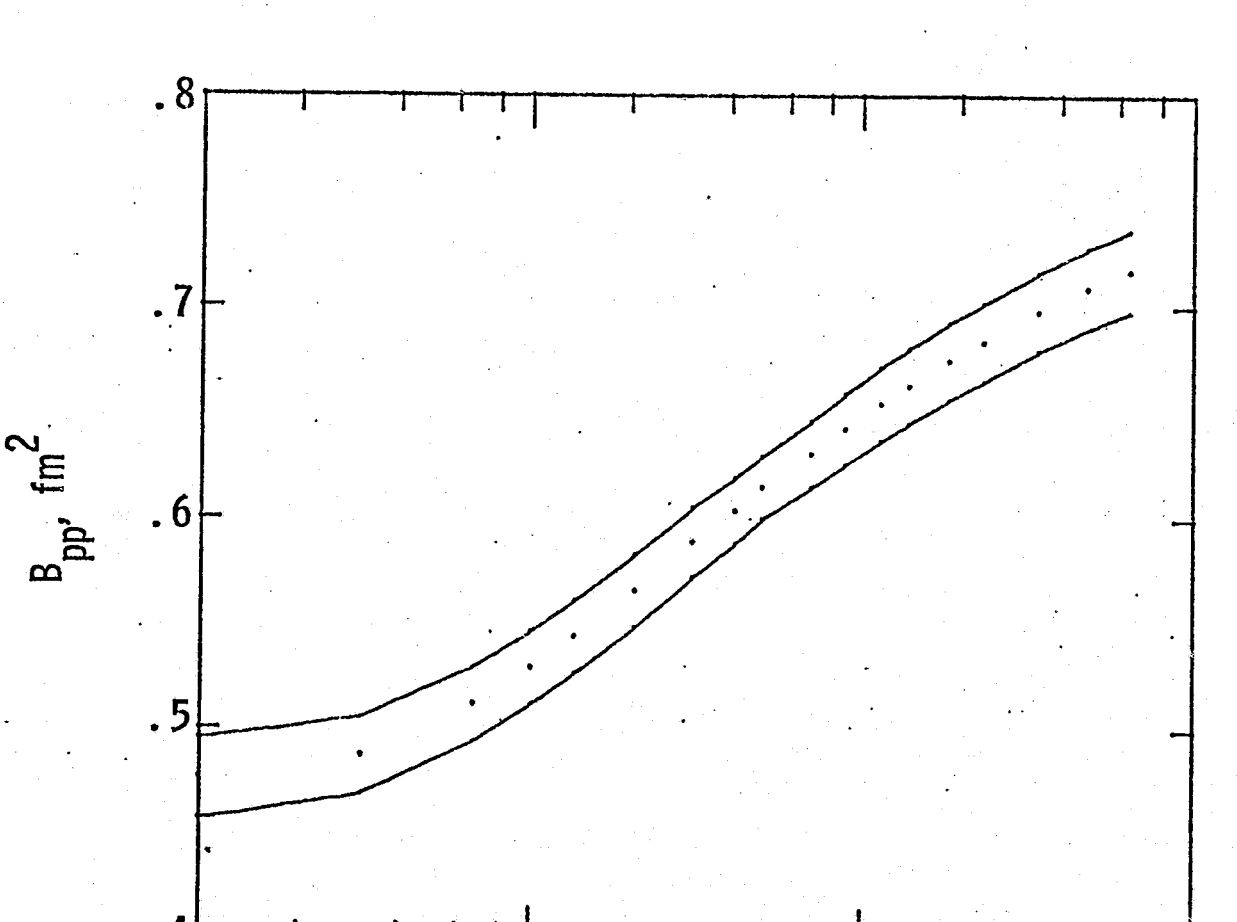

Fig. 9. Proton-proton scattering slope parameter as a function of laboratory energy.

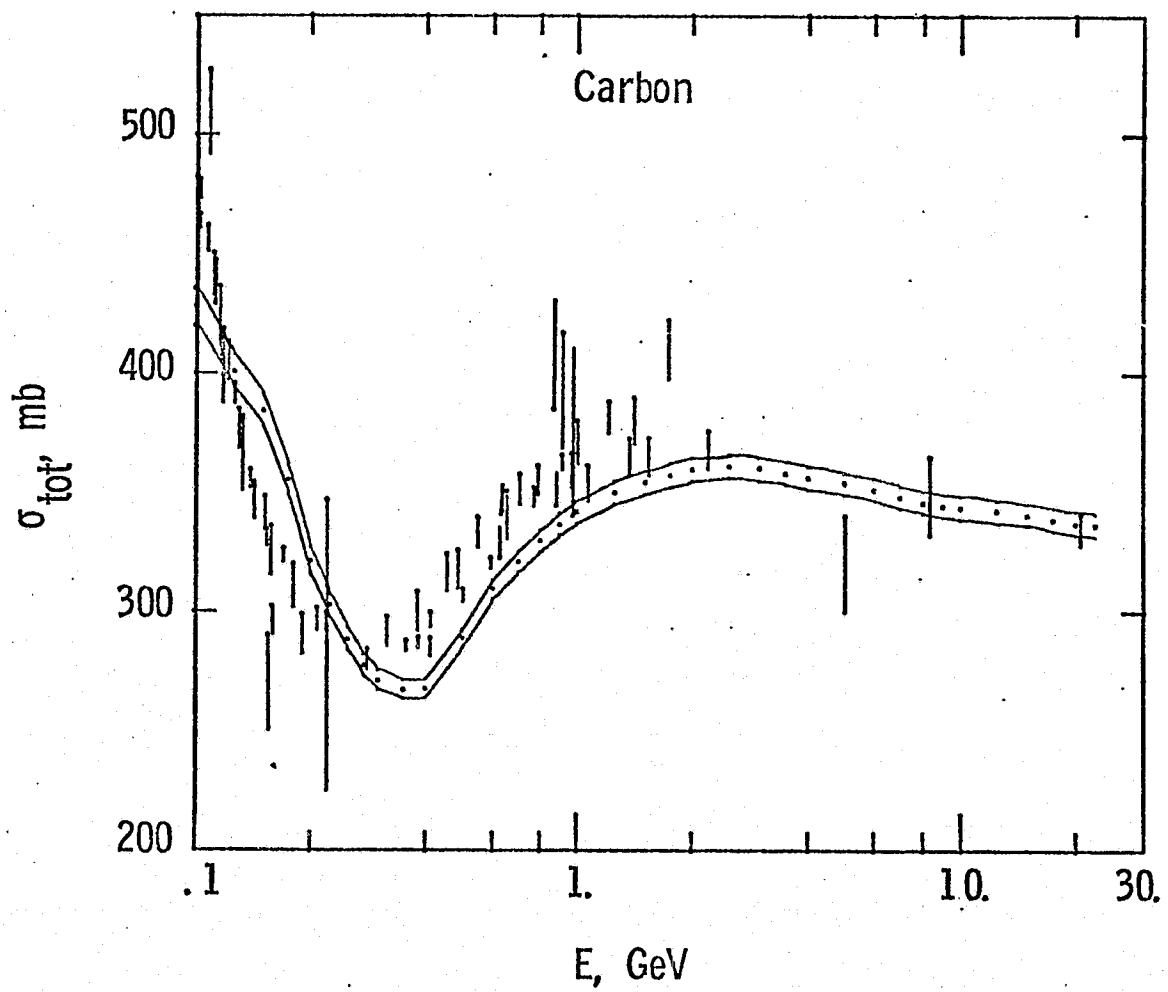

Fig. 10. Nucleon-carbon total cross section as a function of laboratory energy.

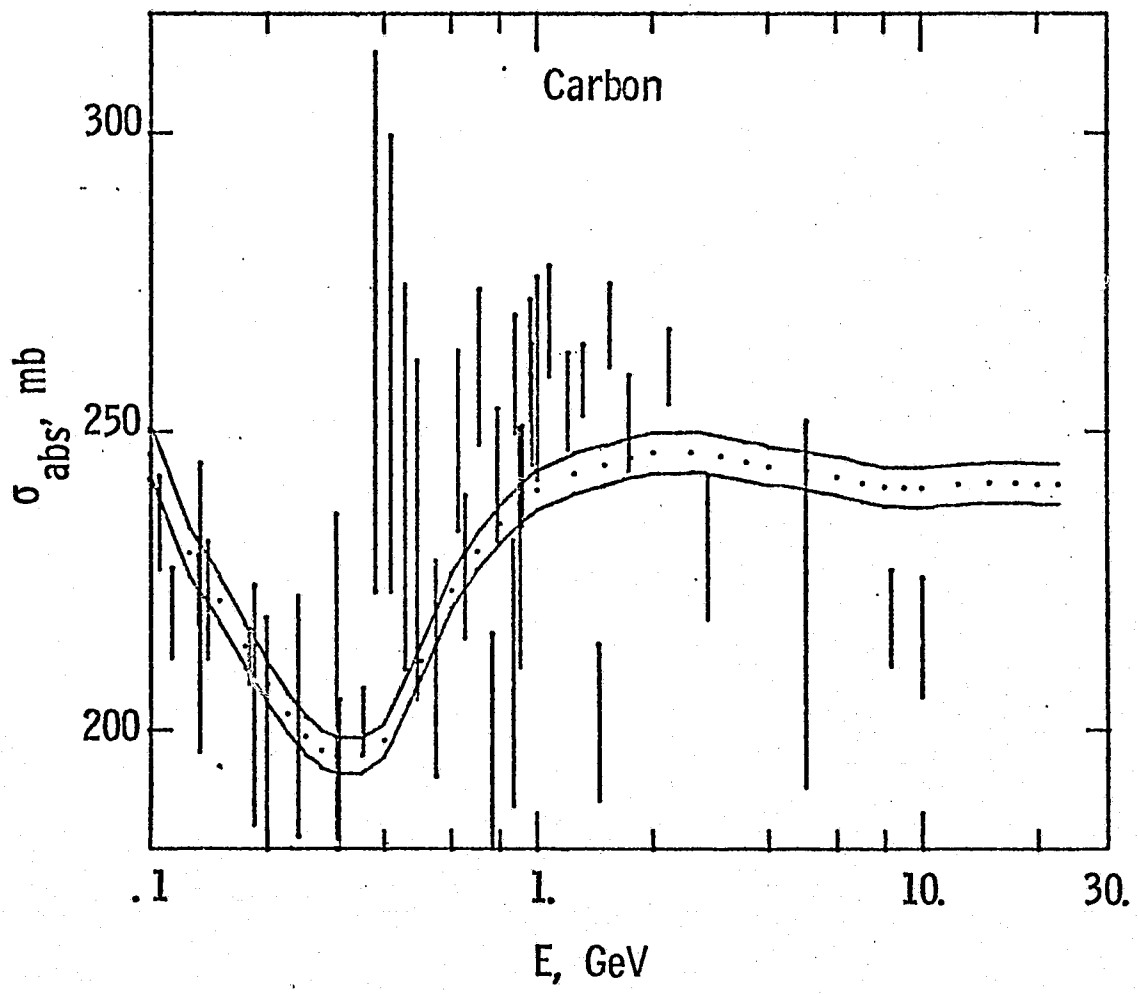

Fig. 11. Nucleon-carbon absorption cross section as a function of laboratory energy.

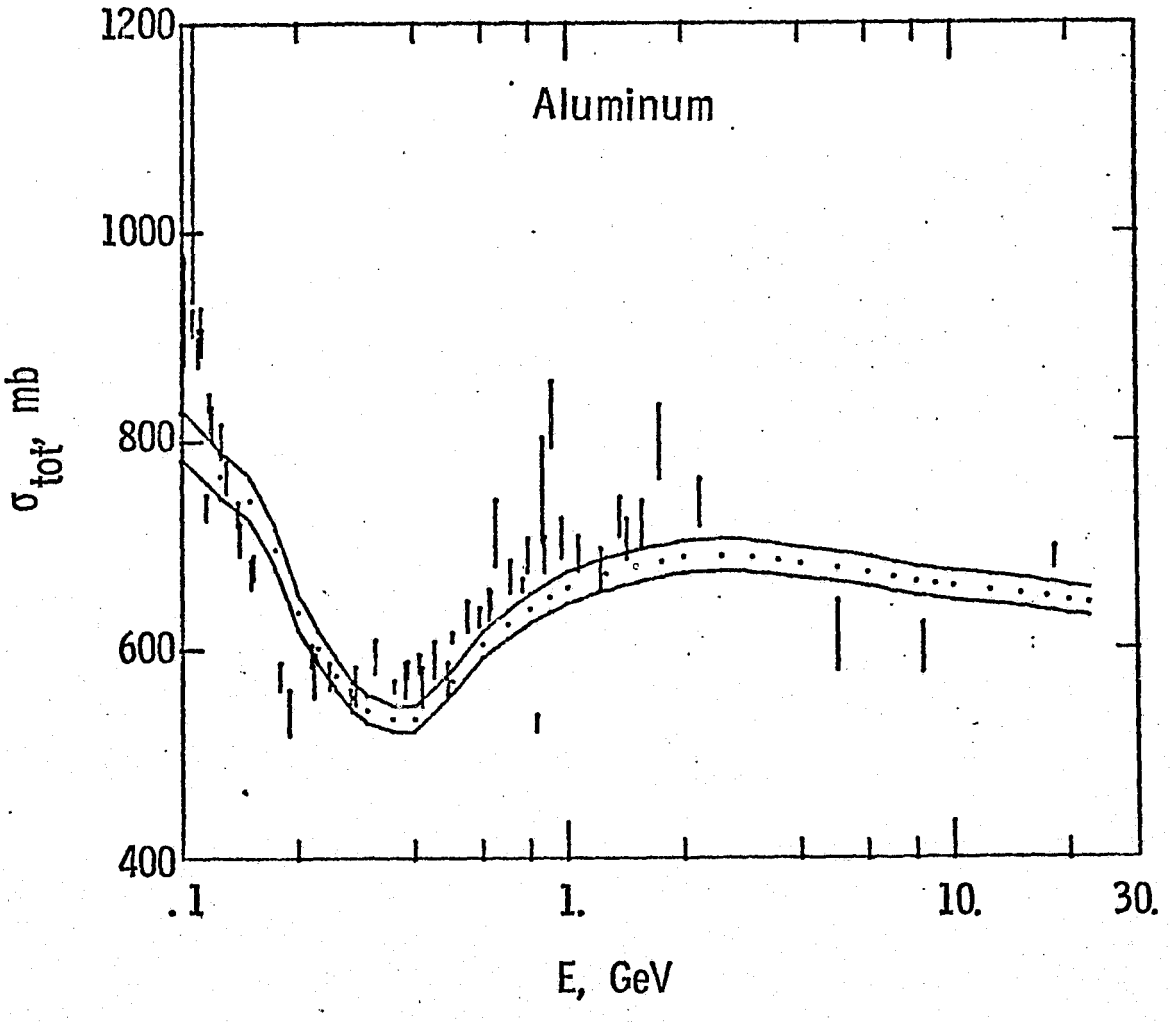

Fig. 12. Nucleon-aluminum total cross section as a function of laboratory energy.

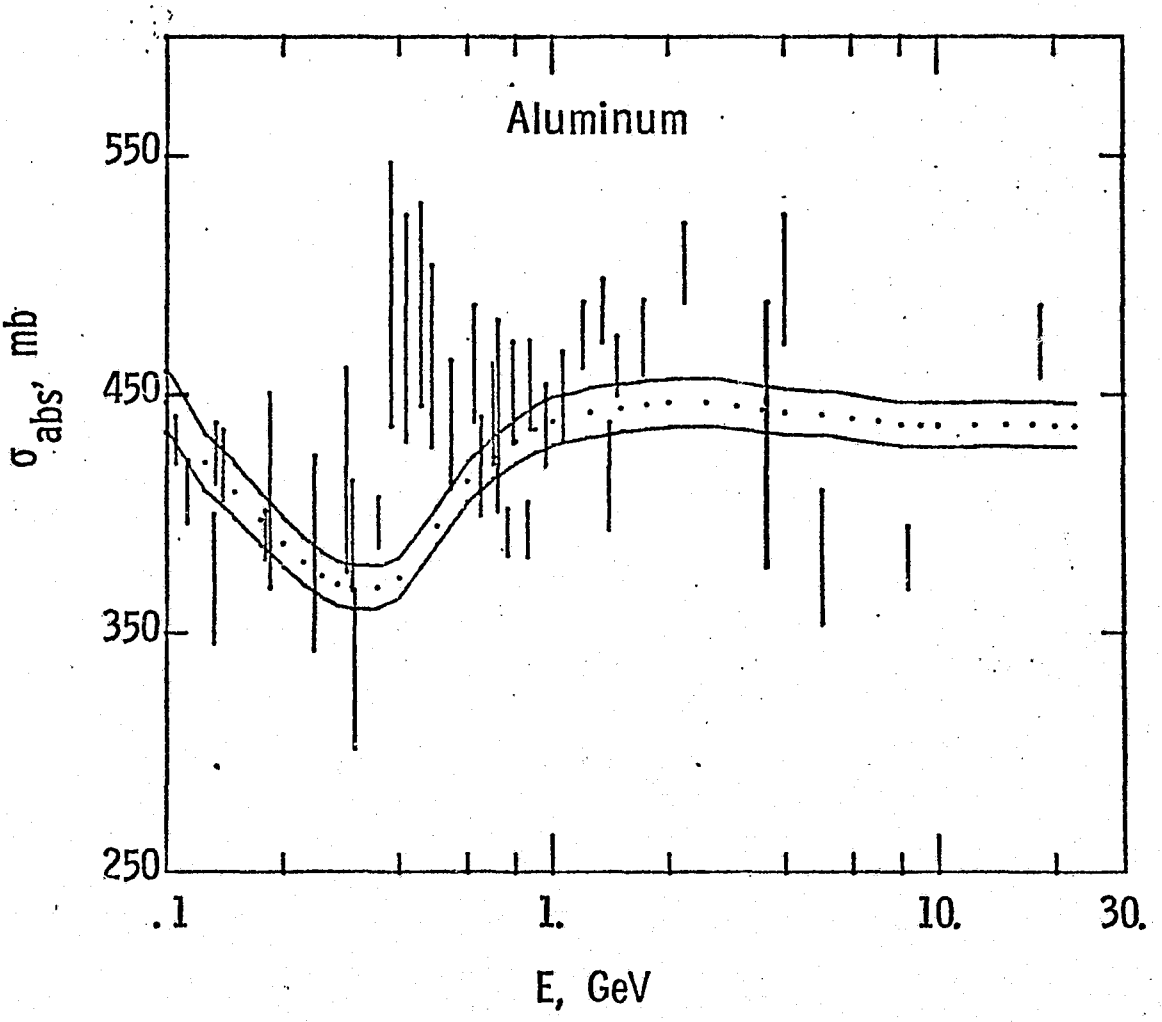

Fig. 13. Nucleon-aluminum absorption cross section as a function of laboratory energy.

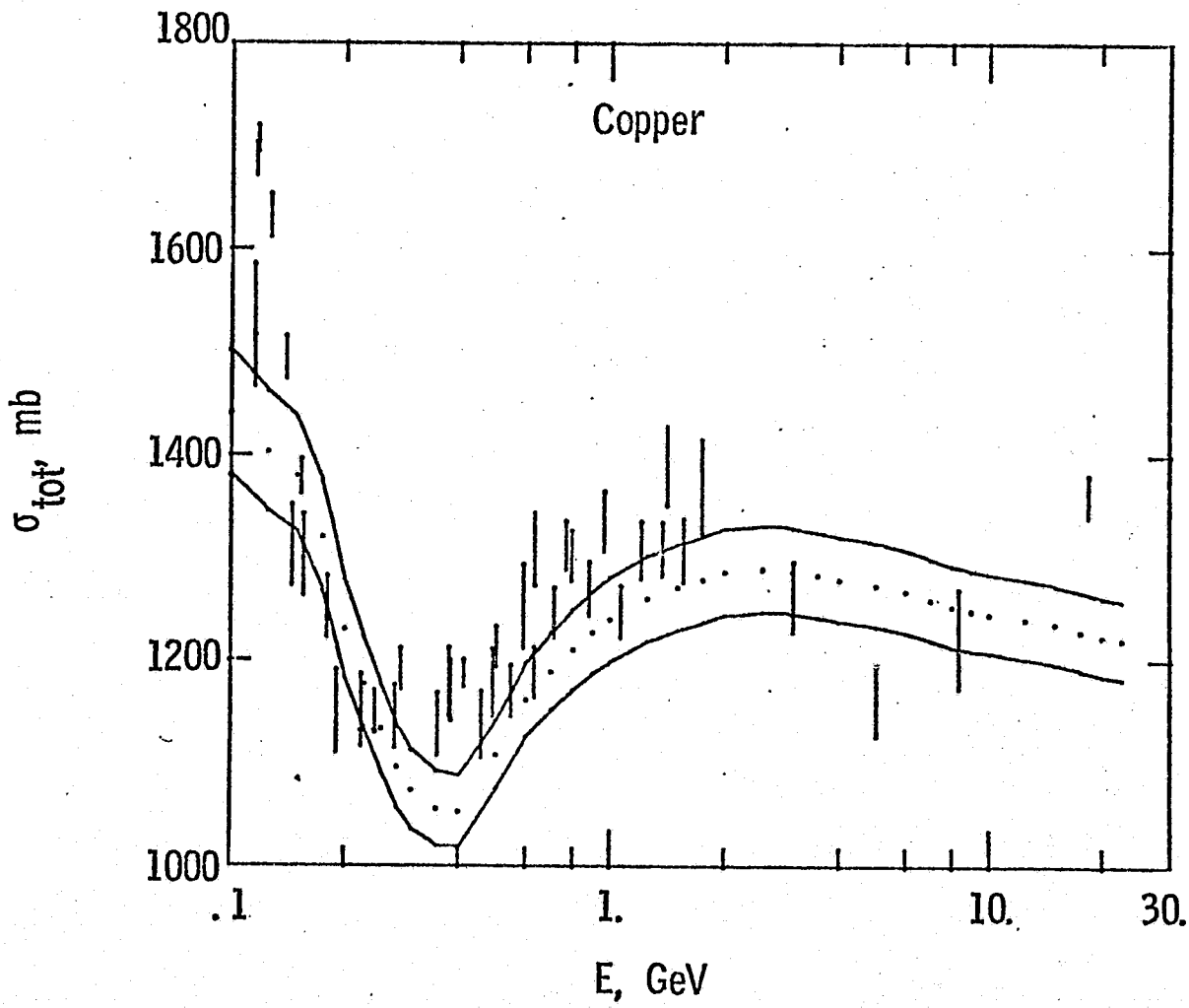

Fig. 14. Nucleon-copper total cross section as a function of laboratory energy.

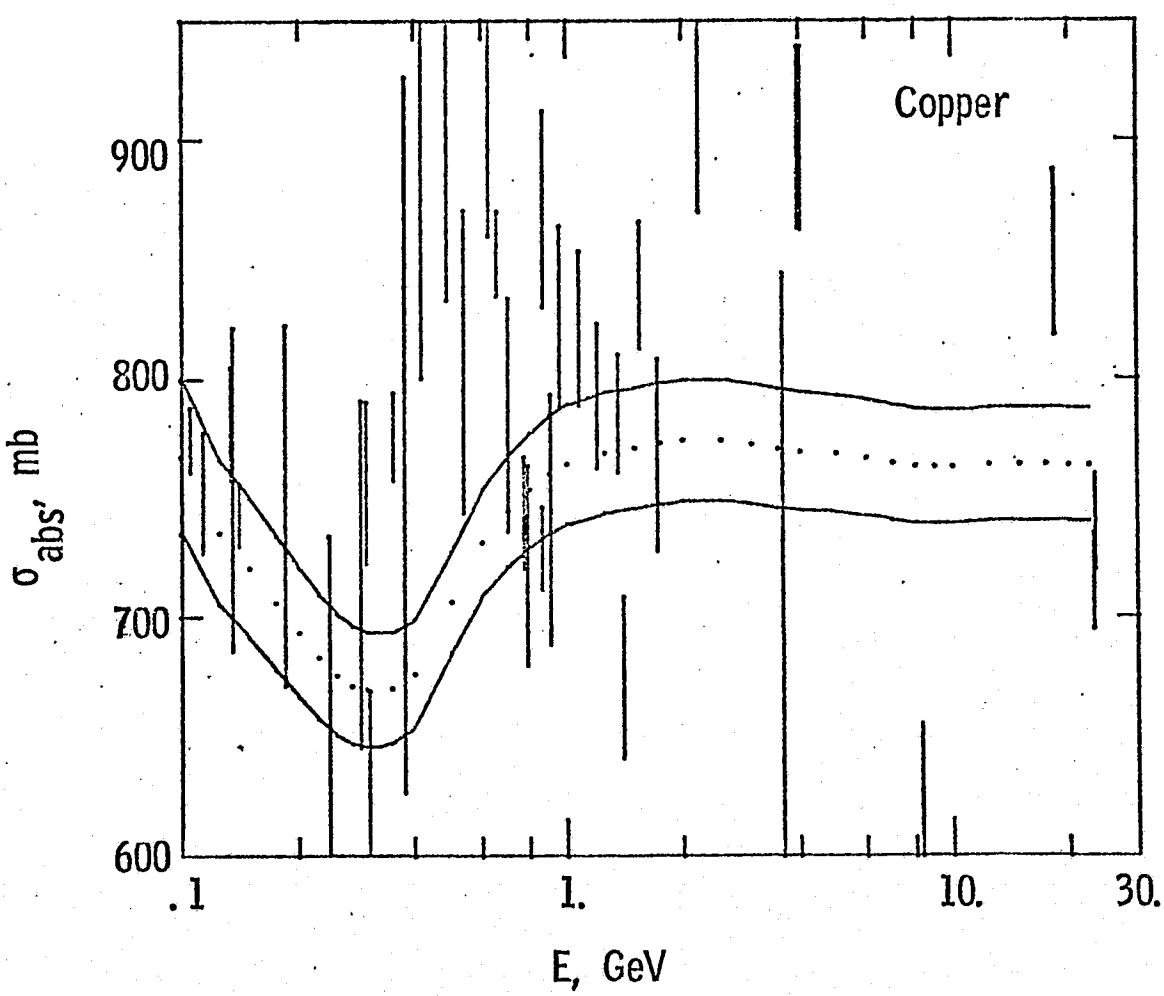

Fig. 15. Nucleon-copper absorption cross sections as a function of laboratory energy.

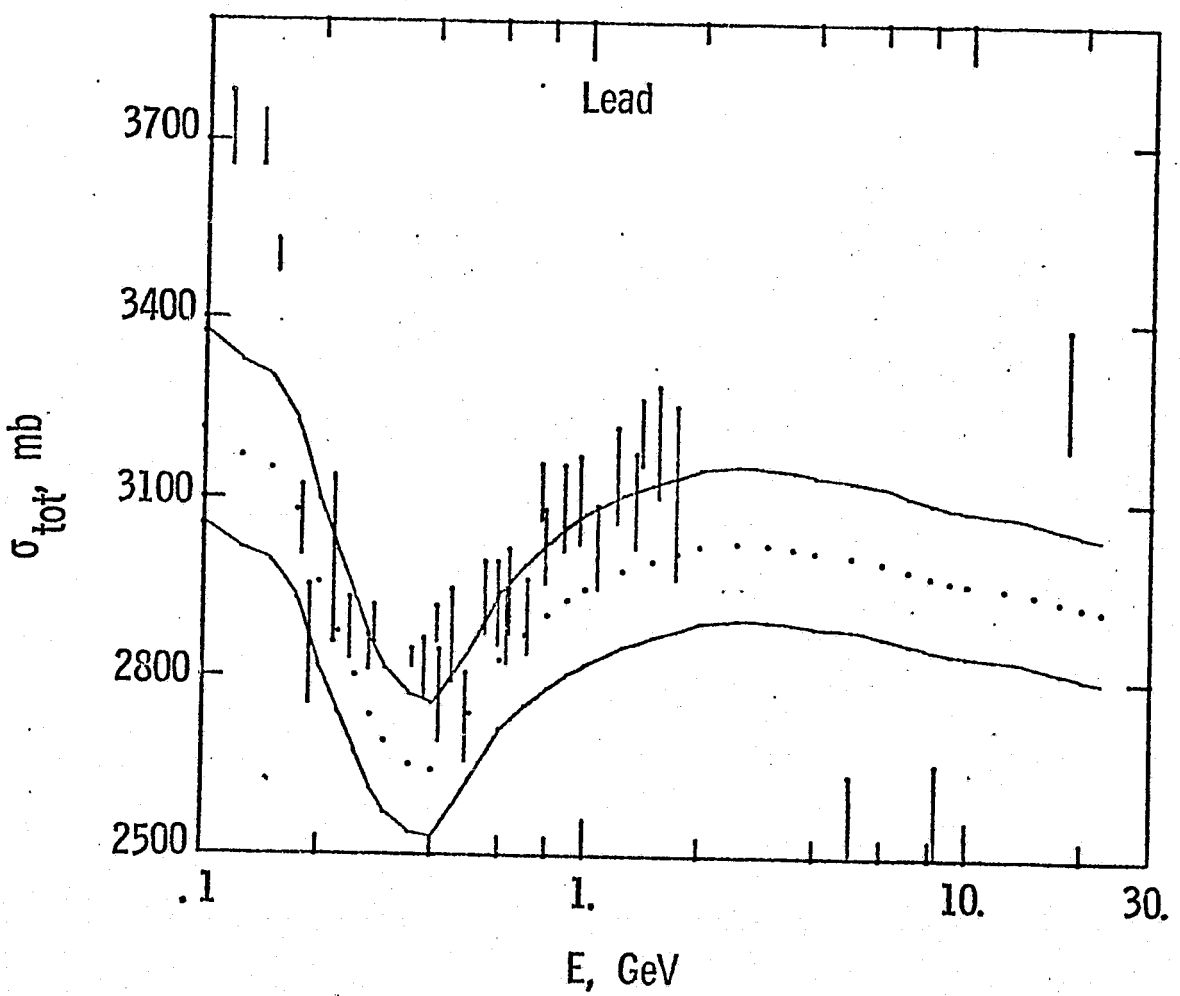

Fig. 16. Neutron-lead total cross section as a function of laboratory energy.

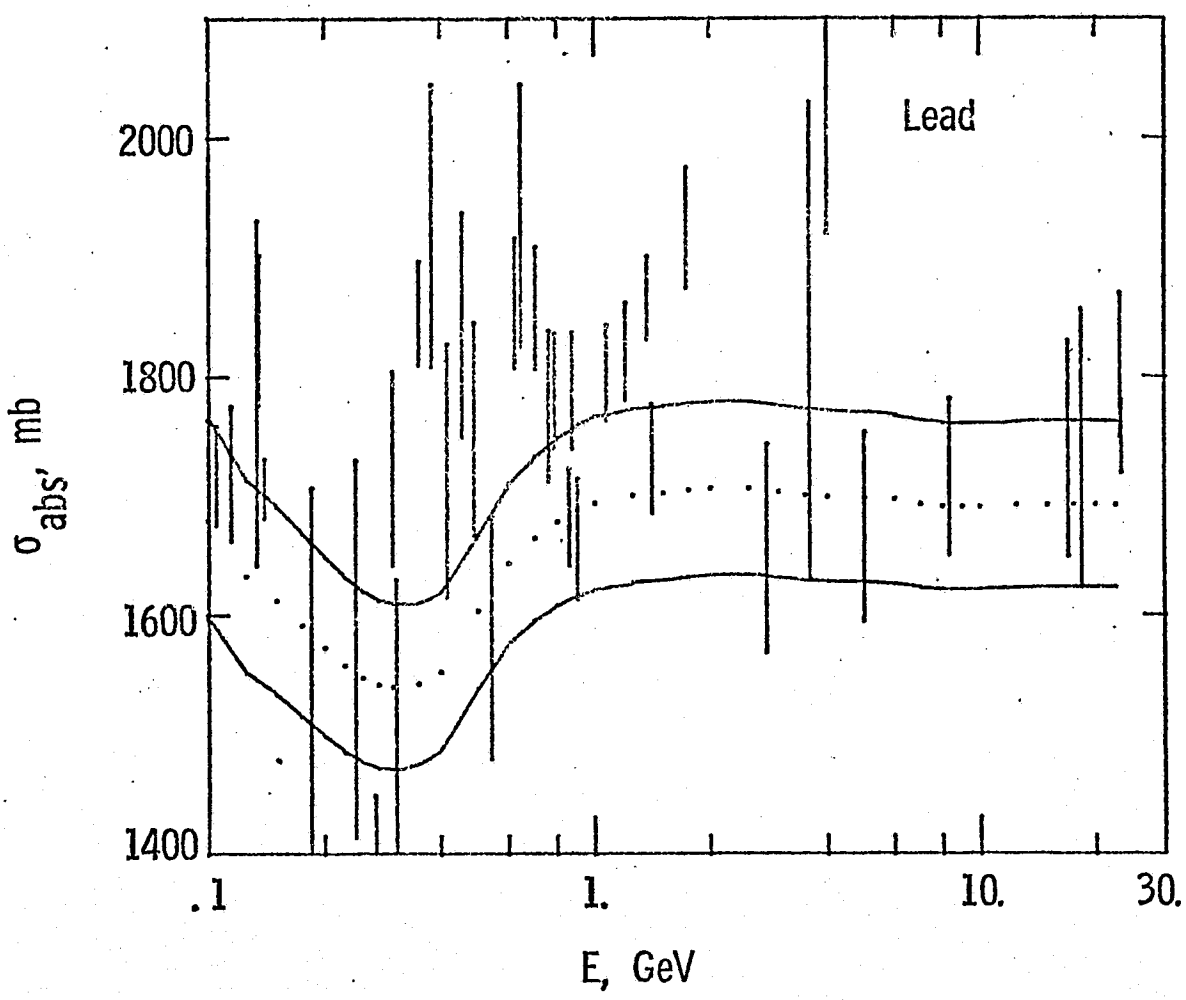

Fig. 17. Neutron-lead absorption cross section as a function of laboratory energy.